Ann. Rev. Astron. Astrophys. 1977. 15:295–362

THE GALACTIC CENTER ✖2116

J. H. Oort
Sterrewacht, Leiden, the Netherlands

INTRODUCTION AND OVERVIEW

This article is partly a review and partly a research paper. The discussion and conclusions can be summarized as follows:

Gravitational field and mass distribution Within $R = 750$ pc this is determined from the rotation of the H I nuclear disk (Table 1). Emission at 2.2 μ from the main stellar population has been used, in combination with data on M31, to estimate the mass distribution in the inner 50 pc. Observations of the Ne II emission at 12.8 μ yield information on the mass inside 0.5 pc. An ultracompact radio source of radius smaller than ~ 10 A.U. is presumably the actual center of the Galaxy. It may have a mass in the order of five million solar masses, and there is a suspicion that it may contain the "engine" responsible for the many expulsion phenomena observed throughout the central region.

Table 1 Mass within R, potential, circular velocity, time of revolution, and density

R (pc)	$M(R)$ ($10^6\ M_\odot$)	$\Phi(0)-\Phi(R)$ (10^4 km^2 sec^{-2})	Θ_c (km sec^{-1})	T (10^6 yr)	$\rho(R)$ ($M_\odot$ pc^{-3})
0.1	0.3[a]	0.64	114	0.006	3×10^7
1.0	4.4[a]	4.4	138	0.045	4×10^5
5	30	8.2	161	0.20	2×10^4
10	70	10.0	174	0.36	7×10^3
20	160	12.2	186	0.67	1.9×10^3
50	490	15.6	206	1.5	
100	920	18.6	200	3.1	1.1×10^2
200	2500	21.9	233	5.4	
500	8300	27.8	268	12	6
1000	16400	32.8	266	24	

[a] Recent dynamical data have shown that the actual mass within $R = 0.4$ pc is about three times higher than the mass of $1.5 \times 10^6\ M_\odot$ interpolated from the table (Section 6.3.2).

Expulsive phenomena Four different regimes of expulsive phenomena have been established; presumably all four are causally connected with the nucleus:

1. Arm-like H I features extending to a few kpc. Their H I masses range up to two million solar masses. The radial motions are generally between 100 and 200 km sec^{-1} (Table 2). The two largest, the 3-kpc arm and the expanding arm at $+135$ km sec^{-1}, may be of a different nature, and they may be parts of resonance orbits instead of results of expulsion. Many expanding features move at an angle with the galactic plane. The origin of the expulsion is unknown. (Figures 11–15).
2. Massive complexes of molecular clouds, within 300 pc from the center. Their relatively slow motions indicate that they must have been expelled. Direct evidence for this is shown by a ring of molecular clouds at $R \sim 190$ pc expanding at an average velocity of 150 km sec^{-1}. One of the giant molecule agglomerations, the "$+40$ km sec^{-1} cloud," may be very close to the center and of quite recent origin. The longitude distribution of the bulk of the molecules is extremely anisotropic: by far the greater part lies at positive longitudes and has positive velocities. The total mass in the molecular complexes is in the order of 10^8 $M_\odot$ (Figures 19, 21, 26).
3. Ionized gas within $R \sim 50$ pc. This also occurs in extended agglomerations, including the "Arc," about 15′ from the center (Figure 31). Again, they have small velocities, from which it may be inferred that they come from nuclear expulsion.
4. High-velocity streams within 1 pc from the center. Velocities determined by the Ne II line at 12.8 μ give evidence of large radial (as well as transverse) motions (Figure 34).

Table 2 H I features with large radial motions at $l = 0°$

	M_{HI} (10^6 $M_\odot$)	V_E (km sec^{-1})	Limits of l (°)		$\langle b \rangle$ (°)	$\langle z \rangle$ (pc)	R (kpc)
3-kpc arm	36[a]	−53	338	6	+0.1	0	4.0
The expanding arm at +135 km sec^{-1} = van der Kruit I	>7[b]	+137	355	22	+0.4	+85	2.2
van der Kruit VII	2	+100	355	0	+1.0	+183	0.9
van der Kruit XII	1.4	−99	358	9	−2.5	−330	2.4
Rougoor 2 = Cohen II	1.2	+73	357	~20	0.0	0	4.0
van der Kruit X	0.07	−162	358	5	−3.0	−436	1.7
feature E	0.06	−170	0		−1.5	−260	?
Cugnon's object[c] = van der Kruit VIII	2:	high	349	354	+3	+500	2?
Mirabel & Turner's object[d]	2	high	351	359	−14	−2400	2.4

[a] Integrated over a full quadrant.

[b] Integrated only over the longitude range 355° to 10°.

[c] This large object has been observed down to 349° longitude where it has its maximum intensity; a possible farther extension is quite uncertain. Its radial velocity of +50 km sec^{-1} is strongly forbidden (Cugnon 1968). As it does not extend to $l = 0°$, its association with the center is uncertain; it *might* be a relatively nearby high velocity complex.

[d] An elongated structure extending from $l = 359°$, $b = -7°.5$ to $l = 351°$, $b = -20°$, pointing away from the center, and having a forbidden radial velocity of +44 km sec^{-1} (Mirabel & Turner 1972). Because of its appreciable distance from the center its allocation to the central region remains uncertain.

The infrared core The same 1-pc region contains a remarkable concentration of discrete sources of far-infrared radiation emitted by dust that is heated partly by the smoothly distributed old stars and partly by young O stars. It is optically thin (Figures 35–38).

Need for a massive black hole? Nothing is known about the mechanism of expulsion, nor of the way in which the nucleus is replenished with interstellar gas on a sufficiently short time scale. Something out of the ordinary appears to be required.

1 POSITION AND DISTANCE OF THE NUCLEUS

The concentration of near-infrared radiation and, in particular, the still unresolved core of the radio source Sagittarius A West define the direction to the galactic center to within about 0.″1. Becklin & Neugebauer's (1975) high resolution map at 2.2 μ shows the centroid to lie near their source 16, at $\alpha = 17^h42^m29^s.3 \pm 0^s.15$, $\delta = -28°59'18'' \pm 3''$ (1950). The position of the unresolved core of Sgr A West is $\alpha = 17^h42^m29^s.291 \pm 0^s.005$, $\delta = -28°59'17''.6 \pm 0''.1$ (1950) (Ekers et al. 1975). The two positions agree exactly. The galactic co-ordinates are $l = -3'.34$, $b = -2'.75$.

At present the most reliable way to determine the distance to the center is by observations of the RR Lyrae variables. These are strongly concentrated toward the center. The dispersion of their mean absolute magnitudes is small, of the order of ± 0.2 mag. However, there is still a rather serious uncertainty, estimated to be about ± 0.15 mag, in the calibration of the absolute magnitude.

From the data obtained by Plaut in an extensive survey of the RR Lyrae variables with the 48-inch Palomar Schmidt in some fields near the center, Oort & Plaut (1975) derived a distance of 8.7 kpc for the center. The estimated mean square error was ± 0.6 kpc, the largest contribution to the error coming from the uncertainty in the mean absolute magnitude, the second largest from the rough way in which the absorptions in the various fields were determined.

To avoid possible confusion in comparisons with other investigators the data and discussions in the present article have all been based on the standard distance of 10 kpc.

2 THE GRAVITATIONAL FIELD AND THE NUCLEAR DISK

Information on the mass density in the central region can be obtained in three ways: (*a*) from the distribution of radiation in the near infrared, (*b*) from the rotation velocity of gas concentrated in the galactic plane, and (*c*) from the density distribution and velocity dispersion of Population II objects.

2.1 *Near-infrared Radiation*

Because of the heavy obscuration in the galactic layer our knowledge of the central region is confined to what we can learn from observations in the infrared, and at mm and radio wavelengths.

Only a limited range of the infrared spectrum, from about 1.5 to 3.5 μ, can be

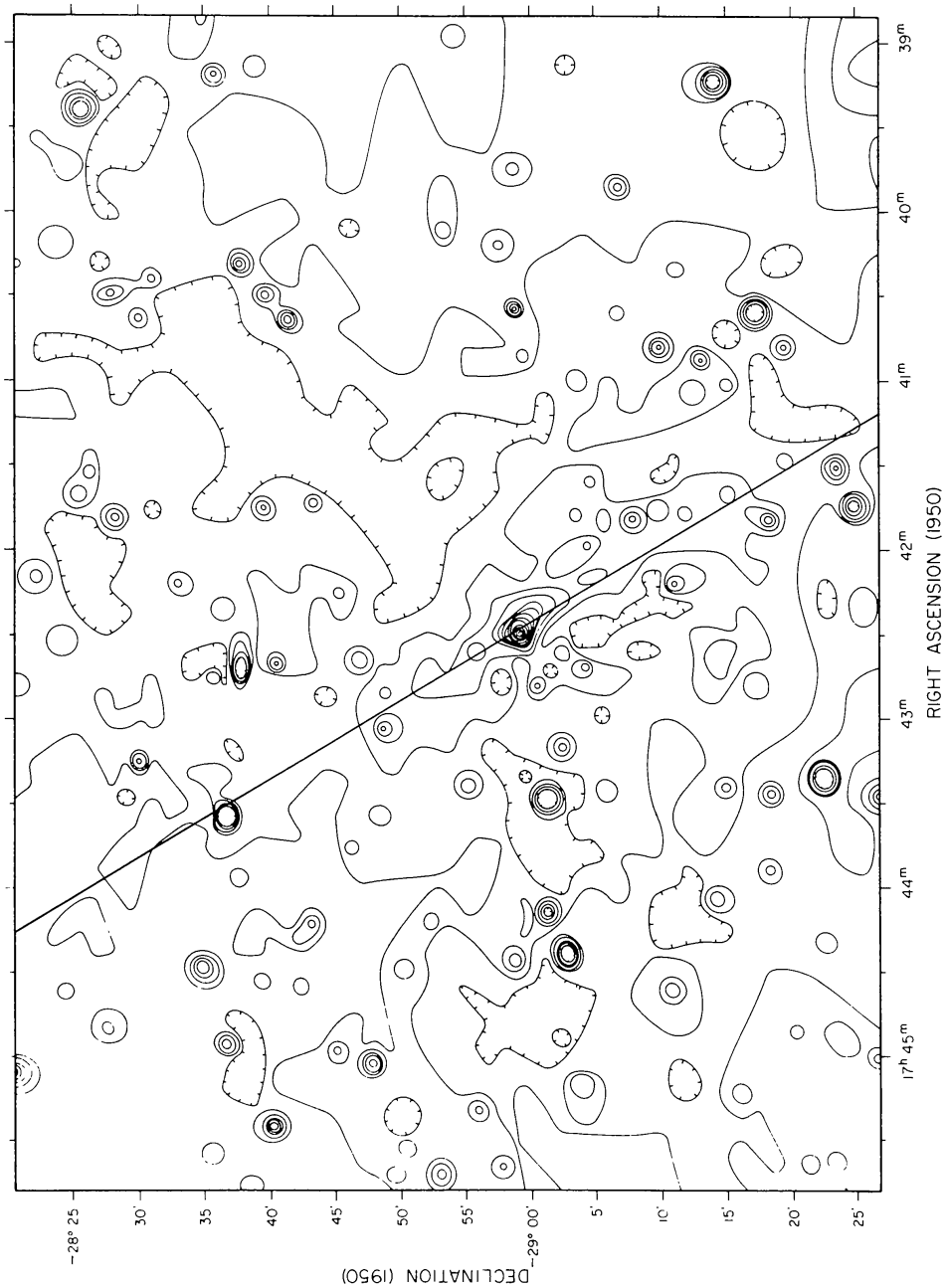

Figure 1 A 2.2-μ contour map of the central 1° of the galactic center made with an angular resolution of 1′.2. The contour levels correspond to 1.7 Jy in a 1′.2 aperture. The hatched areas correspond to point sources whose flux density is greater than 6.5 Jy. The zero level of the map was taken as the average flux 1° east and west of the galactic center; the ticked contours show the direction of decreasing flux. The map was constructed from right ascension drift scans on the 1-m telescope at Las Campanas, Chile; the present data were obtained with only a single measuring beam (Becklin, Neugebauer & Early 1977). The straight line is the true galactic equator ($b = -2.^{\circ}75$).

used for exploring the mass distribution. At shorter wavelengths the absorption becomes prohibitive, while at much longer wavelengths the radiation comes mainly from interstellar dust and gas. Around 2 μ, however, the radiation is largely stellar.

Figure 1 shows the distribution of the surface brightness at 2.2 μ in a $1° \times 1°$ region around the center, as measured by Becklin, Neugebauer & Early (1977). It shows a strong concentration towards the center of the picture, which coincides with what on other grounds is considered to be the actual center of the Galaxy, and a gradual falloff with the distance from this center. The distribution is clearly elongated, with an axial ratio of about 0.4; the elongation is along the galactic equator. The patchiness of the picture is probably partly due to unevenness in the interstellar extinction, which totals about 3 magnitudes at 2.2 μ, and partly to individual stars of very high intrinsic brightness in the central region. The absorption cannot be reduced much further by observing at still longer wavelengths because, as Becklin & Neugebauer (1969) have clearly shown, nonstellar radiation begins to preponderate beyond about 3.5 μ.

The assumption that the radiation around 2 μ is stellar radiation receives support from observations of the center of the Andromeda nebula, where the optical absorption is relatively small, so that the *optical* spectrum can be studied along with the infrared emission. Sandage, Becklin & Neugebauer (1969) have shown that the distribution of the surface brightness is practically identical for various optical and near-infrared wavelengths, including 2 μ. We know from the spectrum that the optical radiation comes from stars, probably principally K giants. The brightness at 2.2 μ corresponds roughly to what would be expected from such stars, and it is

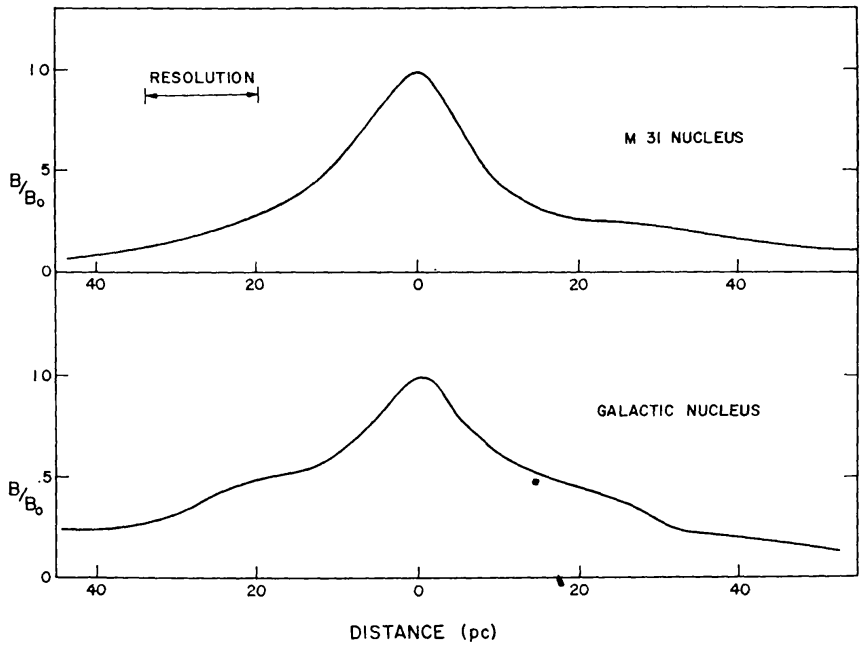

Figure 2 Comparison of distribution of 2.2-μ brightness around the galactic center with that around the nucleus of M31 at the same spatial resolution (Becklin & Neugebauer 1968).

therefore plausible to assume as a working hypothesis that the 2.2-μ radiation gives a measure of the star density. We shall assume that the same applies to our own Galaxy.

The two galaxies resemble each other in the distribution as well as in the absolute intensity of the 2.2-μ radiation (cf Figure 2). However, the light distribution in the innermost part of M31 is less flattened than the 2.2-μ radiation in the Galaxy, and the absolute value of the surface brightness seems to be 2.4 times fainter in M31.

2.2 *Mass-to-Light Ratio. Mass Distribution from 2.2-μ Radiation*

The only way in which we can determine the ratio of the mass to infrared emission is through a comparison with the Andromeda nebula, in which one can probably see the true light distribution down into the nucleus. Mass-to-light ratios (M/L) for its nuclear region have been estimated from various spectral data. These indicate that the bulk of the light is contributed by late-type giants. Population models constructed by Faber give $M/L_V = 15$ (cf van den Bergh 1975). An independent value can be derived from measurements of the velocity dispersion and the distribution of the light density in the nucleus. Applying the virial theorem to these data, Morton & Thuan (1973) obtained $M/L_V \sim 13$. It may be noted that a very similar ratio has been found for the main body of M31 from the rotation curve.

As we know the ratio of the 2.2 μ to the visual brightness we can in this way find the ratio of mass density to that of the infrared emission.

In order to find the mass distribution in our own Galaxy from the measurements at 2.2 μ we can assume as a working hypothesis that the stellar composition of the nuclear regions is the same in the two galaxies. We then have all the data that are needed to obtain the mass density distribution. The resulting gravitational field can finally be confronted with that derived from the rotation of the H I nuclear disk, which gives an entirely independent and essential check on the various assumptions made.

On the basis of Becklin & Neugebauer's 1968 data the following representation of the mass density has been found:

$$\rho(\alpha) = 7.6 \times 10^5 \alpha^{-1.8} M_\odot \,\mathrm{pc}^{-3}, \tag{1}$$

where

$$\alpha^2 = \varpi^2 + z^2(a/c)^2,$$

ϖ being the distance from the rotation axis, z that from the galactic plane, both in pc, and c/a the axial ratio of the surface brightness distribution. The above expression has been taken from an article by Sanders & Lowinger (1972). They used a somewhat more roundabout way than that sketched above to convert the 2.2-μ densities into mass densities. The axial ratio was taken to be 0.4.

Infrared intensities are available only for the region within roughly 50 pc from the center. In order to extend the data to larger distances, which is necessary if one wants to compare them with rotation velocities in the central disk, one must once more recur to a comparison with M31 and make use of the light distribution in its central region.

In view of the similarity of the 2.2-μ radiation in the innermost regions of M31 and the Galaxy, and in view of the fact that the light distributions in the central bulges of different galaxies appear to be practically identical, it is reasonable to assume that the similarity will extend beyond 50 pc. From data collected by Kinman (1965), Ruiz (1976) has derived space densities in M31 up to about 500 pc from the center. Between 10 and 500 pc the density can be well represented by $\rho \propto a^{-1.9}$, if a is the distance from the center measured in the equatorial plane and the axial ratio is assumed to be 1.45. This is practically the same power law as in (1), and supports the assumption made by Sanders & Lowinger (1972) that the mass density in the Galaxy can be represented by formula (1) up to at least 500 pc.

The following section shows that the agreement between the results obtained in this way and the rotation of the central disk is satisfactory.

2.3 *The Interstellar Gas*

The interstellar hydrogen in the central region has been extensively investigated in various ways. It is partly in atomic form, in which it can be observed in the 21-cm line. A large fraction is molecular and is concentrated in dense clouds; the H_2 molecules in these clouds have not been observed directly, but only through the emission or absorption lines of other molecules (CO, OH, H_2CO) that always occur side by side with H_2.

Finally, there are numerous H II regions in the central area. These are observed in the continuous radio spectrum as well as in recombination lines.

The contribution of the gas to the total mass density in the central region is negligible, but the *motion* of the gas gives important information on this total density. The clearest data, so far, come from the 21-cm line observations.

2.4 *The Rotating Nuclear Disk*

In regions where the gas is moving in approximately circular orbits, measurements of its velocity yield directly the gravitational force. Pressure gradients are almost always negligible. In the central region, up to about 4 kpc from the center, large deviations from circular motion occur, so that the velocity of the gas cannot give unambiguous information on the gravitational field. The deviations are at least partly due to gas expulsion from the nucleus. Between 1 and 4 kpc they may also be caused by a deviation of the gravitational field from circular symmetry. We return to these problems in Sections 3 and 4.

For the present context it is important to note that there is a region, between roughly 50 and 750 pc from the center, where the atomic hydrogen appears to move in practically circular orbits, and thus permits the determination of the gravitational field.

Figures 3 and 4, taken from an early investigation of the central region by Rougoor (1964), give a survey of the H I density in the galactic plane, as a function of longitude and velocity. The low-velocity parts, which contain mainly gas outside the central region, have been left blank. A more recent, higher-sensitivity map made with the Dwingeloo telescope has been published by Burton (1970).

The figures give an impression of the complexity of the phenomena in the central region. Most striking is the asymmetry. If the motions were governed principally by the galactic rotation the upper right-hand quadrant should have been a mirror image of the lower left-hand quadrant, and similarly for the lower right-hand and upper left-hand quadrants. Evidently the reality is totally different.

Particularly intriguing are some features with large *radial* motions relative to the center. The most important of these are as follows:

1. The intense ridge at negative velocity is seen in absorption at $l = 0°$. It moves away from the center at a velocity of 53 km sec^{-1}. Figure 4 indicates that it becomes "tangential" around $-22°$ longitude. At the time of its discovery in 1957, when the distance R_0 from the Sun to the center was assumed to be 8.2 kpc, the longitude 22° corresponded to $R = 3$ kpc. The feature was therefore called the 3-kpc arm.
2. Around $l = 0°$ relatively strong emission is seen at velocities up to nearly $+200$ km sec^{-1}. The gas at these velocities does not absorb the radiation of Sgr A; it must therefore lie behind it and move away from the center. The stronger part has been called "the expanding arm at $+135$ km sec^{-1}" (Rougoor 1964) or "feature I" (van der Kruit 1970, Cohen 1975). Figure 3 shows that the high positive velocities of the feature extend to $-5°$ longitude. At negative longitudes the radial velocity due to rotation should be negative; the hydrogen

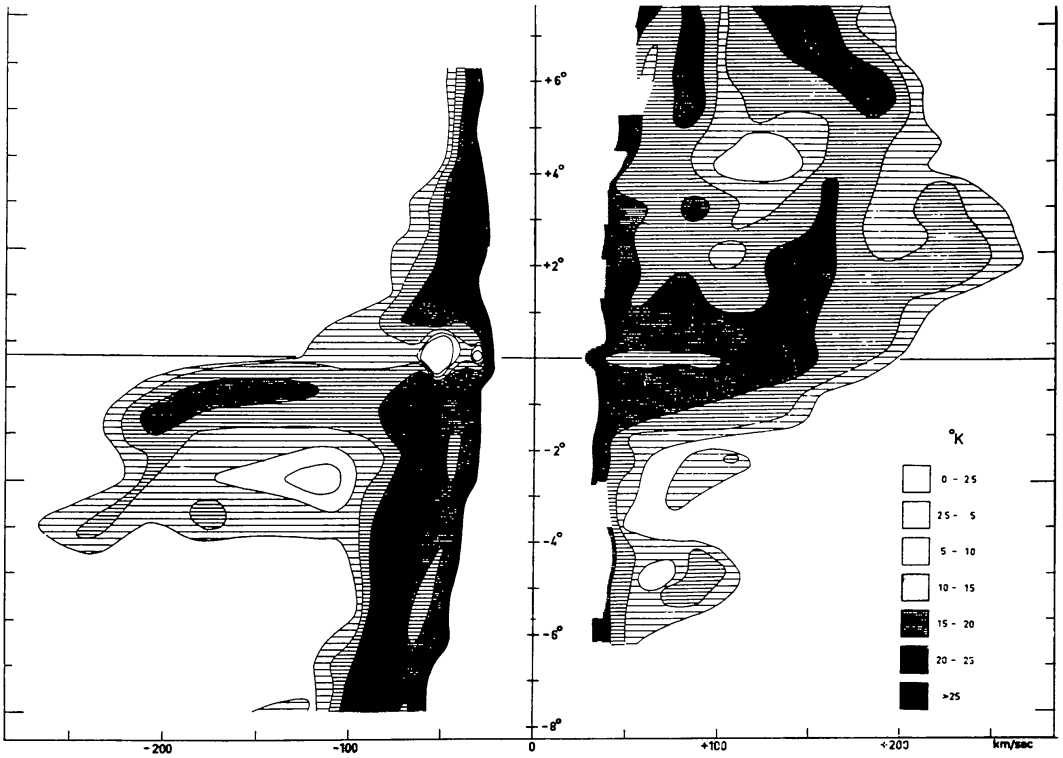

Figure 3 Velocity-longitude contours of atomic hydrogen in the galactic plane between $-8°$ and $+8°$ longitude, observed with the Dwingeloo radiotelescope with a half-power beam of 34′ (Rougoor 1964).

in this part of feature I must therefore have a very large radial component directed away from the center.

A striking feature in Figures 3 and 4 is the wing of high negative velocities between $l = -4°$ and $l = 0°$. I have added Figure 4 to emphasize the uniqueness of this feature. It was first discovered by Rougoor and Oort in 1959, who interpreted it as part of a rotating nuclear disk on the basis of two independent arguments (Rougoor & Oort 1960). The first was the sudden cutoff at the exact longitude of the center, and the lack of any clear sign of expansional radial motions. The second was that the rotation velocities that followed from this interpretation agreed with the circular velocities to be expected if the distribution of the mass near the galactic center were the same as in M31. The mass density in M31 was calculated from the brightness distribution on the assumption that the value of M/L in its central region was the same as that for the main body of the nebula.

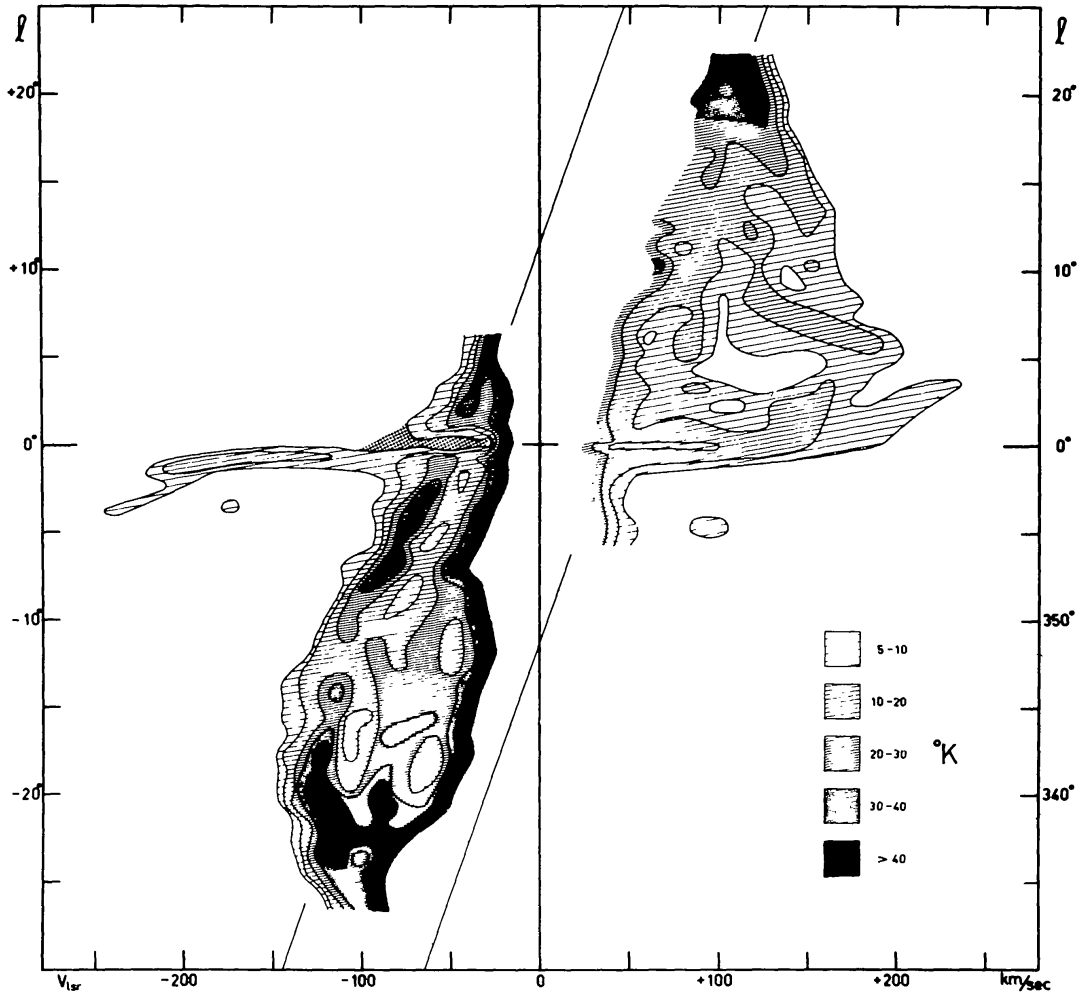

Figure 4 Extension of Figure 3 to greater distances from the center, indicating the uniqueness of the wing ascribed to the negative-longitude half of the rotating nuclear disk (Rougoor 1964).

A complete rotating disk should show a similar *positive* velocity wing at positive longitudes. However, on the positive velocity side the phenomena are muddled by high-velocity expanding gas, so that the other side of the supposed disk does not show up so convincingly. However, one does find a fair symmetry of the two sides if one confines oneself to the highest velocities, as in Figure 5, which gives a comparison of the column densities of H I atoms with velocities above 175 km sec^{-1}.

For somewhat lower velocities there are clearly asymmetries in the part within $l = \pm 1°.5$, as is seen most clearly in Figure 6, for instance in the absence of a counterpart at positive longitudes of the ridge *d*, which is so striking on the negative side. Sanders, Wrixon & Mebold (1977), to whom Figure 6 is due, interpret this feature as a small, steeply inclined arm spiraling into the nucleus. The innermost part of the proposed rotating disk seems to be seriously disturbed on the positive longitude side. *Outside* 1°.5 longitude the disk may well be symmetrical: the hydrogen with velocities from +200 to +250 km sec^{-1} between +1°.5 and +4°.0 longitude corresponds exactly with the gas at −200 to −250 km sec^{-1}

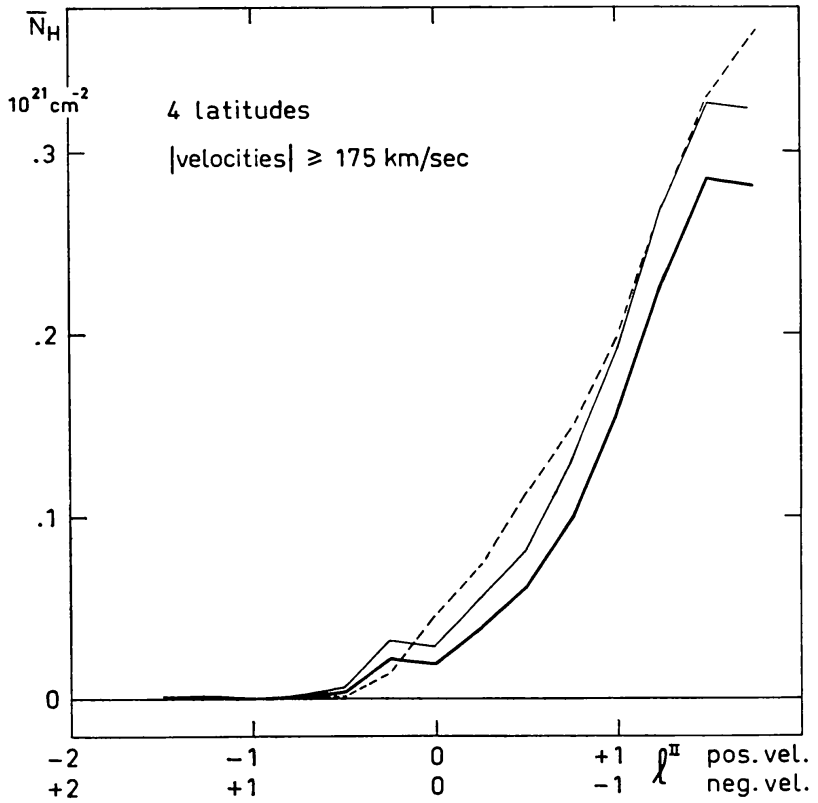

Figure 5 Variation with longitude of the number of hydrogen atoms with velocities above 175 km sec^{-1}. N_H has been averaged over latitudes $b^{II} = +0°.69$, $+0°.44$, $-0°.56$, and $-0°.81$. The heavy line is for the positive velocities above +175 km sec^{-1}, the thin line is for the positive velocities above +170 km sec^{-1}. This latter line coincides fairly well with the dashed curve for negative velocities. The longitude scale for the positive velocities has been reversed (Rougoor 1964).

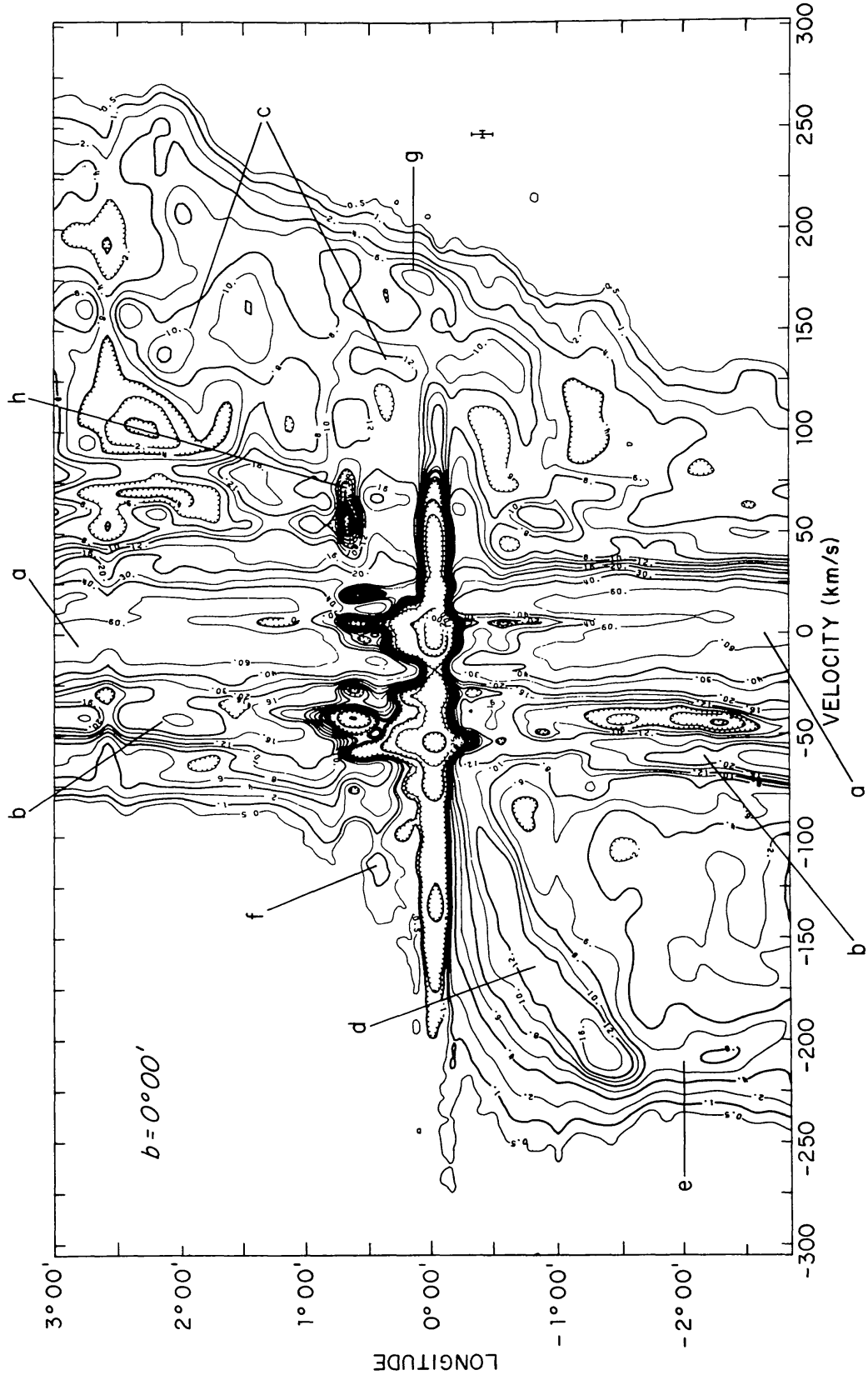

Figure 6 Velocity-longitude contours of H I in the galactic plane within 3° of the center observed with the Effelsberg radiotelescope. Beamwidth 9′ (Sanders, Wrixon & Mebold 1977).

between $-1.^{\circ}5$ and $-4.^{\circ}0$ longitude. Moreover, there is evidence for a similar cut-off at $l = 4.^{\circ}0$ on both sides of the center.

From a combination of the measured rotation in the central disk and data on the light distribution in M31 Rougoor & Oort (1960) derived a rotation curve for the central region down to quite small distances from the center (Figure 7). Assuming that pressure effects are small compared to gravitation they used these data to compute the mass distribution shown in Table 1. The table is intended only to give a general idea of the masses and the gravitational field. For this rough approximation the field was assumed to be spherically symmetrical.

The most extensive comparison of the rotation curve predicted from the light distribution in M31 and the 2.2-μ radiation in our Galaxy with the measured rotations has been made by Sanders & Wrixon (1973). They computed 21-cm line contour-velocity diagrams starting from this predicted rotation curve and assuming various density distributions of the gas. They compared these with a map for the inner $\pm 3^{\circ}$ longitude constructed from observations with the 140-foot Green Bank telescope, with a resolution of 21′ (Wrixon & Sanders 1973). The authors found that the predicted rotation curve (indicated by crosses in Figure 7), which is almost identical with the curve adopted by Rougoor and Oort, could give a good representation of the longitude-velocity diagram if combined with a suitable distribution of the gas density. The density distribution adopted by Sanders and Wrixon is shown by the solid drawn curve in Figure 8. The actual distribution may, however, differ considerably from this curve (cf Sanders, Wrixon & Mebold 1977). Observations extending to larger distances suggest the existence of a thin ring of increased density at $R = 0.7$ kpc, as indicated schematically by the dashed curve. The rotation velocity of the ring is roughly 240 km sec^{-1} (cf Rougoor & Oort 1960 and Burton 1974).

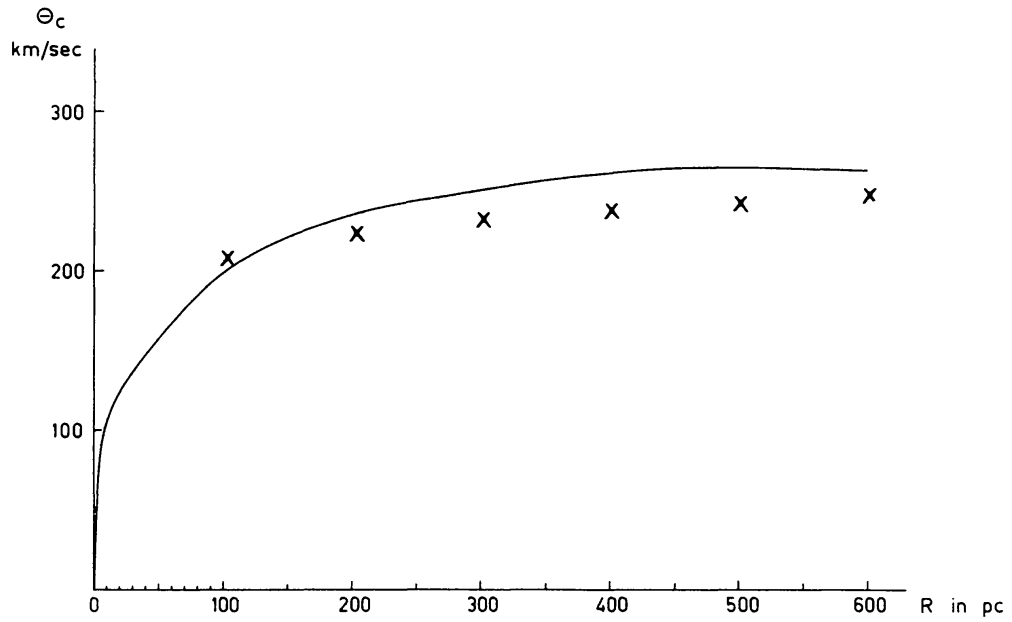

Figure 7 Circular velocity in the central region. The curve is from Rougoor & Oort (1960), the crosses are from Sanders & Wrixon (1973).

From the angle subtended in latitude the thickness of the disk between half-density surfaces is found to be 50 pc for l between $-0.^{\circ}3$ and $-1.^{\circ}5$ (with R between 50 and 250 pc) and 80 pc between $l = -1.^{\circ}5$ and $-3.^{\circ}0$ (with R between 250 and 500 pc). In the ring it rises to about 200 pc, comparable to the thickness of the H I layer in the outer regions of the Galaxy, up to about 10 kpc. Sanders and Wrixon point out that velocity dispersions greater than 100 km sec^{-1} would be necessary to maintain a disk of such thickness. However, the observed line profiles appear to exclude random velocities of such magnitude, and the authors suggest that the observed thickness may be due to the action of magnetic fields. The amount of atomic hydrogen in the nuclear disk is roughly 4×10^6 $M_\odot$; the *total* gaseous mass contained in it must be at least ten times, and possibly as much as fifty times higher, the additional mass being concentrated in dense molecular clouds (cf Section 5.3). The ring between $R \sim 700$ and ~ 900 pc is inclined to the plane at an angle of 8°, having an average latitude of $+0.^{\circ}9$ at $l = -5^{\circ}$ and $-0.^{\circ}5$ at $l = +5^{\circ}$. The small disk *may* have a similar inclination.

Summarizing this section we conclude that there is fair evidence that the wing of high negative velocity hydrogen at negative longitudes should be interpreted as being due to a rapidly rotating disk rather than to gas expelled from the center.

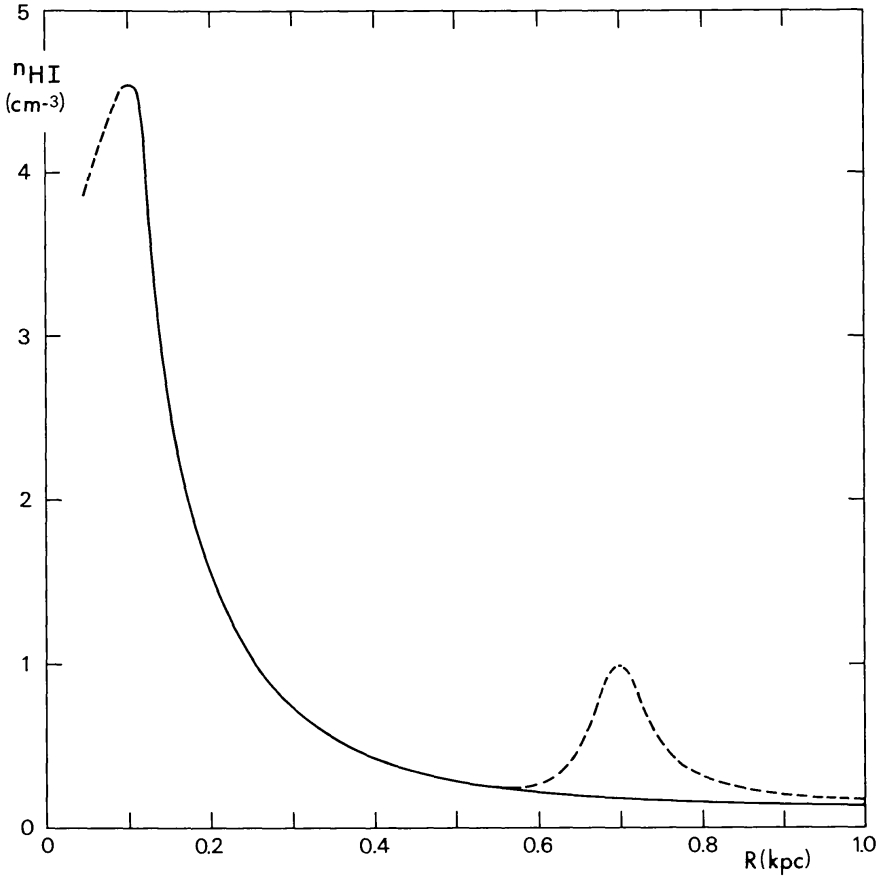

Figure 8 Density of atomic hydrogen in the galactic plane in the model used by Sanders & Wrixon (1973). The dashed secondary hump indicates schematically the ring structure suggested by Rougoor & Oort (1960). Ordinates are numbers of atoms per cm^3.

This interpretation is supported by (*a*) the wing's sharp cutoff at precisely the longitude of the center, and (*b*) the fact that the rotation curve derived from the velocities in the wing corresponds in shape as well as absolute value with what is expected from the 2.2-μ emission in our Galaxy and from the light distribution in the central region of M31. The evidence for the sharp cutoff between $-0.^{\circ}5$ and 0° longitude has been particularly strengthened by the recent very high resolution map made with the Effelsberg telescope by Sanders, Wrixon & Mebold (1977) (Figure 6). These observations may make it possible to find the rotation of the disk from direct measurements down to $R \sim 50$ pc.

Although the model of the rotating disk thus appears plausible, the evidence is not entirely conclusive. In particular, the accumulating evidence for the existence of numerous "expanding" features in the central region must keep us alive to the possibility of an alternative interpretation of the high-velocity wing.

It therefore remains desirable to confirm the gravitational field derived from the disk by data of a different nature, such as can in principle be derived from objects belonging to an old population.[1]

2.5 *Upper Limit to a Compact Mass at the Center*

The existence of various massive expanding features around the center, which is discussed in the following sections, has led to the idea that the Galaxy might contain a massive compact nucleus of unknown nature, possibly a black hole. Such a nucleus might be invisible at optical and infrared wavelengths, and be discoverable only by its gravitational field.

Up to the present the only *direct* source of information on the gravitational field has been the rotation of the nuclear disk, and this could not be measured closer than 50 to 100 pc from the center. The uncertainty at that distance must be at least 10%, corresponding with about $10^8\ M_{\odot}$. This means that we can add an invisible mass of up to $10^8\ M_{\odot}$ at the center without coming into conflict with observations. A specific effort to get as reliable an upper limit as possible to this hypothetical mass has been made by Sanders & Wrixon (1973). This led to the value of $10^8\ M_{\odot}$ mentioned.[1]

2.6 *Possibility of Determining the Gravitational Field from the Density and Velocity Distribution of Population II Objects*

Stars belonging to Population II, which is characterized by a strong concentration to the center and high random velocities, are ideal for an alternative determination of the gravitational field in the central region.

[1] Since this chapter was written the reviewer received extremely important data throwing new light on this problem. Members of the Berkeley team [Wollman et al. (1976), and in particular Wollman (1976)] have determined motions of the ionized gas within 1 pc from the center by observations of the Ne II line at 12.8 μ. These data permit a direct estimate of the mass inside $\sim$0.4 pc, namely $\sim 5 \times 10^6\ M_{\odot}$ (cf Section 6.3.2). If there is a black hole at the center this gives an indication of its mass. If there is no black hole it provides a check on the density distribution in Table 1. Interpolated for $R = 0.4$, this table gives $1.5 \times 10^6\ M_{\odot}$, three times lower than the mass found from the Ne II motions.

Two types of Population II objects can be observed close enough to the center to be of interest, namely planetary nebulae and type IIb OH masers.

Extensive surveys of planetary nebulae by Minkowski (cf Minkowski 1965 for a general description) have clearly brought out their strong concentration towards the center, where, in contrast to their disk distribution through most of the Galaxy, they appear to be distributed nearly isotropically. This is confirmed by the radial velocities, which are known for about 60 nebulae less than 5° from the center. These show no sign of galactic rotation. The distribution is Gaussian, with a dispersion of 125 km sec^{-1}. Although the strong emission lines have enabled investigators to discover these nebulae up to large distances and through considerable amounts of absorption, the absorption close to the center is so strong that between $-5°$ and $+5°$ longitude relatively few have been found closer than 2° from the galactic equator, in the region that is of main interest for the gravitational field. The planetaries in this obscured region *are* discoverable at radio wavelengths, and a search is being made. But owing to their faintness, progress is slow. To obtain a significant accuracy in the determination of the field a considerable extension of the radial velocity data would also be needed.

If the velocity distribution is Maxwellian the gravitational potential Φ can be determined from the following relation

$$\Phi(0)-\Phi(R)=\frac{\log \nu(R)-\log \nu(0)}{\text{Mod disp}^2\, v}, \tag{2}$$

where ν is the space density and v the radial velocity.

For investigating the possibility of a massive nucleus it is essential to obtain observations on objects very close to the center. The minimum distance that can be reached is determined mainly by the space density of the objects used.

An interesting development that promises to provide data of the same kind as are being sought in the planetaries is the recent discovery by B. Baud, H. Habing and others (private communication) that type IIb OH masers in the central region probably share the dynamical characteristics of planetary nebulae, namely a strong concentration towards the center combined with a very large velocity dispersion. These Population II masers can be identified without ambiguity, and their observation provides at once their radial velocity. However, their space density may be too small for a significant test of the field of force near the center.

3 EXPANDING H I FEATURES

Outside the nuclear disk and ring the hydrogen density drops to low values. At our side of the center it only becomes appreciable again when we reach the 3-kpc arm.

This well-defined expanding feature, described on p. 302, has been observed over a galactocentric sector of about 90°. The H I contained in this sector has a mass of $3.6 \times 10^7\ M_\odot$ (Cohen & Davies 1976). The *total* mass is higher because of the presence of H_2, and because some 50% in weight should be added for the helium. From CO observations Bania (1977) has estimated that the H_2 mass is about half that of H I. This leads to a total gaseous mass of about $8 \times 10^7\ M_\odot$ for the observed quadrant of the 3-kpc arm.

It is interesting that the proportion of molecules seems to be much lower in the 3-kpc arm than in the undisturbed medium at similar distances from the center. From Gordon & Burton's (1976) analysis of the CO distribution in the Galaxy the ratio between the column density of H_2 and H I in the general medium around $R = 3$ kpc may be estimated as 3.6 in weight, as against 1.5 in the 3-kpc arm itself.

The second massive feature with a large radial motion, Rougoor's "expanding arm at $+135$ km sec^{-1}," which is situated on the opposite side of the center, is much less regular than the 3-kpc arm. Its H I mass may be estimated at between 1.0 and 1.5×10^7 $M_\odot$, one third, or one half, of that of the 3-kpc arm. Besides these two principal structures there are in the central region a number of smaller features that appear to be similarly moving away from the center. These are discussed in the next section.

Figure 9 gives a sketch of the possible situation of the 3-kpc arm, the expanding arm at $+135$ km sec^{-1}, and the nuclear disk and ring.

Have the radial motions of the 3-kpc arm and the other features been caused by

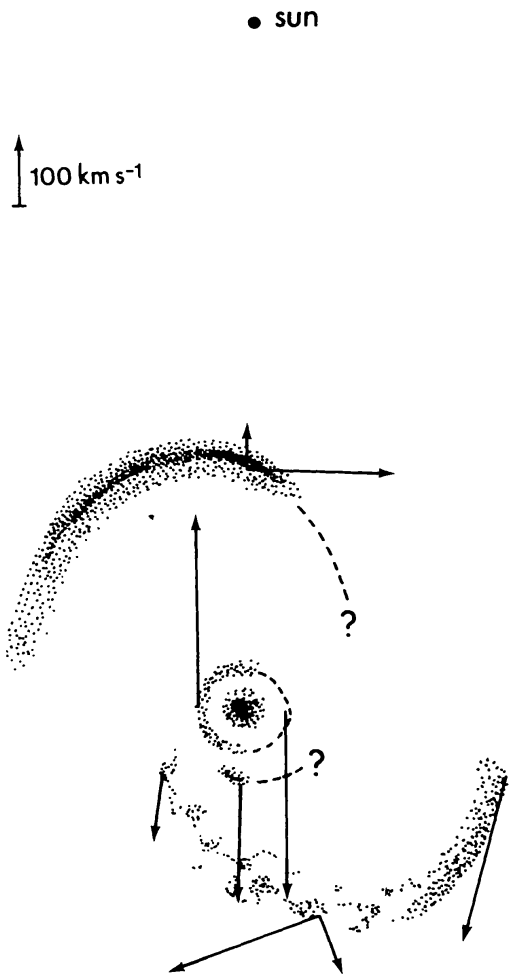

Figure 9 Sketch of the possible situation and motion of the 3-kpc arm, the $+135$ km sec^{-1} expanding arm, and the nuclear disk and ring (Rougoor & Oort 1960).

expulsion of gas from the galactic center, or are they connected with gas accumulated in the region of the inner Lindblad resonance, where highly excentric quasi-steady orbits may exist? The two large expanding arms may lie in such a resonance region. Attempts to represent the general motions within $R \simeq 5$ kpc by a resonance model, or by "dispersion orbits," have been made by Shane (1972) and Simonson & Mader (1973). They have not produced convincing evidence. On the theoretical side no gas-dynamical model has yet been given that bears resemblance to the observed motions. The question therefore remains unanswered.

One difficulty facing all models that ascribe the deviations from circular motion to the gravitational field is the lack of symmetry apparent in the great difference between the expansion velocity of the expanding arm at $+135$ km sec^{-1} and that of the 3-kpc arm, and the equally striking disparity between the entire velocity longitude contours for positive and negative velocities, as shown by Figures 3 and 4. That there is no counterpart of the 3-kpc arm behind the center is shown particularly clearly by CO observations (Bania 1977). Further discussion about the nature of the noncircular motions is postponed to Sections 4 and 5.8.

An apparently very serious obstacle for a gravitational field interpretation is the existence of features outside the galactic plane. The first evidence that H I exists at appreciable latitudes and has motions in a "forbidden" direction (that is, in a direction opposite to that which would correspond to the normal rotation) was found in 1966 by Shane (cf Oort 1968). It was followed by a systematic search by van der Kruit (1970). He observed several features lying distinctly outside the galactic plane and having "forbidden" velocities. At negative longitudes they were found to be situated above the galactic plane, at positive longitudes below it. His conclusion was that the data suggested an ejection of clouds from the nucleus in two roughly opposite directions at a large angle with the plane. The total H I mass of the expanding features lying outside the plane must be about $4 \times 10^6\ M_\odot$ (Cohen & Davies 1976).

Van der Kruit's survey was extended with considerably greater sensitivity to higher negative latitudes by Sanders, Wrixon & Penzias (1972), who used a horn antenna with a beam width of 2°. But by far the most detailed survey was made by Cohen at Jodrell Bank (Cohen 1975, Cohen & Davies 1976). Several new features were found, and already-known features were outlined in much greater detail. A sample of the Jodrell Bank latitude-velocity maps is shown in Figure 10.

Most of the features supposed to be connected with the galactic center are situated within the limits of 5° in l and b of the Jodrell Bank survey or at least pass through this region. Exceptions are the two objects in the last lines of Table 2. One other feature has been found within 10° from the center. It was discovered by Shane as an isolated cloud with a geometrical mean radius of 1° at $l = 8°$, $b = -4°$, and a velocity of -213 km sec^{-1} relative to the LSR (Saraber & Shane 1974). The H I mass is $3 \times 10^4\ M_\odot$ if it lies at the distance of the center. According to the authors it may have been ejected from the galactic nucleus. An unpublished sensitive survey between 349° and 12° longitude, $-10°$ to $+10°$ latitude, where v is between -500 and $+500$ km sec^{-1}, has revealed no other new object of similar or larger size. I am indebted to Dr. Burton for this information.

It is evident that structure and motions in the central region are very complex. Table 2 summarizes data on the more important features having motions deviating strongly from circular orbits. They are arranged in order of their H I mass, shown

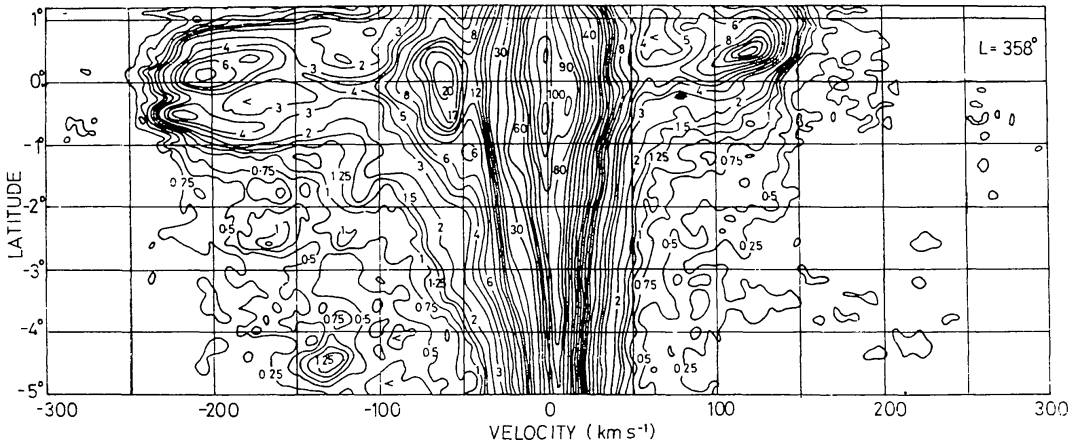

Figure 10 Latitude-velocity contours of H I at $l = 358°$ taken with the Mark IA radio telescope (Cohen 1975). Resolution $13' \times 7.3$ km sec^{-1}. The contours are for antenna temperatures of 0.25, 0.5, 0.75, 1, 1.5, 2, 2.5, 3, 4 K. They should be multiplied by 1.56 to convert to brightness temperatures. Velocities are relative to the LSR. The intense feature on the right is the +135 km sec^{-1} expanding arm, the 3-kpc arm is seen around $b = 0°$, $v = -60$. The powerful feature near $v = -200$ is due to the nuclear disk. The small concentration at $b = -4°.4$, $v = -130$ is feature J1 (see text).

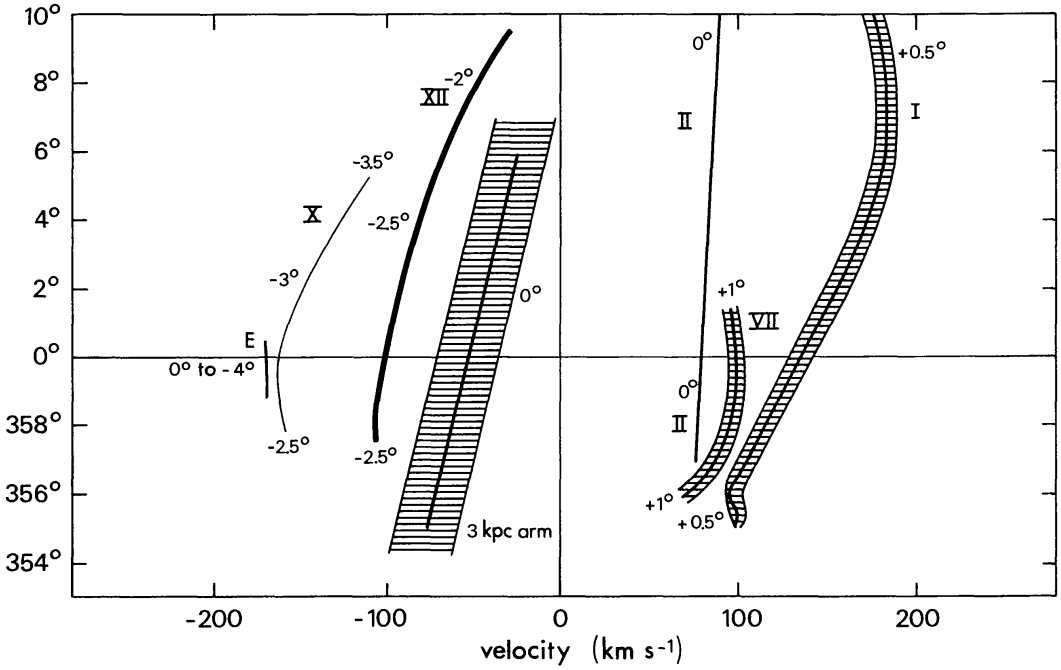

Figure 11 The principal "expanding" features listed in Table 2. Roman numbers refer to the designations by Rougoor, van der Kruit, and Cohen. Small arabic figures indicate average galactic latitudes. Width of the shading or thickness of the curve is roughly proportional to the H I mass per unit interval of l.

in the second column. V_E gives the radial component of the feature's motion at 0° longitude. Negative signs indicate structures on our side, positive signs those on the far side of the center. The next column shows the range in longitude over which the feature is observed. The next to last column gives the mean distance from the galactic plane. All data were taken from the article by Cohen & Davies (1976). For smaller features, not listed in Table 2, reference should be made to Cohen (1975) and Cohen & Davies (1976).

In the last two lines data are given for two features, Cugnon's and Mirabel & Turner's objects (Cugnon 1968, Mirabel & Turner 1972), situated outside the region surveyed by Cohen. Their relation with the galactic center is somewhat uncertain; the second feature is elongated in a radial direction relative to the center.

The situation of the various features in the l/v plane is shown in Figure 11. Figures 12 and 13 show the distribution on the sky of the column density in features XII and VII + J2 respectively.

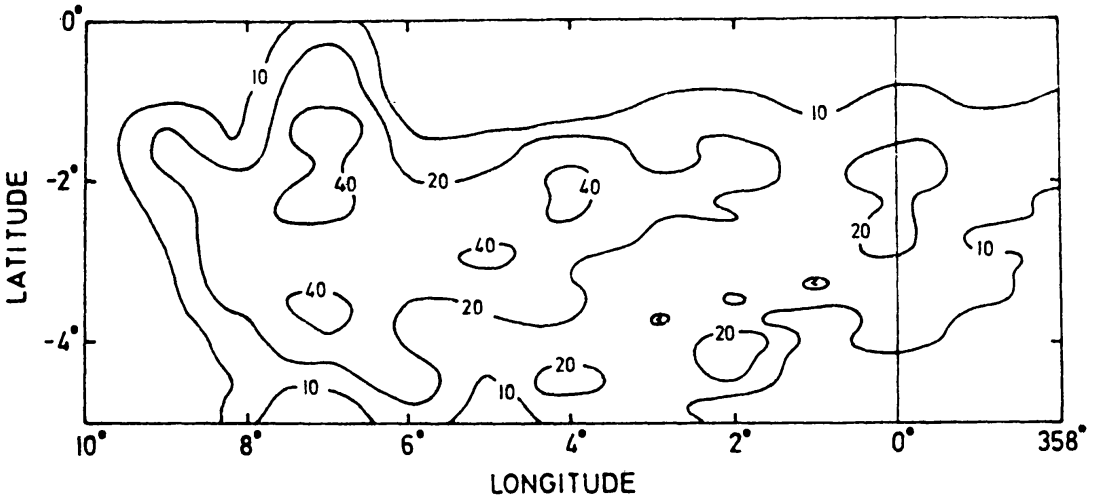

Figure 12 H I column density of van der Kruit's feature XII in units of 10^{19} atoms per cm^2.

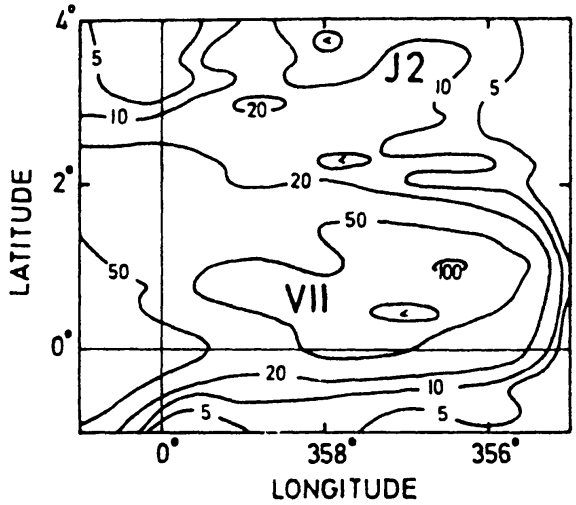

Figure 13 H I column density in units of 10^{19} atoms per cm^2 of features VII and J2.

A general characteristic of most features is that they extend over considerable stretches in longitude. They are apparently parts of rings or arms rather than clouds or jets.

However, the smaller features, E, J1, and J2, may be of a somewhat different nature. E was found by Sanders, Wrixon & Penzias (1972) at $l = 0°$ at a velocity of -170 km sec^{-1}, with a half width of 40–50 km sec^{-1}. It sticks out almost perpendicular to the plane, extending down to $b = -4°$. The authors suggested that it "might be associated with continual high angle expulsion of mass from the nucleus." J1, found by Cohen, is a rather compact cloud centered at $l = 357.°8$, $b = -4.°5$, with a half-width of about 1° in each coordinate and a velocity of -130 km sec^{-1}. It has faint extensions in l, to about 2° on either side (cf Figure 10, and Cohen's Figure 7). The H I mass is $5 \times 10^4\ M_\odot$ if it lies at the distance of the center. J2, similarly found by Cohen, extends from $l \sim 356.°5$ to $\sim 359.°5$ and has a latitude of $+3.°0$. It has a strongly forbidden velocity of $+100$ km sec^{-1}. It is adjacent to, and possibly connected with, feature VII (see Figure 13). Like E it makes a very large angle with the galactic circle. Its H I mass is $3 \times 10^4\ M_\odot$.

In all cases where a feature includes the direction of the center, so that we can see whether or not it absorbs the radiation from Sgr A and thus determine on which side of the center it is situated, the motions are directed away from the center. This applies to four of the six major features listed in Table 2. The two remaining ones are Cugnon's object and van der Kruit's feature XII. If we adopt expulsion as the general cause for all anomalous motions in the central region it is probable that the latter feature is at present likewise moving away from the center. For if it were falling back it would be hard to understand why it has not previously fallen into the disk.

Cohen & Davies (1976) have tried to locate in space all features identified in the central region, in a somewhat similar manner as was done in Figure 9 for the two most important arms. Many have not been observed at their tangent points,

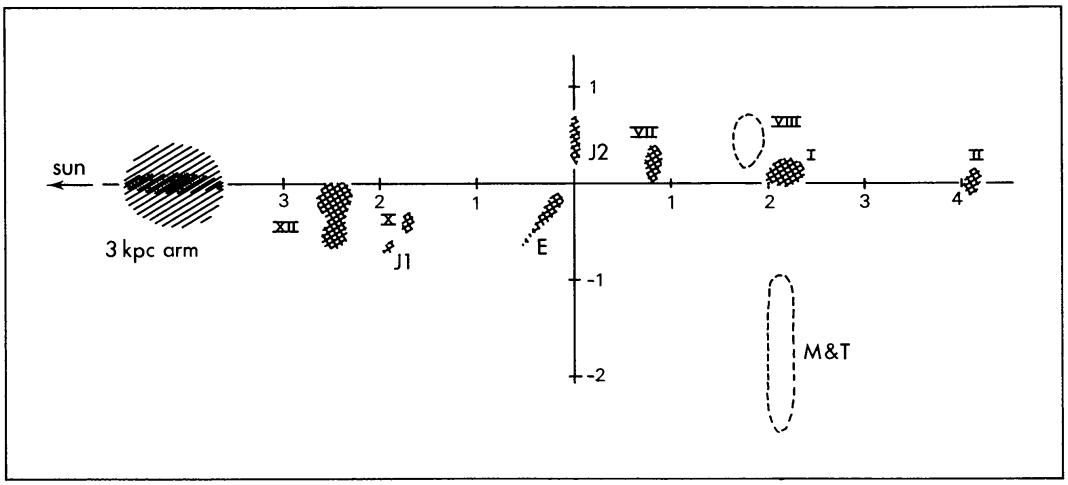

Figure 14 Cross cut perpendicular to the galactic plane through $l = 0°$, schematically indicating the situation of various "expanding" features. Distance scales are in kpc.

so that there is no direct way of estimating their distance from the center. Cohen and Davies determined this distance from the way in which the radial velocity varied with longitude. They assumed that each feature was rotating as well as expanding and that it was lying on a circle. The radius of the circle determined in this way is given under R in the last column of the table. These distances must be considered as quite uncertain, mainly because of the assumption of circular shape. Most features might well be parts of considerably inclined spirals.

It is seen from Table 2 that the majority of the high-velocity arms lie at considerable distance from the galactic plane. This is further illustrated in Figure 14, which gives a schematic cross section at $l = 0°$. The features shown are those in Table 2 plus J1 and J2 mentioned in the text. Cugnon's arm and Mirabel and Turner's feature, which do not extend to $l = 0°$, and whose pertinence to the central region is uncertain, are indicated by dotted contours. It should be stressed again that the distances from the center are mostly uncertain. The distances z from the plane are, however, well determined.

There is reason to believe that at least part of the gas complexes considered owe their large expansional motions and their high z values to ejection of massive clouds from a small nuclear region. Rather direct evidence in support of this thesis is shown by features E and J2, which lie close to the center and point away from it under large angles with the galactic plane.

No recent data on K_z are available, but we can get a sufficient impression of the velocities required to attain the observed distances from the plane from the data in Table 1. Spherical symmetry was assumed in this table; in the actual case the potential differences in the z direction will be higher than in the spherical case for the same distance from the center, so that the velocities cited below, which were computed on the assumption that $\Phi(0)-\Phi(z)$ was equal to $\Phi(0)-\Phi(R)$, will be too low.

From the values of the potential given in Table 1 we find that if there is no friction a body thrown out from the center needs a velocity of 610 km sec^{-1} to reach a maximum distance of 100 pc and 740 km sec^{-1} to get to 500 pc. It is this order of velocity that must have been imparted to gas complexes containing in some cases more than a million solar masses of H I.

We return to this problem and that of the arms in the plane in Section 4 and Section 5.8.

3.1 *Evidence for an Inclination of the Layer of the Expanding H I Complexes*

We have already mentioned that van der Kruit's observations (van der Kruit 1970) indicated clearly that the high-velocity gas near the center is tilted with respect to the galactic equator. At longitudes close to zero the tilt of the layer of forbidden-velocity H I may be quite steep. It is interesting to note that the continuum radiation at a wavelength of 20 cm shows two ridges about 250 pc long and steeply inclined to the galactic equator in the same sense: towards positive b at negative l and towards negative b at positive l (Kerr & Sinclair 1966).

Cohen & Davies' (1976) data fully confirm the tilt. The authors conclude that the

H I within 2.5 kpc of the center forms an inclined layer, with a pole in the direction $l = 124° \pm 28°$, $b = 81° \pm 4°$.

The nuclear disk, with inclusion of its ring, appears to be similarly tilted at an angle of about 6° (R. D. Davies, private communication).

A similar tilt has been observed by Kerr (1968) in the H I, with highest velocities in the *permitted* direction. Integrating in each point over the highest 70 km sec^{-1} he finds column densities as plotted in Figure 15. The tilt appears to extend to $l = 345°$ and $l = 8°$ on the two sides of the center, with average z values of $+100$ and -60 pc respectively. Near the center the angle is about 8°. Kerr suggests that the gas concerned forms a central bar structure which at its outer end might connect up with the 3-kpc arm. However, the evidence for a bar is not convincing.

4 ORIGIN OF THE RADIAL MOTIONS AND THE DEVIATIONS FROM THE GALACTIC PLANE

4.1 *Introduction*

In the twenty years that have elapsed since the discovery of the 3-kpc arm no essential progress has been made toward answering the central question of whether its large deviation from circular motion is connected with a large-scale deviation from axial symmetry in the Galaxy's gravitational field ("the field model") or whether it is due to expulsion of gas from the nucleus ("the ejection model").

Great progress has, however, been made on the *observational* side, in three main directions: (*a*) the identification of other "expanding arms"; (*b*) the discovery in the central region of H I features at considerable distance from the galactic plane,

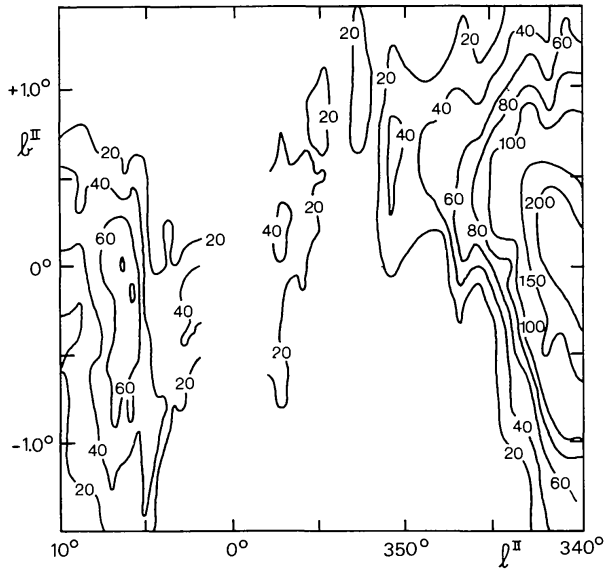

Figure 15 Integrated brightness temperature for atomic hydrogen of highest velocities. For $l > 0°$ the interval over which b^{II} has been integrated extends over the highest 70 km sec^{-1}, for $l < 0°$ it extends also over 70 km sec^{-1}, the lower limit being the lowest velocity observed at each position (Kerr 1968). Note the expanded latitude scale.

some of them quite large and massive; (*c*) the observation of numerous dense molecular clouds in the nuclear disk, mostly with considerable velocity components in radial direction relative to the center.

For these molecular clouds an expulsive origin seems indicated, notwithstanding the severe difficulty presented by their large masses. Similarly, for the jet-like H I features E and J2, which seem to point away from the center and extend to about 700 pc, an ejective origin is strongly suggested. But there are no such directly suggestive circumstances for the bulk of the H I features.

In connection with the confrontation of the two hypotheses two things should be stressed. The first is that violent activity leading to the expulsion of discrete masses of gas at high velocity is apparently of rather common occurrence in the nuclei of massive galaxies. It may be estimated that at least 10% of the spiral galaxies with masses of the order of that of our Galaxy are in a very active Seyfert stage, in which large discrete "clouds" are being continually thrown out from the nucleus at velocities of the order of 1000 km sec^{-1}. Unfortunately we have no sufficient information concerning the total masses of gas that are expelled during a Seyfert stage, so that we cannot make a quantitative confrontation with the phenomena observed in our Galaxy. That in some cases the expelled mass must be quite large is shown by the filaments around NGC 1275.

It is quite possible that the Seyfert stage is intermittent, and that most large spirals pass through active periods that in total might make up on the order of a tenth of their lives.

Another type, or possibly, another stage, of activity is observed in NGC 4258. The strong synchrotron emission of this spiral and especially the remarkable structure of the synchrotron arms has been interpreted as being due to the ejection of clouds with a combined mass of about 10^8 $M_\odot$ and velocities of the order of 1000 km sec^{-1} into two opposite cones at a small angle with the equatorial plane (cf van der Kruit, Oort & Mathewson 1972, van der Kruit 1974, van Albada & Shane 1975, de Bruyn 1977). The case of NGC 4258, which does not seem to be unique, indicates that anisotropic expulsions involving masses of the same order as those of the largest expanding H I features in the Galaxy *can* occur in ordinary spirals. It should be mentioned that at present the nucleus of our Galaxy is in a quiescent stage, showing no resemblance to a Seyfert nucleus. It is interesting that the nucleus of NGC 4258, notwithstanding the enormous activity it must have had in the recent past, shows only moderate activity at the present time.

There is a third nearby galaxy that displays still another type of gigantic nuclear activity, namely NGC 5128. Plasma clouds thrown out in directions roughly perpendicular to the equatorial plane have created a giant radio galaxy. The total energy content in the form of relativistic particles and magnetic fields is at least 2×10^{59} erg.

The second thing to be stressed is that to be acceptable, a theory of the expanding features must also account for the conservation of the nuclear disk.

For the discussion of "field" models a detailed study of the central regions of barred spirals would be desirable. This would, however, go beyond the scope of the present review. But attention may be drawn to the possible existence of mini-bars

in the centers of spirals that are not classified as barred systems. Such small bars have been suggested as mechanisms to activate spiral waves. Attention should also be drawn to the fact that in several of the nearby spiral galaxies small dust arms are seen to spiral in close to the nucleus (cf Sandage 1961), which might indicate a nonaxisymmetric field.

4.2 *Some Expulsion Models*

An attempt to explain the outward motion of the 3-kpc arm and the $+135$ km sec^{-1} expanding arm was made by van der Kruit (1971). His observations of H I outside the galactic plane having suggested that this gas had been expelled from the nuclear region, it appeared natural to inquire whether the large expanding arms *in* the plane could not likewise have received their outward momentum from gas expelled at an angle with the plane, thereby avoiding the destruction of the nuclear disk. He supposed that the ejection took place in two opposite directions, rotating fast around the axis of the Galaxy so that all galactocentric longitudes were covered during the period of expulsion. The ejection should have consisted of a large number of small clouds and was presumably triggered in a small core. Before leaving the nuclear disk the clouds would have swept up disk gas and acquired some angular momentum. Van der Kruit assumed that the clouds would have emerged from the disk around $R = 100$ pc, and that beyond this distance they moved under the sole influence of the gravitational field until coming down again into the gas layer at $R \sim 3$ kpc. They were then rapidly braked by friction, transferring their momentum to the gas in the layer.

Figure 16 gives an impression of the orbits followed by clouds starting with a velocity of 625 km sec^{-1} at $R = 0.1$ kpc under various angles i with the galactic plane. The forces were computed from the Schmidt model, amended in the central region by adding an inhomogeneous central spheroid in order to represent the rotation of the nuclear disk.

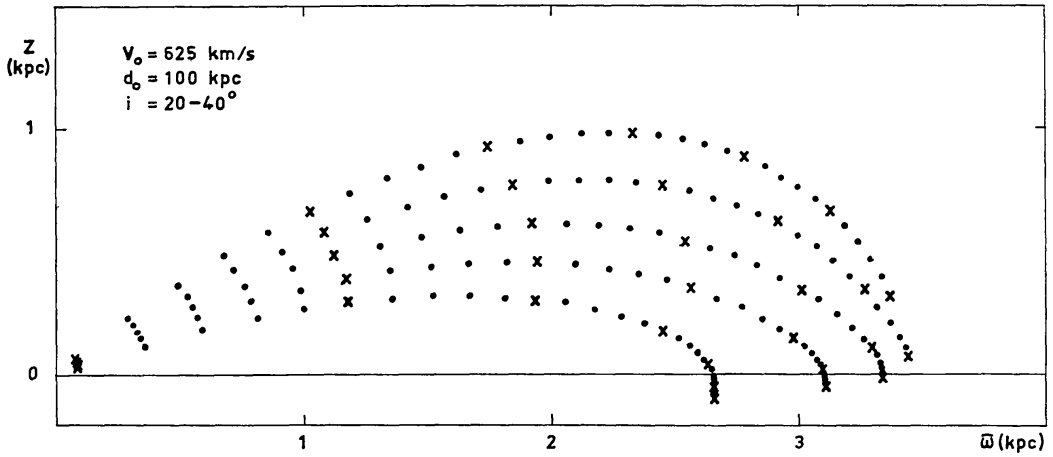

Figure 16 Orbits of gas clouds for an expulsion velocity of 625 km sec^{-1} and inclinations $i = 20$, 25, 30, 35, and 40°. Time interval between dots 5×10^5 yr, between crosses 2.5×10^6 yr (van der Kruit 1971).

According to van der Kruit's calculation the outward motion of the 3-kpc arm may have been caused by an ejection some twelve million years ago of gas clouds with a total mass between five and ten million solar masses, which would have started with a velocity of 600–650 km sec^{-1} at $R = 100$ pc under an angle of 25°–30° with the galactic plane. Similar numbers would be required to produce the motion of the $+135$ km sec^{-1} expanding arm.

The ejection of the massive features observed *outside* the galactic plane was thought to have occurred some six million years ago.

A different attempt to explain the motion of the 3-kpc arm by an ejection process was made by Sanders & Prendergast (1974). They considered the gas-dynamic effect of an isotropic explosion on the normal gas layer and found that a radially oscillating ring of cold gas is produced. In order to get such a ring at the location of the 3-kpc arm the explosion of a central mass of the order of 10^8 $M_\odot$ with a total explosion energy in the order of 10^{58} ergs is required. The arm would oscillate back and forth for a considerable time, estimated as perhaps 10^8 years. During such a period the nuclear disk, which was destroyed by the explosion, might have been restored by the normal mass loss of evolving stars. The principal difficulty is the size of the initial mass which has to be exploded.

4.3 *The Gravitational Field Hypothesis*

We are confronted with two problems: (*a*) the radial motions, and (*b*) the systematic deviations from the galactic plane.

While the first might be attributed to a systematic deviation from axial symmetry in the mass distribution, the second requires that the mass distribution in the center is inclined to the galactic plane. Without such a tilted distribution the field model could hardly produce the Z velocities of the order of 500 km sec^{-1} required to take hydrogen masses up to the observed distances of ~ 300 pc from the galactic plane.

In the central region the only important contributors to the mass density are old Population II stars with high random velocities. It is for these that one would have to assume a tilted distribution.

That such a situation should not be dismissed a priori is indicated by two phenomena: in the first place by the large angles that are often seen between the minor axes of elliptical radio galaxies and their radio axes, and in the second place by the structure of the core of the Andromeda nebula. The circumstance that in double radio galaxies, which also have components close to the nucleus, the latter lie generally in the same direction as the outer components suggests that this direction may be parallel to the rotation axis of the compact nucleus from which the radio emission presumably originates, and that therefore this axis often differs considerably from that of the E galaxy as a whole. As the nucleus is likely to be generically related to the galaxy's inner region its tilt may be an indication that the rotation axis of this inner mass may likewise make an angle with the axis of the main mass of the galaxy.

The stratoscope II observations of M31 (Light, Danielson & Schwarzschild 1974) suggest that its distinctly flattened nucleus is somewhat tilted relative to the major

axis of the main system. The nucleus has a radius of roughly 3 pc. Because of its importance for the present discussion I reproduce in Figure 17 the contour map given by Light et al. for the central 3″ (or 9 pc) of M31, in which I have indicated the direction of the major axis of the entire galaxy. From ellipses fitted to the contours the authors find that on the average these have a roughly 25° larger position angle. A disturbing feature is the somewhat asymmetrical position of the brightest region; this may indicate that the contours are affected by absorption effects.

A somewhat smaller tilt in the same direction had previously been observed by H. M. Johnson (1961). Lindblad (1956) has pointed to a similar small deviation in the isophotes between 300 and 1500 pc radius which he, however, interpreted as being due to a central bar lying in the equatorial plane.

The color and spectrum of the nucleus is identical with that of the surrounding "nuclear bulge." Both consist mainly of later-type stars, and may be assumed to reflect the mass distribution.

If the tilt is confirmed by observations at longer wavelengths it would indicate that the plane of symmetry near the center of a galaxy can be appreciably tipped with respect to the general equatorial plane. This would evidently be a discovery of fundamental significance.

It is possible that the H I features outside the galactic plane in the center of our own Galaxy indicate that *its* central plane of symmetry is similarly tilted, at an angle of perhaps 10°. In that case part of the anomalous features could be naturally understood on the basis of the field hypothesis. There would, of course, remain the need for a nonaxially symmetric mass distribution to explain the large radial motions.

A considerable amount of work has been done to explain the observed motions by dynamical models without the aid of an explosion (see, for instance, Sanders &

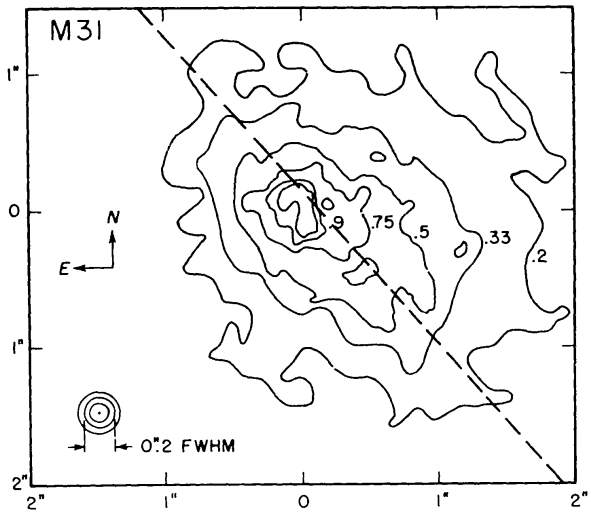

Figure 17 Contour map of the nucleus of M31. The levels are labeled by the fraction of peak intensity. (Light, Danielson & Schwarzschild 1974.)

Huntley 1976), but it has not yet proved possible to construct a plausible model that reproduces the observed structures and motions in a convincing way.

Peters (1975) has tried to represent the H I velocity longitude diagram for the central region by gas moving in concentric elliptical orbits with axial ratios of about 0.5. He suggested that such orbits might be sustained by a bar-like perturbation, but no quantitative dynamical foundation was given.

4.4 *Ejection or Gravitational Field?*

We close this section by summarizing the main difficulties encountered by either model.

4.4.1 PROBLEMS WITH THE EXPULSION HYPOTHESIS The most serious problem is the vastness of the mass that has to be expelled. Van der Kruit estimated that a quantity of H I of between 0.5 and 1.0×10^7 $M_\odot$ would have had to be expelled to give the 3-kpc arm its outward velocity. Cohen's high-sensitivity survey has increased the H I mass of the 3-kpc arm by a factor of 1.8. If one includes the hydrogen in molecular form as well as the helium the total gaseous mass becomes a factor of 4 higher than that considered by van der Kruit. The resulting amount of gas to be expelled would then become approximately 3×10^7 $M_\odot$. This is for a collimated ejection; an isotropic ejection would require some five times more. The ejection took place roughly ten million years ago. Averaged over such a period the mass loss from the region within $R = 50$ pc would be of the order of 10 $M_\odot$ per year. Such a quantity cannot be replenished by evolving stars. Normal evolution of the stars within $R = 100$ pc would yield no more than 0.0004 $M_\odot$ per year (cf van der Kruit, Oort & Mathewson 1972). Even including all stars within 500 pc would yield but 0.004 $M_\odot$, so that it would take 10^{10} years to produce the gas needed for the outward momentum of the 3-kpc arm to be caused by expulsion. The expulsion hypothesis can for these massive features only be maintained if the central region is replenished by infalling material. The rate of infall would then have to be at least two orders of magnitude higher than that indicated by the high velocity complexes in the vicinity of the Sun. Alternatively one might consider the possibility that there is a mechanism (provided perhaps by a massive black hole) that would disintegrate stars at a much faster rate than normal evolution (cf also p. 343).

The collimation assumed by van der Kruit forms another problem. It is possible, however, that the collimation is only apparent, and is in reality an effect of selection, i.e., the clouds expelled under small inclinations may be stopped in the disk and transformed into molecular clouds, while those with very large inclinations might not have become dense enough to be observable.

The nucleus today shows nothing like the degree of violence that should have existed in order to eject such high-velocity features as listed in Table 2. The turbulent ionized gas seen in the nucleus is negligible in quantity as well as velocity compared to what is needed for such ejections (see Section 6). For the expulsion theory to be acceptable one must suppose that a radical change in the activity of the nucleus has taken place in the past ten million years.

4.4.2 PROBLEMS FOR THE GRAVITATIONAL FIELD HYPOTHESIS It is difficult to see how a field due to probably well-mixed stars with high random velocities could produce jet-shaped features, like E and J2 of Table 2, pointing away from the center under a very large angle with the galactic plane. It seems equally difficult to construct a field that could have imparted to the numerous dense molecular clouds observed in the nuclear disk their considerable velocities without at the same time systematically affecting the H I in the disk. But in particular it is hard to conceive that the recently confirmed, almost complete ring of molecular clouds, which has a radius of 190 pc and is expanding at a velocity of 150 km sec^{-1} (cf Section 5.5), was produced by an asymmetry in the field.

Whether it is possible or impossible for the field model to explain the large H I features outside the plane depends entirely on whether or not the central mass distribution can be tilted. And even if it *is* tilted there would still remain, beside E and J2 already mentioned, a number of other features, for instance X and J5 of Cohen's survey, which would lie so far outside the tilted plane as to require some ejection or infall mechanism to explain them.

4.4.3 CONCLUSION The molecular clouds in the nuclear disk and some of the highly inclined H I features near the center have probably been formed by ejection. For the large H I features at 1 kpc and farther we do not know. For these we may have to revert to the hypothesis of a tilted bar structure. For both hypotheses the actual driving mechanism has until today remained hidden. The problem is reconsidered in Section 5.8 in connection with the molecular clouds.

4.5 *The Disk's Magnetic Field*

The large differential rotation in the nuclear disk tends to increase the magnetic field strength on a short time scale. It is conceivable that it would become sufficiently strong to affect appreciably the motion of the gas. The problem has been discussed by Sanders & Wrixon (1973) in connection with the thickness of the disk. They noted that a velocity dispersion of about 100 km sec^{-1} would be needed to maintain the observed z distribution of the H I. So high a dispersion seems incompatible with the structure observed in the plane. According to the authors the largest dispersion permitted by these latter observations is 24 km sec^{-1}. They concluded that either cosmic-ray pressure or magnetic pressure contribute primarily to the support of the disk. If it is magnetic pressure a field on the order of 20 μG would be required. Sanders and Wrixon suggest that by the wrapping in the disk the field strength is increased to a "quasi-static equilibrium value, where further increase is prevented by loops of force rising out of the plane and dragging some neutral gas along. This might also account for the high-velocity features outside of the plane near the center."

A limiting factor is the brightness temperature of the nonthermal radio emission from the disk region. If the density of cosmic ray electrons in this region is comparable to that in the solar neighborhood the maximum permissible field strength would be on the order of 10^{-5} G. Such a strength would be quite insufficient to throw out massive gas streams at velocities of several hundred km sec^{-1}, as would be required for most of the features listed in Table 2.

5 MOLECULAR CLOUDS AND TOTAL GAS DENSITY

5.1 *Introduction*

Inward from about 4 kpc the interstellar density decreases considerably and remains low until we reach the edge of the nuclear disk at $R \sim 750$ pc. This low-density region is the domain of the "expanding" H I features discussed in Section 3. In the nuclear disk the "expanding" regime changes again into a more orderly state in which the H I motions seem to be practically circular. But at a few hundred parsecs from the center a third radical change occurs. The density increases strongly, and the hydrogen is almost entirely in the molecular state and is mostly concentrated in massive and dense conglomerations whose motions deviate widely from the rotation of the nuclear disk described in Section 2. The conglomerations are further characterized by very large internal velocity dispersions. They lie close to the galactic plane and are quite thin in the z-direction (20 or 30 pc).

The knowledge of this inner region has come mainly from observations of interstellar molecules, especially hydroxyl, formaldehyde, and carbon monoxide. The most compelling evidence on the great abundance of molecular hydrogen and on the large masses of the nuclear aggregates has been provided by CO.

5.2 *Total Gas Density Derived from Carbon Monoxide Observations*

CO is observed in emission in the $J = 1 \rightarrow 0$ rotational transition at a wavelength of 2.6 mm. It occurs largely in dense cool clouds where it is shielded from dissociation by ultraviolet radiation, and it is excited through collisions. In order to populate the upper level of the 2.6-mm transition with a Boltzmann distribution corresponding to the excitation temperatures of about 15 K found from the observed emission profiles, particle densities of the order of 10^3 cm^{-3} are required. As the density of hydrogen atoms is far too small the only particles that can be sufficiently numerous to excite the CO are hydrogen molecules.

Minimum cloud masses have been estimated from these considerations. Such estimates are, however, quite uncertain, because the cloud agglomerations considered are probably very inhomogeneous, and it is impossible to determine "filling factors."

The mass estimates given in the following are based on the intensities of the CO emission. If a feature is optically thin in the CO line and the distribution over the levels concerned is "thermalized," the total number of CO molecules per cm^2 can be directly computed from the measured surface brightness. A practical difficulty is that all the more important features in the central region have a large optical thickness in the ^{12}CO line, and that at the time of writing of this report measurements of the fainter ^{13}CO line are still scarce: they are limited to the Sgr B2 complex (cf Section 5.7) and some small other regions. Solomon et al. (1972) as well as Liszt et al. (1975) measured ^{12}CO to ^{13}CO ratios in a small part of the +40 km sec^{-1} feature near the galactic center. For the integrated profile the latter found an average ratio of about 7. The former observed considerable variation of the ratio with velocity, with extreme values of $\sim$5 to $\sim$18. As the terrestrial abundance

ratio of the two carbon isotopes is 89, these measurements may give an impression of the degree of saturation of the ^{12}CO line. However, other investigators have argued that the clouds might *not* always be optically thick (cf Leung & Liszt 1976). A summarizing discussion of the problem has been given by Gordon & Burton (1976).

Most observations have been made in the ^{12}CO line. In their large survey of CO in the Galaxy Gordon & Burton (1976) use the following semi-empirical formula to derive the column density of CO per cm^2

$$N(CO) = 3.43 \times 10^{14} \frac{^{12}CO}{^{13}CO} \int T^*(^{12}CO)\, dv = 1.6 \times 10^{16} \int T^*(^{12}CO)\, dv, \qquad (3)$$

where T^* is the antenna temperature corrected for antenna and atmospheric losses, and v is in km sec^{-1}. For the abundance ratio $^{12}CO/^{13}CO$ they adopt a value of 40 suggested by Wannier et al. (1976).

In order to find total hydrogen masses we must know two other things, namely, 1. the relative number of the carbon atoms that have been condensed onto solid particles, and 2. the abundance ratio of H to C.

1. From a comparison of the CO emission and the optical extinction of a dust cloud, Milman (1975) has found an upper limit of 0.1 for the fraction of carbon in the form of CO, while on theoretical grounds Leung & Liszt (1976) also found 0.1. In most mass estimates a 10% value has been adopted, but this should be considered with very great reserve. Gordon & Burton also use this fraction. Assuming a carbon abundance of 1:3000 they thus arrive at a ratio $n(CO):n(H_2)$ of 6×10^{-5}. The same ratio was used by Bania (1977) in his investigation of the molecular clouds near the center.

The uncertainty in the fraction of the C that has not condensed onto solid particles introduces a great uncertainty in the mass estimates of the molecular clouds. In particular it is questionable whether the fraction derived from observations in the neighborhood of the Sun is also applicable to the cloud complexes near the center, which have formed and evolved under rather different conditions. There are, indeed, indications that the absorption in the central region is considerably less than what would be expected from the high column densities of gas derived by Bania on the assumption that only 10% of the carbon atoms would be in CO. Using formula (3) and the ratio $n(CO)/n(H_2)$ given above, we find from Figure 21 in the central 2 or 3° a column density of 8×10^{23} hydrogen atoms per cm^2. If the dust-to-gas ratio, or the ratio between the number of H atoms and the visual extinction, were the same as that near the Sun, this column density would correspond to a visual extinction of roughly 300^m, roughly half of which might lie in front of the center. From photometric measures at various wavelengths in the infrared Willner (PhD thesis, 1976) quotes a visual extinction of about 28^m in front of the central sources. The general extinction in the galactic disk is probably between 10 and 15^m, leaving only about 15^m for the extinction in the dense central region, which differs by a factor of ten from the above estimate from the CO observations. This may indicate that in the region of the molecular clouds near

the center a much larger fraction of carbon is in gaseous state than the 10% found from observations near the Sun.

An independent estimate of the gas-to-dust ratio may be obtained from measurements of the surface brightness in the mm range, such as have been made by Westbrook et al. (1976) in Sgr B2. From the flux at 1 mm combined with the temperature determined from the far-infrared spectrum they derive the column density of the dust particles in g cm^{-3}. As, with normal abundances, about 1/1000 of the hydrogen can condense onto solid particles, an estimate of the mass of the solid particles will yield also an estimate of the total gaseous mass. In this way the authors found a hydrogen mass of 10^5 $M_\odot$ for the central 1′ of Sgr B2. A comparison with the core mass of 6×10^5 estimated by Scoville, Solomon & Penzias (1975) from CO observations indicates again that the assumption that only 10% of the carbon is in CO, on which the latter estimate is based, may not apply in the central region.

2. An analogous problem is presented by the general abundance of C and O. All published mass estimates rest on the assumption that the abundances are the same as those in the Sun and its surroundings, namely $n(\mathrm{H})/n(\mathrm{C}) \sim 3 \times 10^3$. However, since there is considerable evidence that the abundance of at least some heavier elements, such as O and N, is an order of magnitude higher in the nuclear region of spirals than in the outer parts, the published mass estimates of molecular features in the central region may also on this account be too high.

In view of the above arguments it seems that recent mass estimates of molecular clouds in the central region may be an order of magnitude too high. In the following parts of this section two mass estimates for the hydrogen will therefore be given: (*a*) that of the authors, and (*r*) a ten times lower value. In the reviewer's opinion the second may be closer to the truth.

Notwithstanding these various uncertainties, important information can be obtained on the general molecular density in the Galaxy, and in particular on the very high density in the nuclear region. The most complete general survey to date is that of Gordon & Burton (1976), who observed from $l = 10°$ to 36° with a sampling interval of 0°.2, and over some samples at higher longitudes. They found that the fraction of molecular hydrogen increases gradually towards the center. While in the surroundings of the Sun the masses of atomic and molecular hydrogen in a column perpendicular to the galactic plane are roughly the same, between 2 and 6 kpc from the center the mass of atomic hydrogen diminishes to about one fifth of that of the molecular component. In the nuclear disk it is still smaller, while in the innermost two or three hundred parsecs it seems to become almost negligible.

The total gas density has a maximum between $R \sim 4$ and ~ 7 kpc; it drops sharply inside 4.0 kpc, and between 2 and 4 kpc the density per column perpendicular to the galactic plane is only about four tenths of that between 4 and 6 kpc. The entire region between roughly 1 and 4 kpc is remarkably devoid of gas. It is not known what causes this. It may be that the gas has been used up by more intensive star formation which might, for instance, be caused by the increase of the angular

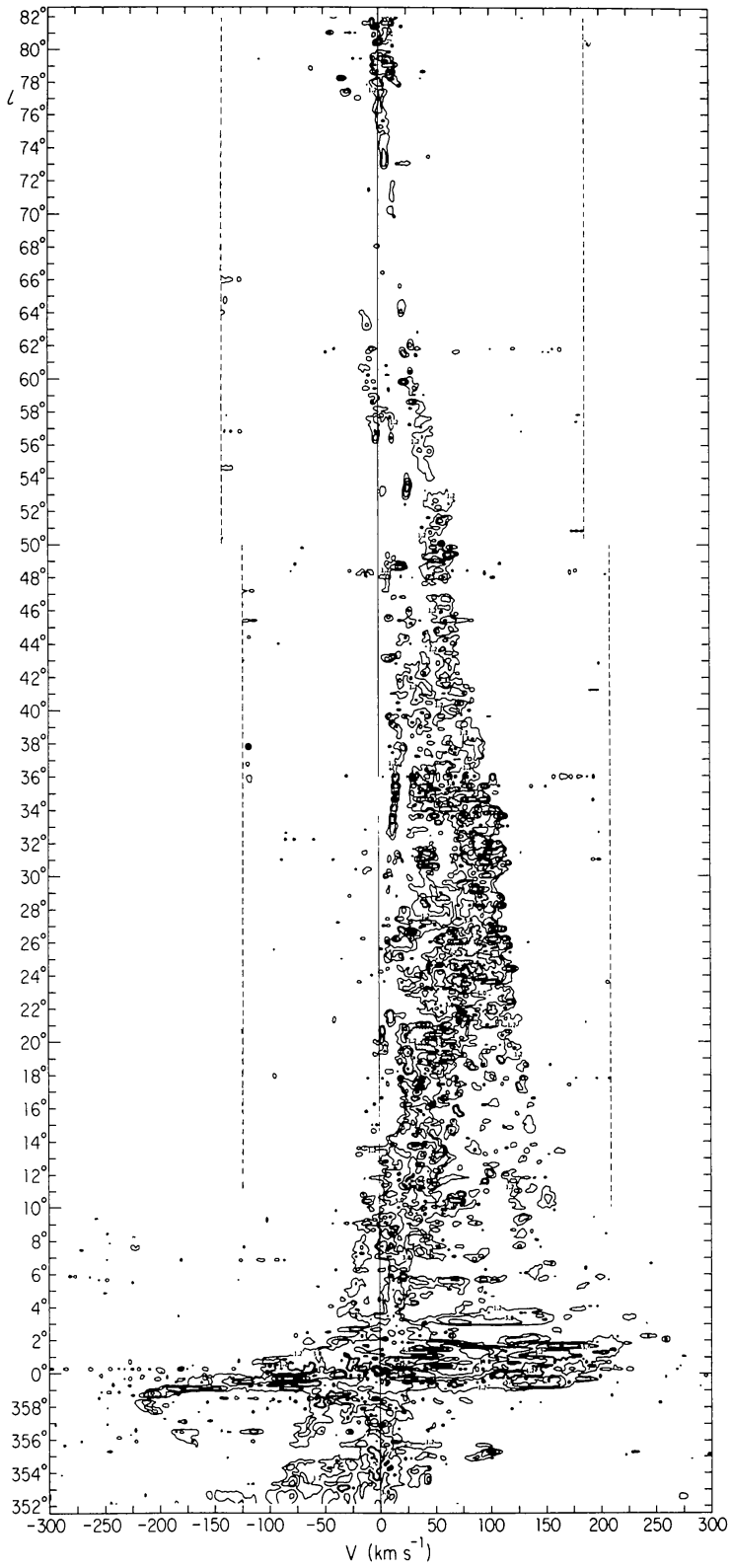

Figure 18 Distribution of CO in longitude and velocity at $b = 0°$ from $-8°$ to $+82°$ longitude, from observations with the 11 m NRAO telescope on Kitt Peak. Beam width 65″. (Burton & Gordon 1977 for $l > 10°$; Bania 1977 for $l \leqq 10°$.)

velocity towards the center and the consequent greater frequency with which the gas meets the spiral pattern (cf Oort 1974a; Segalovitz 1975); or, alternatively, the gas may have been swept away by expanding arms.

The gradual increase in molecular density from $l = 85°$ to $l = 21°$ and the sharp rise within 4° from the center may be illustrated by Figure 18, which gives the ^{12}CO intensity as a function of v and l. An instructive complement to this figure is shown in Figure 1 of Gordon & Burton (1976), which gives an l/v contour diagram between $l = 36°$ and 10°, beautifully illustrating the cloudy structure of the CO, as well as the remarkably sharp velocity cutoff around 110 km sec^{-1} between $l = 36°$ and 21°.

Two things stand out in Figure 18 as well as in Gordon & Burton's Figure 1: the high intensity and very large velocity spread between $l = +4°$ and $-4°$ and the absence of velocities larger than about $+60$ km sec^{-1} between $l = 21°$ and 4°. This absence reflects the general lack of gas between $R = 800$ and 3500 pc; the lower velocity CO observed in this longitude range lies outside 4 kpc. The large velocity dispersion at $|l| < 4°$ is due in part to the rotation of the nuclear disk, and for an equally important part to features with large noncircular motions. The latter are similar to what has been found in H I. However, the observations of the molecules have made it possible to study these motions in greater detail and nearer to the center.

5.3 *Distribution and Motions of Molecules in the Nuclear Disk. CO Observations*

The first somewhat complete survey of CO emission from the central region was made by Scoville, Solomon & Jefferts (1974), who gave an instructive longitude velocity contour diagram at $b = 0°$. Recently these observations have been greatly extended by Bania (1977) and by Liszt et al. (1977), with a much finer grid and at various latitudes. The observations at $b = 0$ are illustrated in Figures 19 and 20. In the part within $|l| = 1°$, from Liszt et al., the latitude is $-2'45''$ and the longitudes are counted from the galactic center position at $l = -3'20''$, $b = -2'45''$. Observations were also made at other latitudes, up to 12′ (35 pc). No important new features appeared in these, but they indicate the thinness of the CO layer: the half-width of the main part appears to be between 30 and 40 pc.

Although there is some CO emission over the entire extent of the H I nuclear disk, the high-intensity radiation is limited to the interval from roughly $l = -1.°5$ to $+2.°0$. The strength of this concentration is illustrated in Figure 21, showing the intensity integrated over all velocities as a function of l. Tentatively we infer from these data that the molecular clouds are almost wholly concentrated in a region within $R \simeq 250$ pc. From this figure Bania estimated the total H_2 mass within $R = 300$ pc at (*a*) $3.5 \times 10^8\ M_\odot$; the alternative value (*r*) is $3.5 \times 10^7\ M_\odot$ (see p. 325).

The broad strip of low-velocity emission in Figure 19 is from gas outside the central region. At $v \sim -50$ km sec^{-1} the 3-kpc arm is visible in emission as well as absorption. Absorption is also observed in the low-velocity gas. Evidently there must be clouds of extremely low temperature.

The strongest emission is very asymmetrical relative to the center, by far the greatest part lying at positive longitudes. Within this large region of high intensity

two concentrations may be noted: one around 0′ longitude and one around 45′. Both extend over about 15′ (40 pc) in longitude as well as in latitude, and comprise a wide range of velocities, from about 0 to 80 km sec^{-1} for the first, and 40 to 100 for the second. The first has been referred to as the +40 km sec^{-1} cloud, or as the Sgr A complex; it may, or may not, be connected with the nuclear source of the Galaxy. The second contains the unique H II region Sgr B2; we shall therefore refer to it as the Sgr B2 complex. It is possible that it has a weak counterpart on the opposite side of the center, around $l = -30'$, $v = -100$ km sec^{-1}. Around $v = +25$ and $v = +90$ there appear to be "bridges" between the Sgr A and Sgr B2 complexes.

All of this gas has velocities in the direction of galactic rotation, but its average radial velocity is much smaller than would be expected on the basis of the rotation curve discussed in Section 2.4 for clouds with circular motion around the center. If we accept the rotation curve derived from the H I observations, we must conclude that the CO clouds have very large systematic deviations from circular motion. The low radial velocity cannot be explained by situating them far from the "sub-

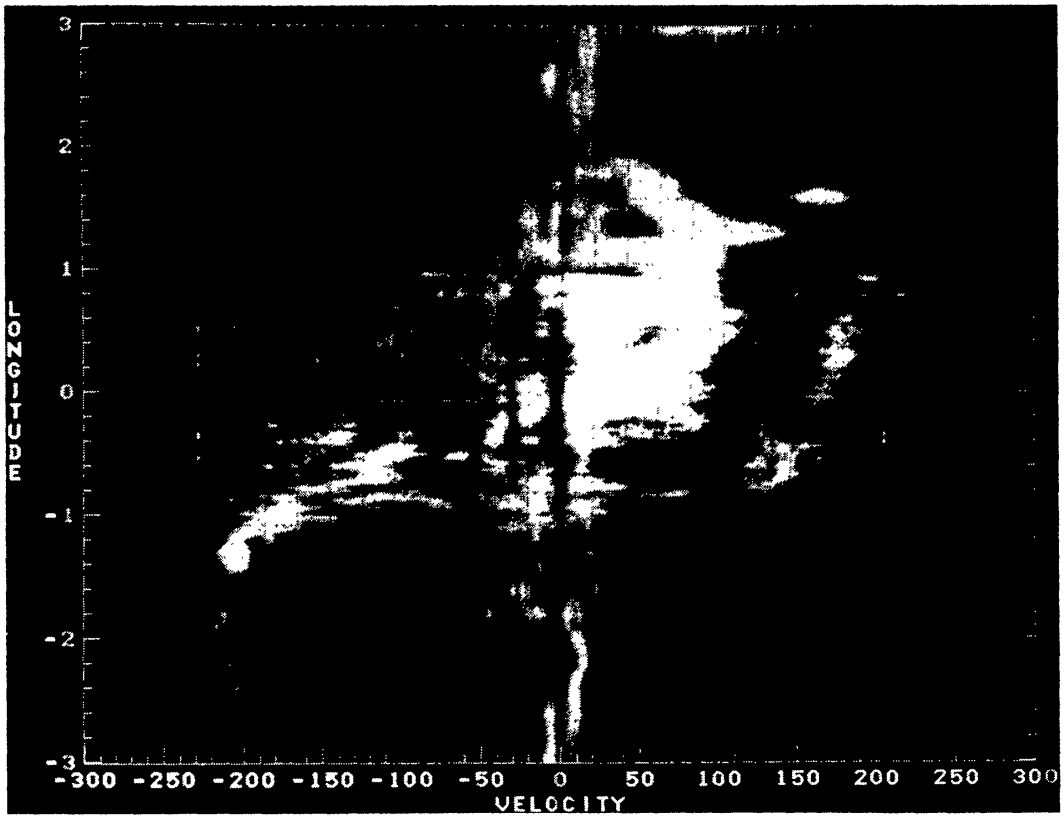

Figure 19 CO distribution in l and v at $b = 0°$ between $-3°$ and $+3°$ longitude, from observations with the 11 m NRAO telescope on Kitt Peak. Beam width 65″. Spacings 12′ between $|l| = 2°$ and 3°, 6′ between 1° and 2°, 2′ for $|l-3'|$ between 10′ and 60′, and 1′ for $|l-3'| < 10'$. The part between 359° and 1° is from a study by Liszt et al. (1977). (Bania 1977).

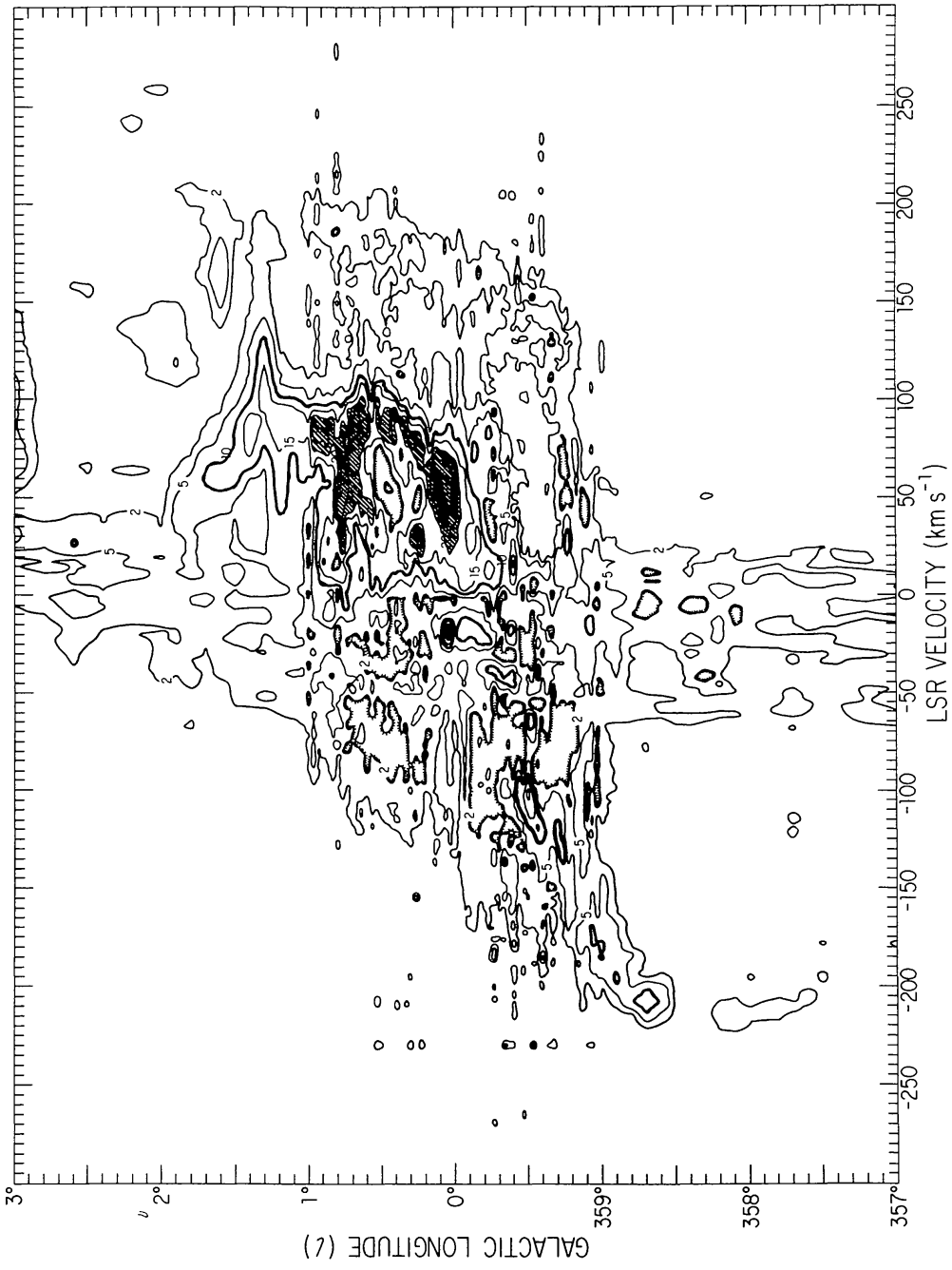

Figure 20 Longitude velocity contour map of ^{12}CO emission at $b = 0$ from the same data as Figure 19. Contour levels are drawn at $T^* = 2, 5, 10, 15, 20, 25, 30$ K. Heavy line: 10 K contour; hatched areas are above 20 K; black is above 30 K.

central points" because, as we have argued above, they must in all likelihood lie within about 250 pc from the center.

The most remarkable features in Figure 19 are the almost straight ribbons at large negative as well as large positive velocities, extending from $l = -50'$ to $l = +60'$. At $l = 0$ their velocities are -125 and $+165$ km sec^{-1}, respectively. From evidence to be discussed below it is clear that the -125 km sec^{-1} feature lies on our side of the center, while the $+165$ km sec^{-1} ribbon lies behind it. Both features are thus moving away from the center. Their slopes in the v/l diagrams indicate that they have also transverse velocities. These are in the direction of the galactic rotation, but lower by factors of ~ 4 and ~ 8 respectively than the circular velocities at $R \sim 200$ pc.

A feature at $l \sim 3°.2$, $v \sim 50$ to 150 km sec^{-1} merits special mention because of its high intensity and remarkably large spread in velocity. It might be connected

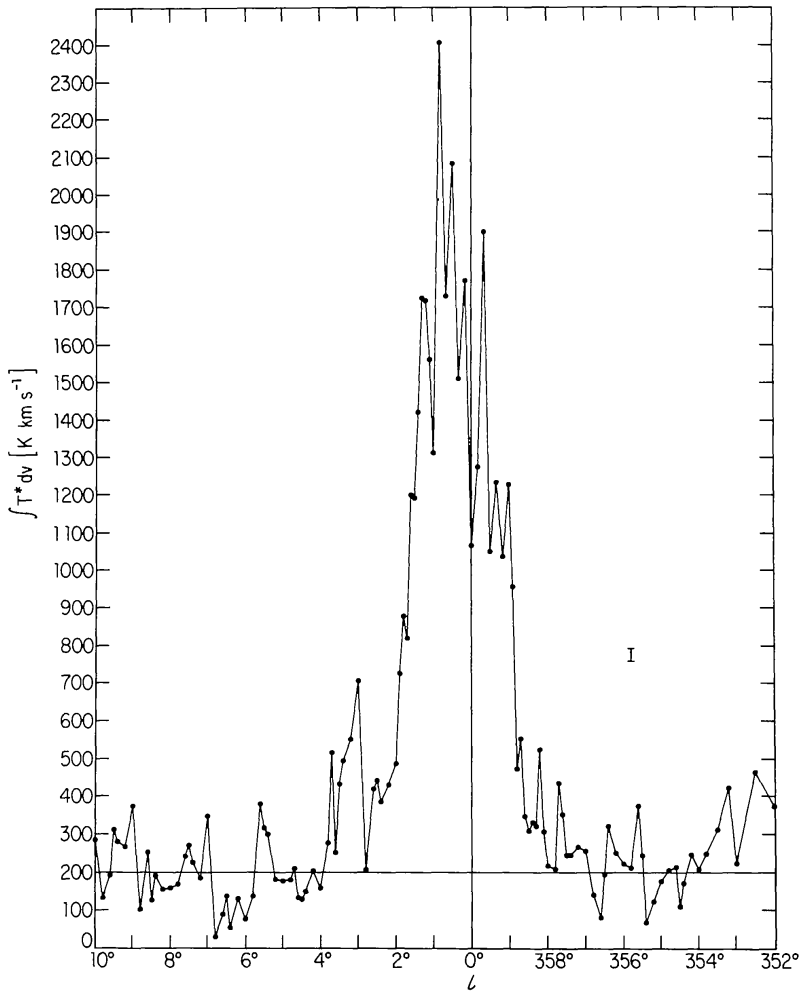

Figure 21 CO emission at $b = 0'$ integrated over all velocities as a function of galactic longitude. Ordinates are $\int T^* dv$, T^* being proportional to the antenna temperature (see text) (Bania 1977).

with the large 100-μ infrared source at the same position. Half of it is visible at the upper edge of Figure 19.

5.4 *Distribution and Motions of Molecules in the Nuclear Disk. OH and H_2CO Observations*

Figure 22 shows the absorption spectrum of Sgr A in OH (full drawn curve) and H I (dashed curve) (Bolton et al. 1964). There are two extremely deep and wide absorption bands in the OH radiation, centered on the velocities of the -125 km sec^{-1} feature and the $+40$ km sec^{-1} complex discussed above in connection with the CO observations. The fact that they are here seen in absorption proves that they must lie in front of Sgr A, or at least of an important part of Sgr A. Their great widths in velocity are probably due to the fact that they consist of various fairly large clouds or sheets with different velocities rather than to the velocity dispersion of a swarm of compact cloudlets. For, as Scoville, Solomon & Penzias (1975) have remarked in their discussion of Sgr B2, the great depths of the absorption lines are hard to explain unless the "clouds" would at each velocity cover the entire

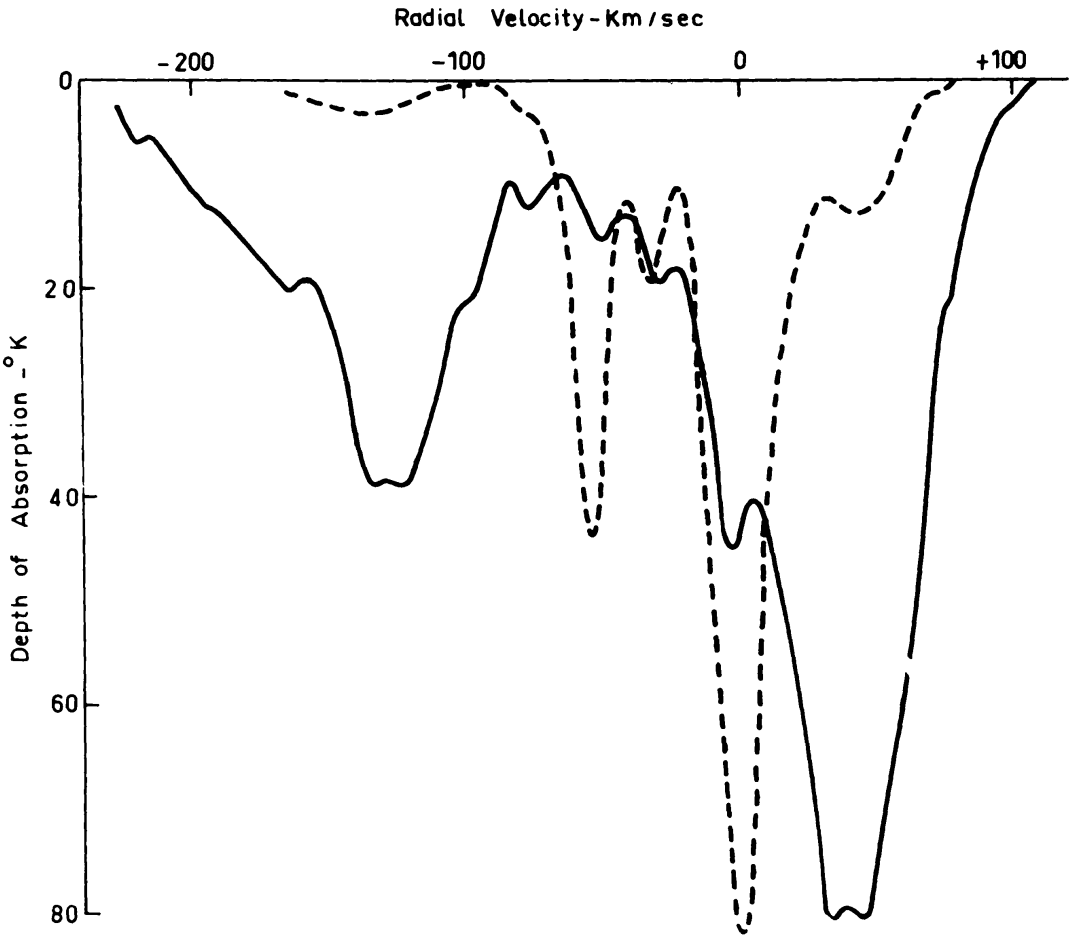

Figure 22 Absorption profile of Sgr A observed with the Parkes telescope (Bolton et al. 1964). Full curve: OH; dashed curve: H I.

continuum source. To effect this with randomly moving small clouds would require such large numbers that they would collide on a time scale short compared to the presumable ages of the features concerned. The wide dispersion has been observed equally in H I and formaldehyde in the $+40$ km sec^{-1} feature. From the extensive observations of H I, OH, and H_2CO made by Sandqvist (1970) with the 40-m Green Bank telescope at high-velocity resolution, the half power width of the $+40$ km sec^{-1} feature may be estimated at 50 km sec^{-1}. The -130 km sec^{-1} band in OH gives 48 km sec^{-1}.

The great difference between the dashed and continuous curves in Figure 22 illustrates once more the enormous concentration of molecules relative to H I in these features close to the center. There is relatively little OH absorption at zero velocity, illustrating on one hand that the molecules in the 10-kpc path between the Sun and the center are relatively scarce and on the other hand that the molecular gas *within* the central region is largely, if not entirely, concentrated in complexes with large radial motions.

It is also interesting to compare the conditions in the 3-kpc arm at -53 km sec^{-1} with those in the two arms in the nuclear region. Figure 22 shows that in the former the opacity in OH is considerably smaller than that in H I. In the two nuclear arms the optical depth of OH is clearly very much *larger* than the H I optical depth, so that the abundance of H I relative to that of OH must be much smaller than in the 3-kpc arm.

The first and most extensive observations of molecular clouds in the central region were of hydroxyl (Bolton et al. 1964; Robinson & McGee 1970; McGee et al. 1970). They were made in its absorption line at a wavelength of 18 cm. Strong absorption was found between $-1°$ and $+2°$ longitude. According to Robinson (1974), weaker absorption can be traced to $l \simeq 4°$, but notwithstanding considerable searching none has been found between $-1.°5$ and $-3°$. The absorptions as measured in the brightness temperature depend on the brightness of the background. Because of the very large variation of this background in the central region they do not give anything like a representative picture of the quantity of the absorbing gas. To a certain extent this can be remedied by plotting what has been called the apparent opacity defined as $\tau_a = -T_{\text{line}}/T_c$, where T_{line} is the temperature measured in the line relative to that outside, and T_c is the temperature of the source behind the cloud, supposed to be high compared with the excitation temperature of the line.

Figure 23 gives a contour diagram at $b = 0°$ of the apparent opacity of the 1667 MHz OH line as measured recently in Jodrell Bank (Cohen & Few 1976). The 1665 line was also measured, and gives a full confirmation of the 1667 results. Striking features are the row of "clouds" at high negative velocity between $l \sim \pm 1.°0$, the $+40$ km sec^{-1} complex at $l = 0°$, and the concentration of dense features between $l \sim 0.°5$ and $2°$ and $v \sim -50$ to $+100$ km sec^{-1}.

The contour diagram of the 6-cm absorption line of H_2CO (Figure 24) shows the same features, and in addition, the 3-kpc arm. The observations, which give the apparent opacity at $b = -12'$, are due to Scoville & Solomon (1973). The beam width is 6.'6.

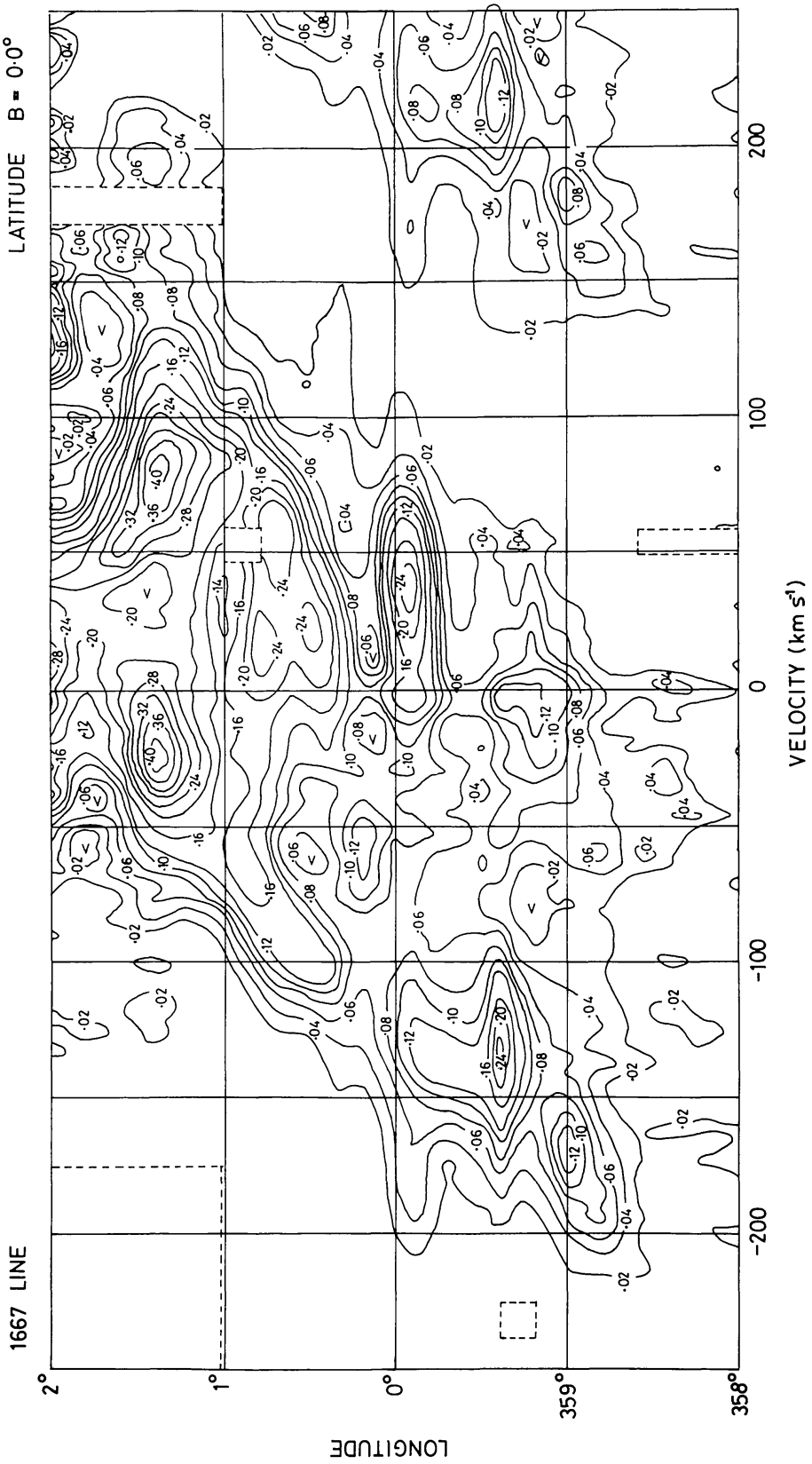

Figure 23 Longitude velocity map of apparent opacity of the 1667 MHz line of OH at $b = 0°.0$ from observations with the Jodrell Bank Mark I telescope. The wing on the right-hand side is due to the 1665 MHz line; the real velocities for this wing are 350 km sec^{-1} lower than indicated at the bottom. The half power beam width is 11′, the velocity resolution 6.1 km sec^{-1} (Cohen & Few 1976).

The string of negative-velocity clouds seen in both pictures coincides essentially with the negative-velocity feature of the CO emission. The fact that it is seen in absorption against the continuous radiation of the central radio sources over the entire longitude range from 359°.0 to 1°.4 shows that it lies in front of these, and is moving outward. In Figure 23, which extends to sufficiently high positive velocities, no trace is seen of the +165 km sec^{-1} feature. This holds for both the 1667 MHz and the 1665 MHz line: within 1° from the center there is no absorption above +100 km sec^{-1}. It is thus evident that the +165 km sec^{-1} feature lies behind all the brighter continuum sources, including Sgr B2, and that it is moving outward.

5.5 *The Expanding Molecular Ring*

It has been suggested by various authors (Kaifu, Kato & Iguchi 1972 from OH observations, Scoville 1972 from H_2CO data) that the string of negative-velocity clouds would form part of an expanding ring around the center. The suggested locus of such a ring is sketched in the full-drawn curve in Figure 24. The ring would have a radius of about 250 pc, an expansion velocity of ~140 km sec^{-1}, and a rotation of 50 km sec^{-1}. The velocity half-width is estimated at 41 km sec^{-1} by Cohen & Few (1976), who give a column density of 8×10^{15} T_s OH molecules per cm^2 (where T_s is the excitation temperature in °K, which is probably around

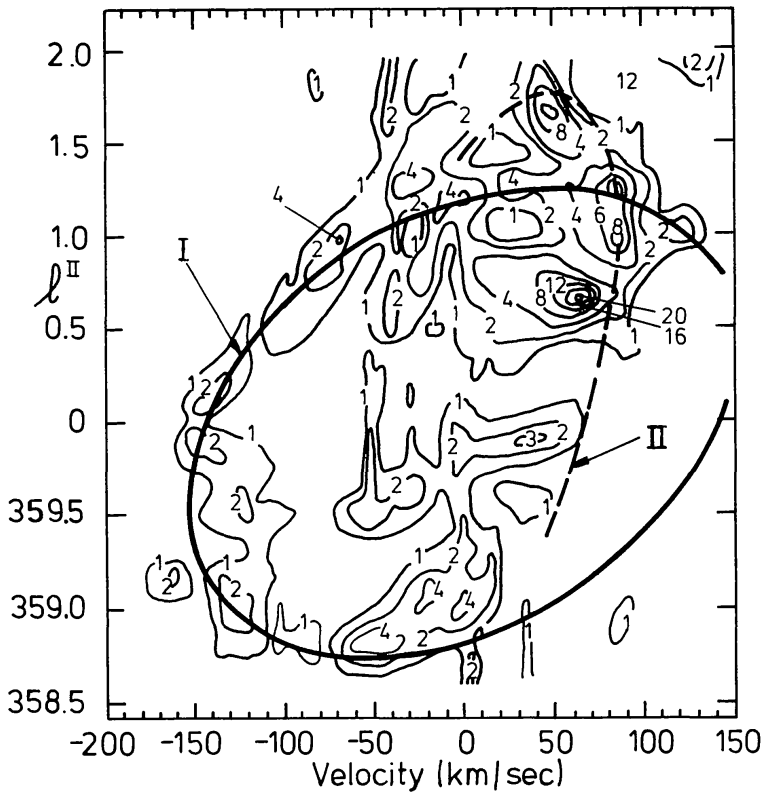

Figure 24 Contours of apparent H_2CO absorption averaged for $b = -2'$ and $-12'$. Beam width 6'.6, velocity resolution 1.6 km sec^{-1}, 6' grid in l (Scoville & Solomon 1973). Full curve: locus of expanding molecular ring as suggested by Scoville (1972).

15 K). The mighty Sgr B2 complex might belong to the "ring." But its most convincing part is the string of negative velocities. In the OH and H_2CO data there is no good evidence for the existence of the opposite half. The half that *is* observed is interesting enough, in showing that the mechanism which has produced these apparently "expanding" cloud complexes must have worked in a coordinated manner over a sector of about 180°. It is therefore unlikely that it would be connected with supernova explosions.

That there is no evidence in the OH and H_2CO absorption for the existence of the opposite half may be due to the fact that this would lie behind the majority of the continuum sources. The earlier CO observations did not show clear evidence for either the front or the rear side of the hypothetical ring, no doubt partly due to the fact that the front side is centered about 6′ below the galactic plane. However, as described in Section 5.3, the recent more complete observations by Liszt et al. at $b = -2'45''$ (Figure 19) show clearly the more or less continuous ribbon at negative velocities as well as a very similar ribbon at high positive velocities. It is tempting to believe that these two features have resulted from one explosive event, and show the "ring" in a somewhat more complete form. Bania (1977) has approximated the features by a ring of radius 190 pc, expanding at an average velocity of 150 km sec^{-1} and rotating with a velocity of 65 km sec^{-1}. The observed emission is somewhat asymmetrical, the positive velocity side having a 20 km sec^{-1} higher expansion velocity than the average of 150 km sec^{-1}, while the negative velocity side has a 20 km sec^{-1} lower expansion velocity than the average, but such asymmetries are to be expected in expulsive phenomena, especially since there must have been considerable interaction with ambient gas. In this case they are all the more probable in view of the glaring asymmetry in longitude of the denser CO at smaller velocity. Because of its greater completeness Bania's model of the ring appears preferable to that derived earlier from the OH and H_2CO observations.

Atomic hydrogen in the ring has been observed by Cohen (1977). From a comparison of the observed profile with emission profiles he found an average excitation temperature $T_s = 92$ K. The cool molecular clouds are therefore embedded in a much hotter H I medium. This medium has a thickness in the z direction of about twice that of the molecules.

In the same article Cohen has given data illustrating the systematic increase of the ratio of the optical thickness of OH and H_2CO to that of H I with decreasing distance from the center. With optical thicknesses integrated over all velocities the ratio changes by more than a hundred between $R = 10$ kpc and the nuclear region.

5.6 *The +40 km sec^{-1} Feature*

Of the two wide absorption bands in the spectrum of Sgr A, one has been interpreted as being caused by the expanding ring discussed in the preceding section. The other, though resembling the first in its width (both have a half-width of roughly 50 km sec^{-1}), appears to be connected with a rather different object. Contrary to the ring the +40 km sec^{-1} feature is strongly concentrated in a small region, near the direction of the center. As may be seen in Figure 20 it contains

Table 3 Observations of the $+40$ km sec^{-1} feature near Sagittarius A

Gas	Authors	Region		Method	Beam
		l	b		
HI	Sandqvist (1970, 1973, 1974)	6′ diam.		lunar occ.	40″ × 70″
HI	Schwarz, Shaver & Ekers (1977)	8′ diam.		ap. synth.	25″ × 120″
OH	Sandqvist (1970, 1973, 1974)	6′ diam.		lunar occ.	40″ × 70″
OH	Bieging (1976)	10′ diam.		ap. synth.	3.′25
H_2CO	Sandqvist (1970, 1973, 1974)	6′ diam.		lunar occ.	40″ × 70″
H_2CO	Gardner & Whiteoak (1970)	359° to 1°	0′ to -12′	pencil beam	4′
H_2CO	Scoville, Solomon & Thaddeus (1972)	359.°4 to 2.°2	-2′	pencil beam	6′
H_2CO	Scoville & Solomon (1973)	358.°5 to 1.°0	-2′, -12′	pencil beam	6′
H_2CO	Fomalont & Weliachew (1973)	5′ diam.		ap. synth.	40″ × 120″
H_2CO	Whiteoak, Rogstad & Lockhart (1974)	4′ diam.		ap. synth.	20″ × 40″
CO	Solomon et al. (1972)	359.°7 to 2.°8	-2′	1′ to 2′ grid	1′
CO	Sanders & Wrixon (1974)	-10′ to $+10$′	0′	1′ grid	1′
CO	Liszt, Sanders & Burton (1975)	-4′ to 0′	-5′ to -2′	1′ grid	1′
CO	Liszt et al. (1977)	-60′ to $+60$′	-7′ to $+1$′	1′ to 5′ grid	1′
CO	Bania (1977)	352° to $+10$°[a]	0′	6′ grid	1′
HCN	Fukui et al. (1977)	~ -12′ to $+24$′	~ -10′ to $+8$′	2′ grid	2′

[a] For the part between 359° and 1° the data were taken from Liszt et al. (1977). The 6′ grid quoted is for $|l|$ between 1.°0 and 2.°0; for the remainder of the survey it was 12′.

the strongest CO emission observed anywhere in the central region. It has therefore been generally thought that it might be connected with the nucleus, and has consequently been the subject of numerous investigations, an overview of which is given in Table 3.

The center of the feature, as inferred from Figure 20, lies practically at $l = 0'$. At $+40$ km sec^{-1} it has a half-width of about 15′ (45 pc) in l. It extends from $\sim +25$ to $\sim +75$ km sec^{-1} in velocity. Between $+70$ and $+100$ km sec^{-1} a sort of bridge connects it with the other main concentration of CO, which lies around Sgr B2, at $l \sim 0.^{\circ}7$.

A rough outline of the "cloud" can also be obtained from the absorption data, cf Cohen & Few (1976) (Figure 23), Sandqvist (1974), and Bieging (1976) (Figure 25). From the latter we find the OH extending over an area of half-widths of about 12′ in l and 6′ in b, centered at $l \sim -3'$, $b \sim -6'$; the longitude coincides with that of the galactic center, the latitude is 3′ below it.

All maps that have sufficient resolution show that there is considerable internal structure. This is seen very clearly in the high resolution charts of Whiteoak, Rogstadt & Lockhart (1974). These authors pointed out that the most extensive absorption is found in the vicinity of the eastern component of the central radio source (Sgr A East), while no absorption is seen against Sgr A West (which is supposed to be the real nucleus of the Galaxy; see Section 6). This has been taken as an indication that the main part lies behind the nucleus, and may have been expelled, as tentatively sketched in Figure 26, in which it has been supposed that

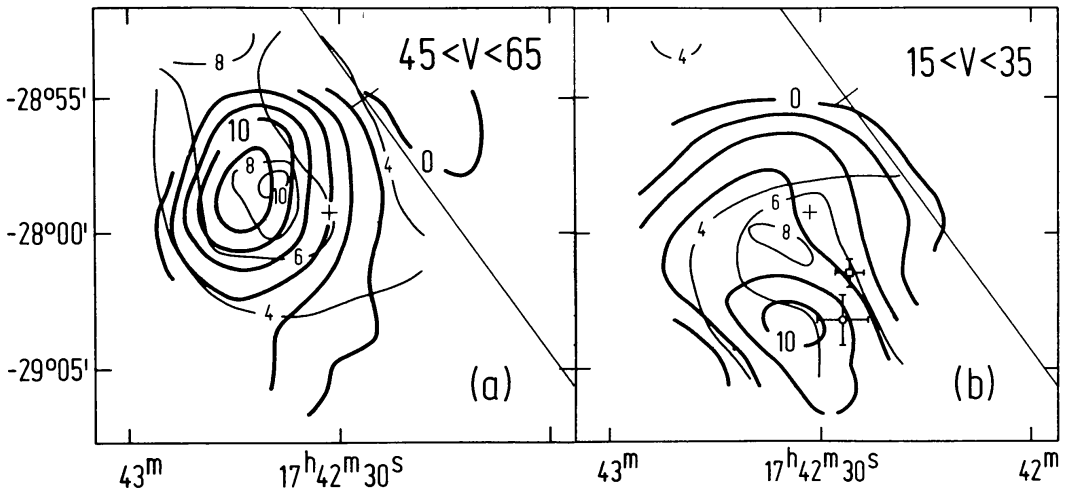

Figure 25 (*a*) Comparison of OH and CO distributions in the direction of Sgr A, integrated over the velocity range 45 to 65 km sec^{-1}. *Bold contours:* $N(\mathrm{OH})T_s$ in units of 3.2×10^{14} cm^{-2} K^{-1}. *Light contours:* ^{12}CO peak line antenna temperature in K, from Solomon et al. (1972). The cross marks the 1.67 GHz continuum peak. The straight line is the galactic equator, on which zero longitude has been marked. (*b*) As for Figure 25a, for the velocity range 15 to 35 km sec^{-1}. Positions, with error bars, of peak emission from 2 mm H_2CO and 12 mm NH_3 lines are indicated by the open square and circle, respectively (Bieging 1976).

Sgr A East lies behind the center. It should be emphasized, however, that the distribution of the H_2CO as indicated by Whiteoak et al. is quite irregular, and shows large variation in optical depth and in velocity over the 4′ field they surveyed. The small absorption in the direction of the Western component might well be accidental, and cannot therefore be taken as a proof that the object lies *behind* Sgr A West.

The alternative is that the $+40$ km sec^{-1} gas lies in front of both central sources and is moving towards them. Some investigators have suggested that it is part of an extended positive velocity mass covering a large sector of the central region, and that the coincidence of the dense concentration with the position of the central source is purely accidental. However, such a model is contradicted by what we know about the gas between $+70$ and $+100$ km sec^{-1} that forms the bridge with Sgr B2, and by the high-velocity part of Sgr B2 itself. This gas, which the CO observations show to be quite dense, is all but invisible in the OH and H_2CO absorption maps; it must therefore be situated behind all the continuum sources in this sector, and must be moving away from the central region, just like the ring at $+165$ km sec^{-1}.

Considering the evidence presently available it appears probable that the $+40$ km sec^{-1} cloud is actually related with the center and that it may have been expelled. The fact that no specific peculiarities are observed at the center itself may be because the molecules have formed only at some distance from the explosive source.

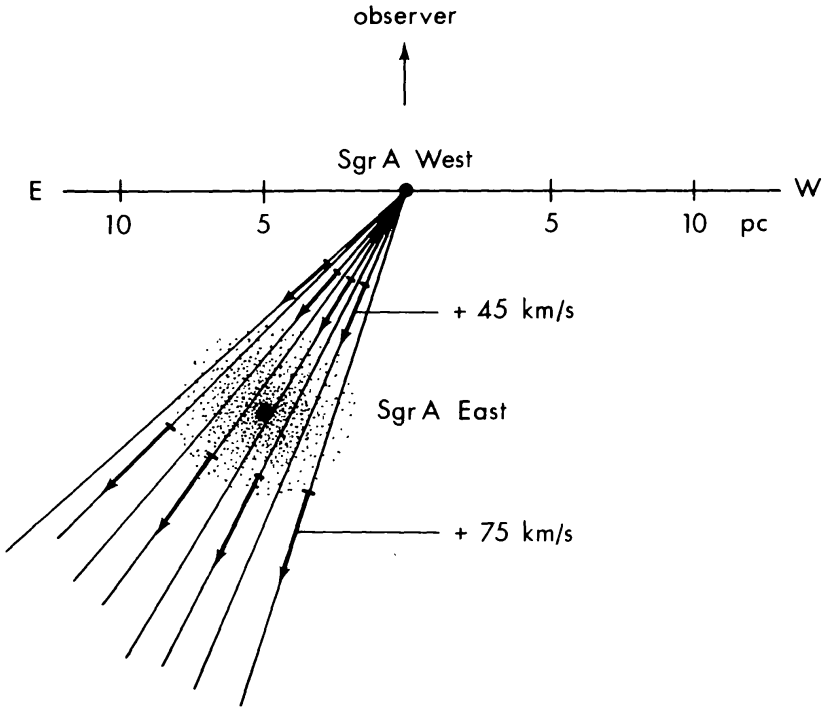

Figure 26 Possible situation of the gas showing CO emission between $+25$ and $+90$ km sec^{-1}, and seen in absorption in OH and H_2CO between $+30$ and $+70$ km sec^{-1} (Oort 1974b).

We now return to the structural and dynamical properties of the feature. The structures found by Whiteoak et al. have typical dimensions of $2' \times 1'$. Liszt, Sanders & Burton (1975) found striking differences in intensity and velocity structure on scales of $1'$ in l and b. The velocities are high on the Eastern and higher longitude side, and low in the opposite part. A similar tendency may be seen in Figure 25. This may indicate that the feature is rotating, in the same sense as the galactic rotation, but more slowly than the circular velocities in the central part of the nuclear disk (Table 1). Alternatively, the velocity differences might have been caused by asymmetries in the expulsion process.

Interesting new observations have been made in the hydrogen cyanide emission line at 3.4 mm by Fukui et al. (1977) at the Tokyo Observatory. The contours of maximum antenna temperatures in Figure 27 show an elongated structure, with the half-intensity contour extending over roughly $16'$ in longitude and about $5'$ in latitude. The authors point to the fan shape of the outer contours; they believe that their observations support the ejection hypothesis.

All anomalously moving molecular features found in the nuclear region can also be observed in H I. The $+40$ km sec^{-1} cloud has been seen by several observers in the 21-cm absorption spectrum of Sgr A. An accurate profile has been given by Sandqvist (1970). In a recent investigation Schwarz, Shaver & Ekers (1977) have derived a column density of about 1.3×10^{22} cm^{-2} for H I. Cohen (1977) found

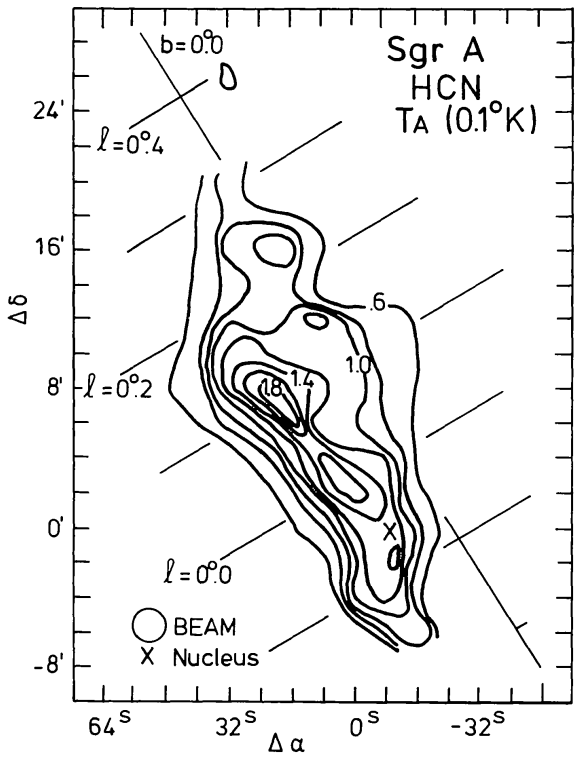

Figure 27 Contours of maximum antenna temperature of HCN emission from the $+40$ km sec^{-1} cloud as a function of α and δ measured at the Tokyo Astronomical Observatory (Fukui et al. 1977).

the spin temperature of the ambient H I to be 110 K, and the ratio of OH to H I column densities as 4×10^{-5} (if the temperature of the molecules is supposed to be 20 K). Again, the molecular clouds appear to be floating in a much hotter surrounding medium.

So far as I am aware no observable quantity of ionized hydrogen has with certainty been identified with the +40 km sec^{-1} cloud. It differs in this respect from many other dense CO concentrations, and in particular from the nearby Sgr B2 complex.

A rough estimate of the mass of the cloud can be made from the contour map of Figure 20. Assuming that the thickness is half that of the dimensions in the plane, and adding 50% helium, we find the mass within the 20 K contour to be (*a*) 4×10^6 $M_\odot$; the alternative value (*r*) is 4×10^5 $M_\odot$ (see p. 325). If we include the surrounding region up to $\Delta l = 10'$, the mass becomes a factor of 10 higher.

5.7 *Sagittarius B2*

Next to the galactic nucleus itself and the +40 km sec^{-1} cloud, the most striking object in the nuclear region is Sgr B2. It is a strong radio source, containing at least seven compact H II regions that are intrinsically as bright as the Orion nebula (Martin & Downes 1972). It is a unique object in the Galaxy, a uniqueness that may be connected with a possible origin from explosive activity in the nucleus. It has become especially famous because the combination of large mass with high density has made it one of the richest hunting grounds for new species of inter-

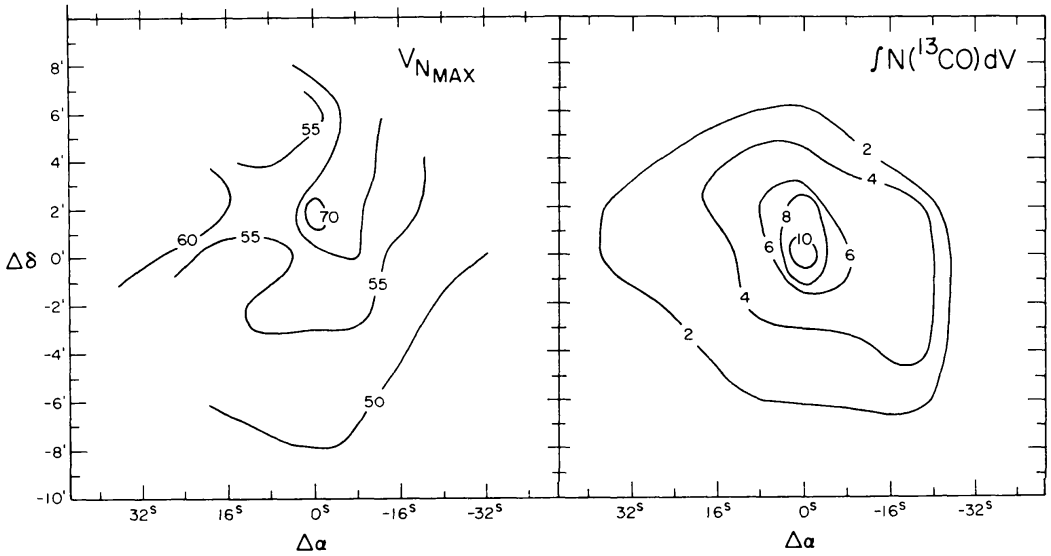

Figure 28 Right: Column density of ^{13}CO in the Sgr B2 cloud with velocities between +30 and +75 km sec^{-1}. Contour unit 5.7×10^{16} cm^{-2}. Origin of coordinates is the OH maser at the center of the cloud at $\alpha_{1950} = 17^h44^m11^s$, $\delta_{1950} = -28°22'30''$. This lies 1^s east and 15″ south of the 2-cm continuum peak. Left: Velocity variation over the cloud. Numbers give the velocity in km sec^{-1} at the maximum column density (Scoville, Solomon & Penzias 1975).

stellar molecules. In Figure 20 the Sgr B2 region stands out as an elongated patch of strong CO emission centered around 40′ longitude and extending from +45 to +100 km sec^{-1} in velocity. The region has been the subject of numerous studies, on interstellar molecules, on the H II regions in its densest part, and on the radiation in the far infrared. It is impossible in the scope of this article to present an adequate discussion. I therefore limit myself to a summary of the properties that appear to be the most relevant in connection with the general structure and dynamics of the nuclear region as a whole. Most of the data cited are from a recent article by Scoville, Solomon & Penzias (1975), in which references to other investigations may be found.

Sgr B2 is an agglomerate of gas and dust clouds; the best-defined part has a diameter of roughly 10′, or 30 pc. Scoville et al. made extensive measurements of ^{12}CO, ^{13}CO, and CS emission over the cloud with a beam of about 1′; they also observed the 2-cm K-doublet of H_2CO in absorption. Because the ^{13}CO line is generally optically thin they could derive CO column densities and determine the structure and space density in the cloud. The column densities are shown in Figure 28, which illustrates the more or less isolated character of the cloud and its strong central concentration. The velocity structure is complicated. At each position the dispersion is large, averaging about 15 km sec^{-1}. Differences in systematic velocity across the cloud are of the same order as the "dispersions" found in a column through the cloud. These observations give "strong evidence that structured flows in the cloud are at least as large as random motions" (quoted from the article by Scoville et al.).

From their ^{13}CO intensities the authors derived a mass (*a*) of $3 \times 10^6\ M_\odot$ for the 10′ diameter cloud, with about 20% in the core; the alternative mass (*r*) is $3 \times 10^5\ M_\odot$.

They point out that their mass is just about equal to the mass that according to the virial theorem could keep the cloud together in the face of its internal motions. However, as the observed velocity distribution over the face of the cloud shows no sign of its having been kept together by its own gravitation, I believe that it is more likely that the agreement of the two mass determinations is fortuitous, and that the velocity differences are not governed by the cloud's mass.

We return to this problem as well as to that of the motion of the entire feature in Section 5.8.

Scoville et al. also discussed the relation between gas and dust in Sgr B2 and came to the conclusion that the two constituents may well be in approximate thermal equilibrium, at a temperature between 20 and 30 K.

Detailed maps of the distribution and temperature of the *dust* have been published by Harvey, Campbell & Hoffmann (1976) at 53, 100, and 175 μ, and by Westbrook et al. (1976) at 1 mm wavelength. From the surface brightness at 1 mm the latter derived a mass of $10^5\ M_\odot$ for the central 1′.

5.8 *Masses and Dynamics*

If we accept the gravitational field derived from the H I nuclear disk (Table 1), the dynamics of most molecular clouds in the nuclear region must be far from

equilibrium conditions. For, as pointed out in Section 5.3, their velocities are generally much lower than the rotational velocities inferred for the H I disk. The bulk of the molecular clouds must therefore have been expelled, presumably from the nucleus.

Fairly direct evidence for such expulsion is shown by the expanding ring and the $+40$ km sec^{-1} cloud.

In order to reach the "ring" at $R = 190$ pc with a radial velocity component $\Pi = 150$ km sec^{-1}, an object moving unimpeded through the interstellar gas would have to start from the nucleus at a velocity of 692 km sec^{-1}. This is derived from Table 1. Should there be any invisible point mass in the center the initial velocity should of course be higher.

Such a picture of clouds expelled at high velocity and decelerated solely by the gravitational field cannot, however, be realistic. Even if compact clouds of sufficient density to move freely through the surrounding medium could have been formed—which is not impossible—no plausible expulsion model can be devised in which all *observed* velocities are nearly an order of magnitude smaller than the required ejection velocities.

We are thus led to the conclusion that the dynamics of the expelled molecular clouds are largely determined by forces other than gravitation. Their motions have presumably been braked by interstellar "friction," and they must therefore consist for an important part of swept-up gas. That the molecular features contain much swept-up gas is confirmed by the fact that they possess angular momentum, although less than what would correspond to the circular velocities listed in Table 1. It is evident that if the friction is taken into account the initial velocities of the clouds which caused the formation of the "ring" must have been considerably higher than the 692 km sec^{-1} estimated above.

The acceleration of the large molecular complexes may have been a gradual process, due to the outward pressure exerted on existing disk gas by the collisions of many small, presumably ionized, clouds ejected at high velocity. A mechanism of this kind is directly suggested by what is observed in Seyfert galaxies.

The *main mass* of the CO may be ascribed to another eruptive period in which the accelerated clouds did not move out as far as the ring, and may at present be near their maximum distance. Liszt et al. (1977) have drawn attention to a pattern extending from about $\Delta l = -50'$, $v = -160$ km sec^{-1}, through $\Delta l = -30'$, $v = -100$, across $v = 0$ at $\Delta l = 0$ to $\Delta l = +30'$, $v = +90$, which looks like a disk rotating at a constant angular velocity. This may well be part of a very anisotropic ring, rotating, at $|l| \sim 30'$, at roughly half the circular velocity given in Table 1.

The $+40$ km sec^{-1} complex, extending from the nucleus to about $R = 50$ pc, may be the most recent formation, perhaps no more than half a million years old. The apparent absence of H II regions in this exceptionally dense structure might be considered as a confirmation of its youth.

The time scales for the other features are uncertain. If the outer ring is on its first journey outward it would be about one million years old. But if, as is quite conceivable, it has moved back and forth, it could be five to ten times older. The

age of the remainder of the CO is hard to estimate, but it is unlikely to be much greater than the time of revolution—at this distance about three million years—because otherwise it could hardly have remained so far from an equilibrium stage as it evidently is.

As in the case of the expanding H I features the question arises how the H I nuclear disk can have survived these eruptions. On the positive longitude side it may indeed have been swept away from the region inside 200 pc where the dense CO is observed (cf Section 2.4). On the other side, where the rotating disk *is* observed down to $R \sim 50$ pc, there is little CO, except for the expanding ring. This latter has apparently been ejected at an angle with the plane, for it is inclined at some 10°.

An intriguing problem is presented by the large *masses* of the molecular features and the rate of ejection needed to form them. The total hydrogen mass within 300 pc is estimated to be between 3×10^7 and 3×10^8 $M_\odot$ (Section 5.3); with 50% helium mass added the total gaseous mass becomes (*a*) 5×10^7, (*r*) 5×10^8. From integrations of Figure 20 the mass of the expanding ring is roughly estimated to be between 3×10^6 and 3×10^7 $M_\odot$, and that of the +40 km sec^{-1} cloud insofar as it lies within the $T^* = 20$ contour to be between 10^6 and 10^7 $M_\odot$.

Even if only 10% of the mass consisted of gas expelled from the nucleus, the rest having been swept up, and even if we suppose that the expulsion of this mass of gas would occur only once in 10^7 years, the nucleus would still have to expel on the order of a solar mass per year in high-velocity clouds; and this is certainly an underestimate, because it does not take account of the gas expelled at an angle with the disk.

The gas produced by evolving stars in a core of 1-pc diameter is many orders of magnitude less than what is required (cf Section 4.4). Additional gas might be produced by stellar collisions or tidal disruptions by a massive central black hole (cf Salpeter 1964, Lynden-Bell & Rees 1971, Frank & Rees 1976, and references given therein), but it is highly unlikely that this could produce the amount needed. Nor can infalling gas from the halo or from outside the Galaxy supply more than a minor fraction of what is needed.

The only way out that I see is a *circulation* of the clouds. As we have seen, the molecular agglomerates have transverse velocities considerably smaller than the circular velocities. They will therefore fall back towards the center. The minimum distances R they can reach are mainly determined by their angular momenta; they may average a few tens of parsecs. The clouds cannot get into the core proper unless they get rid of their angular momenta. It is not at all clear how this could be accomplished. Magnetic fields cannot be of sufficient strength. Though the fast differential rotation—revolution periods ranging from ~40,000 years at $R = 1$ pc to ~400,000 years at $R = 10$ pc—is likely to set up strong turbulence, it is doubtful whether this would suffice to effect the rapid redistribution of angular momentum required.

An attractive alternative idea, suggested in a discussion with E. N. Parker and H. G. van Bueren, is that the gas would intermittently contract into a dense ring at $R \sim 20$ pc and be expelled by an outburst of *radiation* and relativistic particles

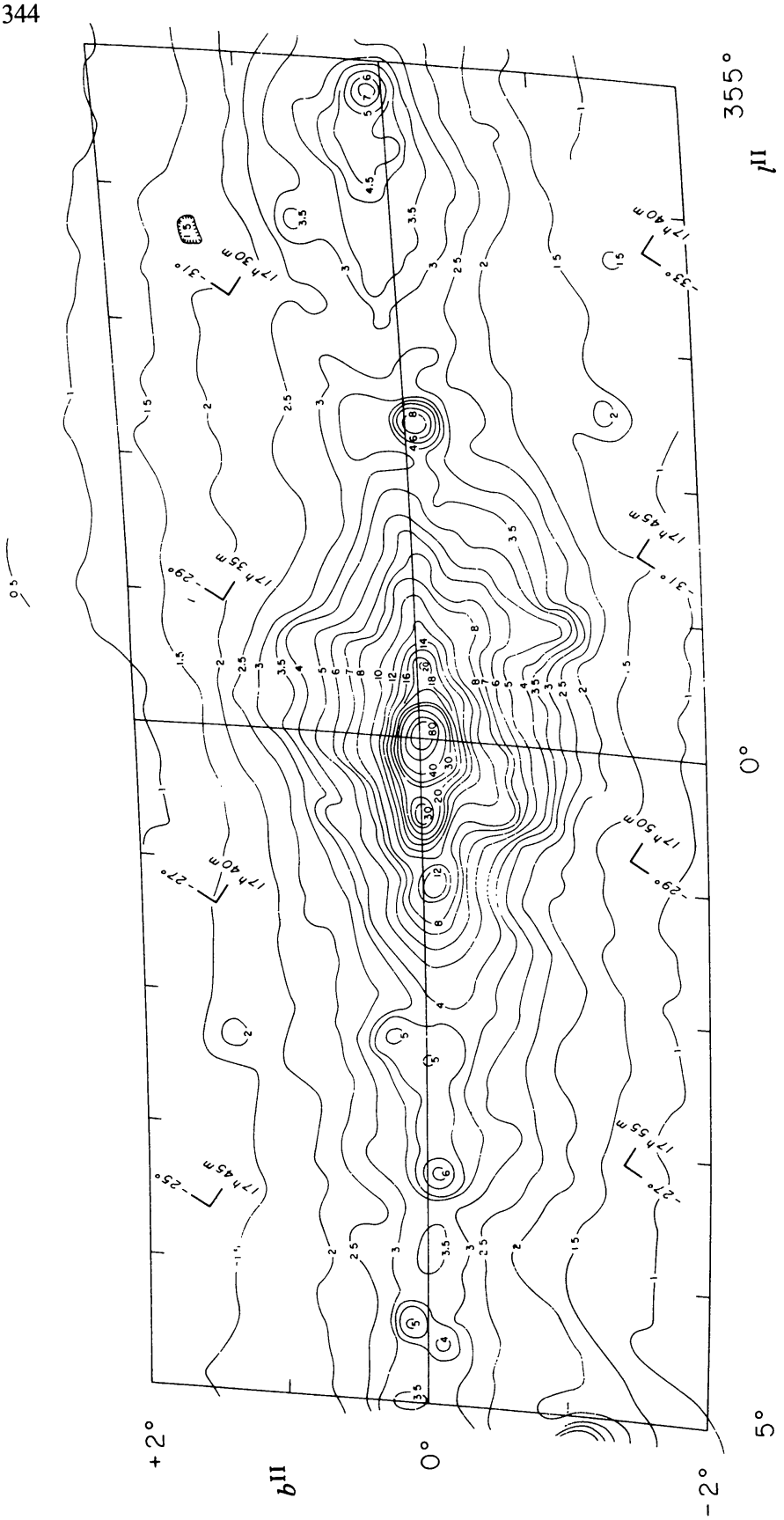

Figure 29 The galactic center in nonthermal radiation. From a survey at 11-cm wavelength made with the 140-ft antenna of the National Radio Astronomy Observatory with a beam width of about 11′. At 11 cm the nonthermal radiation dominates (Altenhoff et al. 1970).

from the nucleus. The energy required for the outward impulse (10^{55} or 10^{56} ergs) and the intervals of the order of 10^6 years would be comparable to what is observed in some radio galaxies.

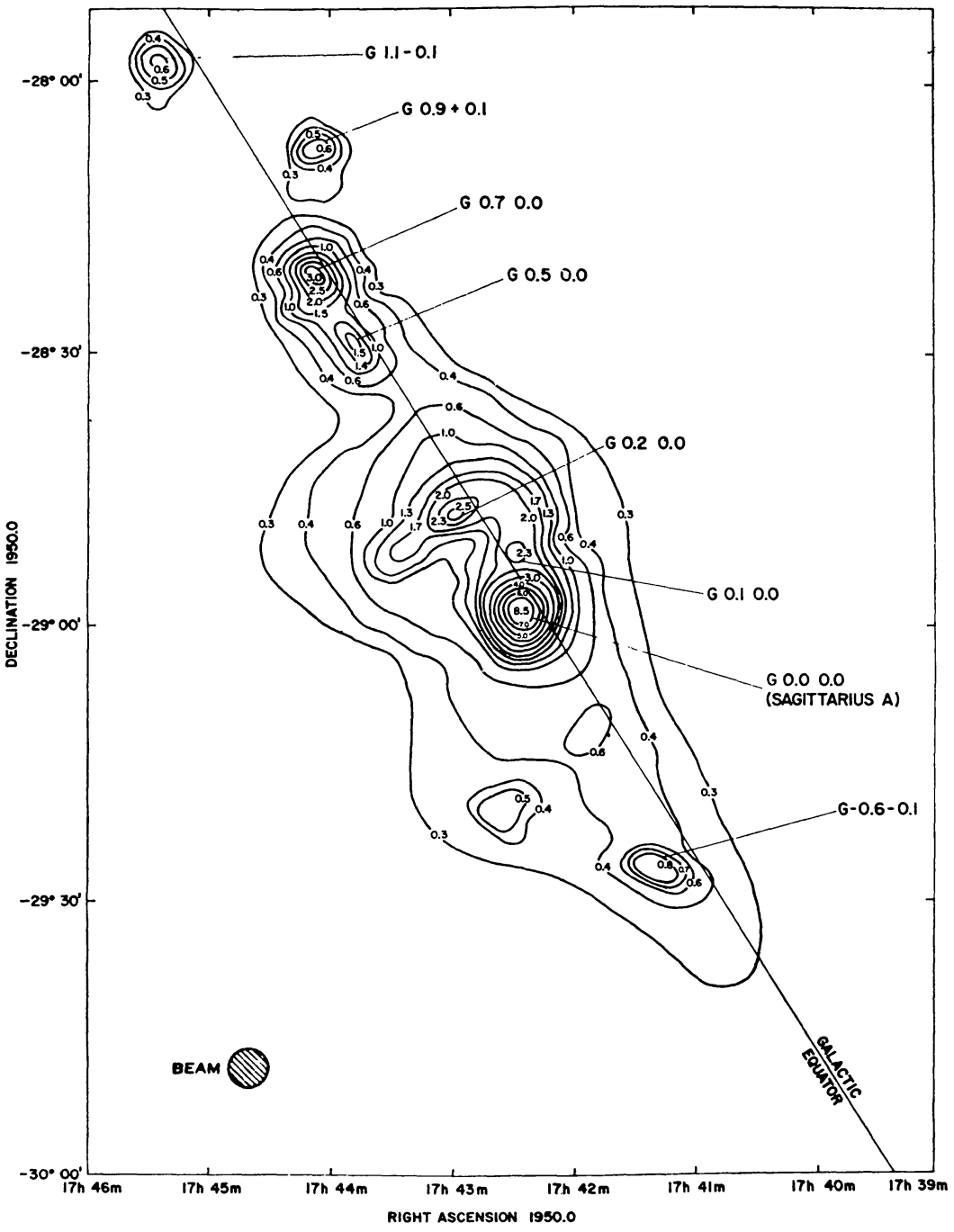

Figure 30 Distribution of thermal radiation around the galactic center. From a survey at 3.75 cm by Downes & Maxwell (1966) with the 120-ft Haystack antenna; beam 4'.2; contours represent antenna temperature.

6 EMISSION AT RADIO FREQUENCIES AND IN THE 12.8-μ NEON II LINE

The central region emits a mixture of thermal and nonthermal radio waves. Figures 29 and 30 show the general distribution of the two kinds of radiation. The first, at 11 cm, gives a good impression of the general distribution of the synchrotron radiation outside the galactic plane. At the lowest latitudes it is mixed with thermal emission. For $|b| < 0.^{\circ}25$ a purer picture of the nonthermal component may be obtained from a map at 75-cm wavelength made with the Molonglo Cross telescope (Little 1974).

Figure 30, at 3.75-cm wavelength, shows mainly the thermal emission. The thermal character is indicated by the spectral index as well as by the observation of recombination lines. Moreover, at longer wavelengths, the central body of ionized gas can be seen in absorption against the nonthermal radiation (cf Mills 1956). The observations with Mills' cross at λ 3.5 m show a striking dip extending to approximately 1° from the center.

The outer diameters are roughly 5° × 2° (900 × 350 pc) for the nonthermal, and $1.^{\circ}5 \times 0.^{\circ}5$ (260 × 90 pc) for the thermal radiation. Both are strongly concentrated towards the center. In both domains the contours have significant irregularities, on scales of 20′ and less. In addition there are a number of discrete sources; the strongest have been marked by their galactic coordinates in degrees preceded by G, which is the usual way of designating sources and concentrations in the central region. A few are fore- or background objects, but all bright sources with $|l| < 2.^{\circ}5$, with the possible exception of G 0.87+0.10, lie in the central domain. They are listed in Table 4, the data of which are from an article by Mezger, Churchwell & Pauls (1974). For Sgr A, which will be extensively discussed in Section 6.3, only the nonthermal component is given. The electron density for a homogeneous source is designated by n_e, E is the emission measure, and L_c the number of Lyman quanta required for the ionization.

Table 4 Radio sources near the galactic center (Mezger, Churchwell & Pauls 1974)

Source	$S_{5\,\mathrm{GHz}}$ (Jy)	α	V_{lsr} (km sec^{-1})	n_e (cm^{-3})	E (10^5 pc cm^{-6})	L_c (10^{49} sec^{-1})
G 357.66−0.09	15.7	−0.4				
G −0.53−0.06	15.4	−0.7				
G −0.05−0.05 (Sgr A)	190	−0.7				
G 0.07+0.01	80	−0.1	−41	105	2.8	71
G 0.18−0.03	157	−0.1	−26	76	2.3	139
G 0.53−0.03	36	−0.2	+46	96	1.9	31
G 0.67−0.02 (Sgr B2)	48	−0.2	+63	201	5.6	42
G 0.87+0.10[a]	8	+0.2				
G 1.15−0.06	10	0.0	−22	98	1.3	9
Region $1.^{\circ}5 \times 0.^{\circ}5$[b]	410			16[b]		360

[a] Uncertain whether this source belongs to the central region.

[b] Half widths 61′ × 20′ in $l \times b$; a homogeneous spheroid of this size would produce the observed radiation if $n_e = 16$.

All central region sources lie in an extremely narrow layer, between $-0.^{\circ}09$ and $+0.^{\circ}01$ latitude. Their average distance from the true plane of symmetry, at $b = -3'$, is $\pm 1.'4$, or 4 pc.

6.1 *Thermal Emission*

The thermal radiation comes in part from giant H II regions. These lie all at positive longitudes, thus showing the same asymmetry in distribution as CO. The strongest appear to be directly related with molecular clouds: Sgr A is, as we have seen, probably connected with the mighty $+40$ km sec^{-1} complex, while Sgr B2 coincides in position and velocity with the second densest agglomeration of clouds. Details on the structure of the six brightest sources may be found in an extensive review by Downes (1974).

The emission profiles of the sources, and of the central area in general, discern themselves from H II regions in other parts of the Galaxy by the generally high velocities of the various components, and especially by their widths. From measurements in the region within $1.^{\circ}5$ longitude, Pauls & Mezger (1975) find a median half-width of 54 km sec^{-1} for the components considered to lie spatially near the center, as against 20 km sec^{-1} for foreground or background components.

The emission within $\sim 20'$ from the center has a peculiar structure, as indicated in Figure 31 (Pauls et al. 1976). Beside the compact central source Sgr A we note, firstly, the striking asymmetry in longitude already mentioned, and, secondly, a structure which the Bonn group has called the Arc, formed by a string of extended "clouds." The combined flux density of these clouds at 5 MHz is about 240 Jy according to Mezger (1974). Pauls et al. have measured recombination line velocities at 15 points in various parts of the field. Along the western branch of the Arc the radial velocities range from -48 km sec^{-1} around the longitude of the center to about -20 at the sharp bend in the north. In the northern arm the velocities are small. At first sight it seems surprising that these velocities are an order of magnitude smaller than the rotation velocities indicated by the H I nuclear disk and the mass model discussed in Section 2, or than the motions to be expected if the virial theorem would be applicable. We are again tempted to question whether we have not been radically mistaken in our interpretation of the H I motions as those of a rotating disk. It appears to me that the difficulties one is faced with if one attempts to interpret the H I in a different manner are so great that this alternative can practically be eliminated, and that we must therefore accept that the H II velocities deviate widely from those corresponding to the virial theorem. This is not so unlikely as it may have seemed at first, because already the peculiar shape of the Arc by itself indicates that it is due to expulsion. In features resulting from a gradual expulsion the lowest velocities required to reach a certain distance will strongly preponderate and may not give any indication of the gravitational field.

In Figure 31 a small extension of the Sgr A source toward greater longitude may be noted. In the tip of this protuberance a velocity of $+45$ km sec^{-1} was found, deviating rather strongly from the velocities in neighboring regions. It might be connected with the $+40$ km sec^{-1} molecular cloud.

It is possible that the Arc clouds are not smooth structures, but are made up of swarms of smaller components. Recent Westerbork observations of some of the

Arc "clouds" at wavelengths of 21 and 6 cm have indicated that they indeed contain a considerable number of compact H II regions, which seem to lie preferentially near the Arc's outer edge. I am indebted to J. Wouterloot in Leiden for this provisional account of his observations.

According to Mezger, Churchwell & Pauls (1974) the discrete thermal sources listed in Table 4 would together require 34 O6 supergiants to provide for their ionization, while 43 more are required to ionize the extended H II regions. This shows that star formation in the region must be taking place at a rapid rate. The abundance of the large and dense molecular clouds fully supports this.

There is of course the possibility that the ionization is partly due to collisions among the various fast moving features.

6.2 *Nonthermal Emission*

It is unknown whether the relativistic electrons responsible for the radiation have been supplied by the galactic nucleus or by supernovae. In view of the fast rate of

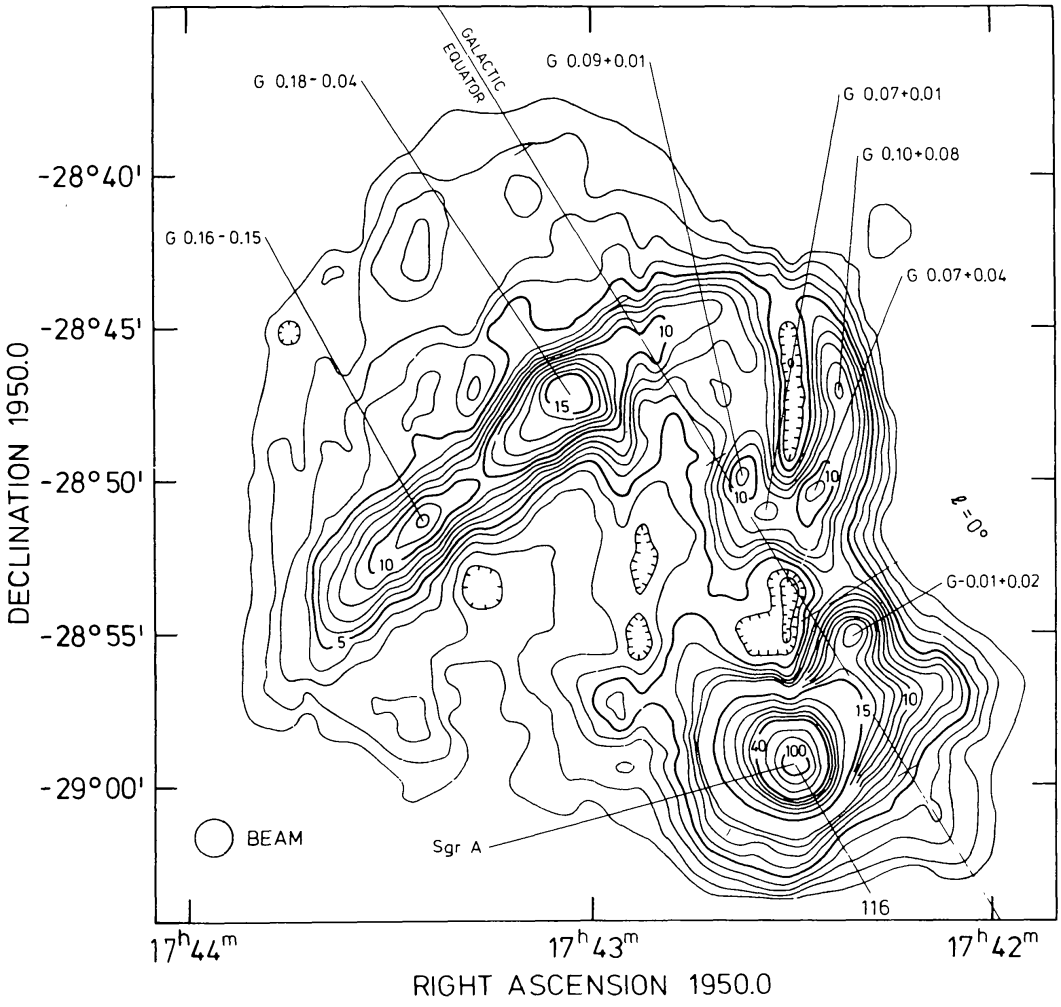

Figure 31 Map of thermal radiation between −10′ and +20′ longitude showing Sgr A and the Arc structure. This 10.7-GHz (2.8-cm) map (beam width 1′.3; contour unit 0.285 K) was made with the 100-m Effelsberg telescope (Pauls et al. 1976).

star formation the frequency of supernovae is probably considerably higher than elsewhere in the Galaxy.

A number of discrete nonthermal sources are known in the central region, three of which are listed in Table 4. The one connected with Sgr A is further discussed in the following section.

A transient radio source, presumably identical with a transient X-ray source, was found by Davies et al. (1976) at 53″ from the center, in position angle 223°. It was found on March 30, 1975, when it had a flux density of 0.48 Jy at 0.96 GHz. It was invisible ($S < 0.05$ Jy) on 6 other days in the period 1974/75.

A sketch of various features in the disk's central part is given in Figure 32.

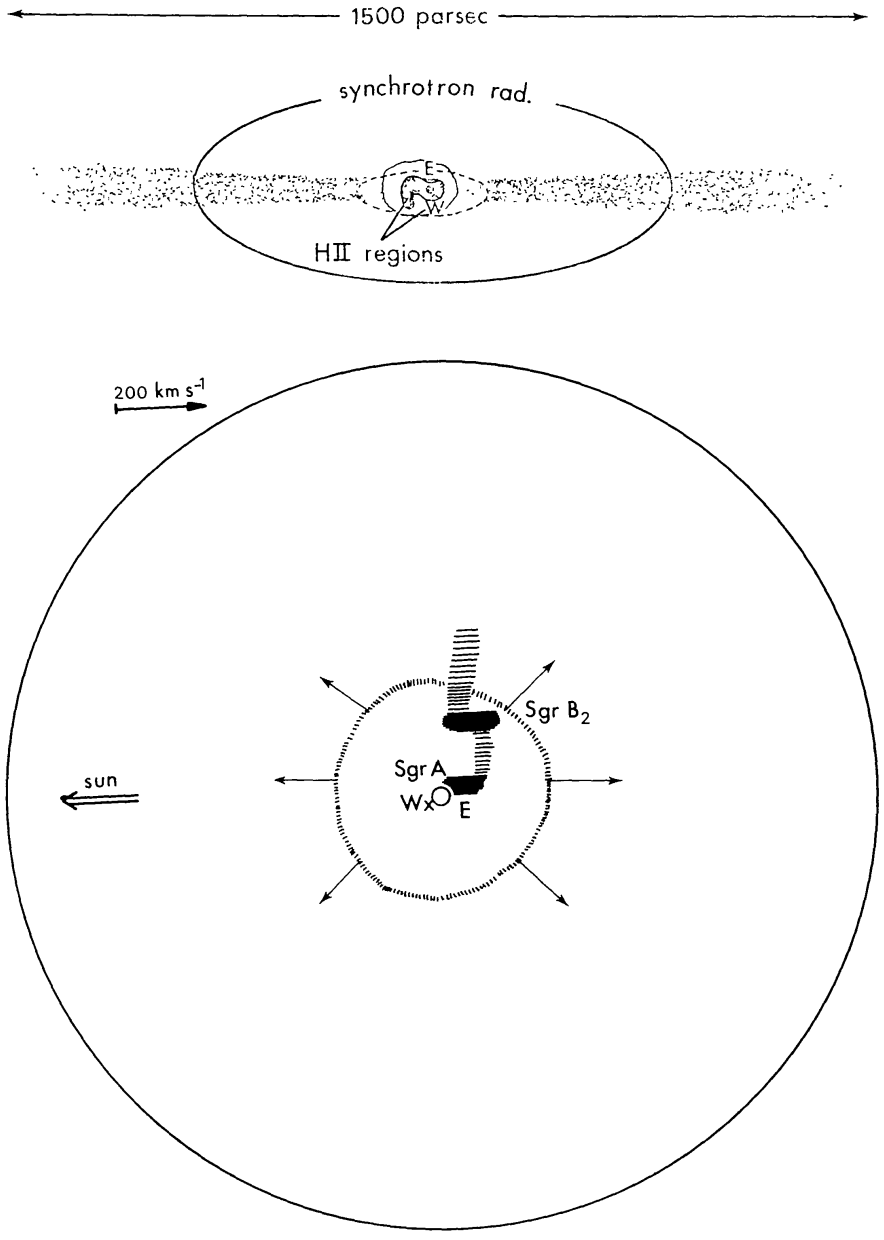

Figure 32 Sketch of the situation of the molecular clouds and other nuclear features relative to the H I disk.

6.3 *Sagittarius A*

As may be seen in Figures 29 and 30 the thermal as well as the synchrotron emission increase gradually with decreasing distance from the center. A new sharp increase sets in around $R = 2'$. Figure 33 (Ekers et al. 1975) shows a map of this inner region, which is called Sgr A. The map is on a 5 times larger scale than that of Figure 31, which itself is on a 3 times larger scale than Figure 30. All three are for cm wavelengths. Figure 33 was obtained from a combination of observations with the synthesis telescope at Westerbork and the Owens Valley radiotelescope. The angular resolution is 6.″3 × 34″ (or 0.3 × 1.7 pc). Many other maps exist,

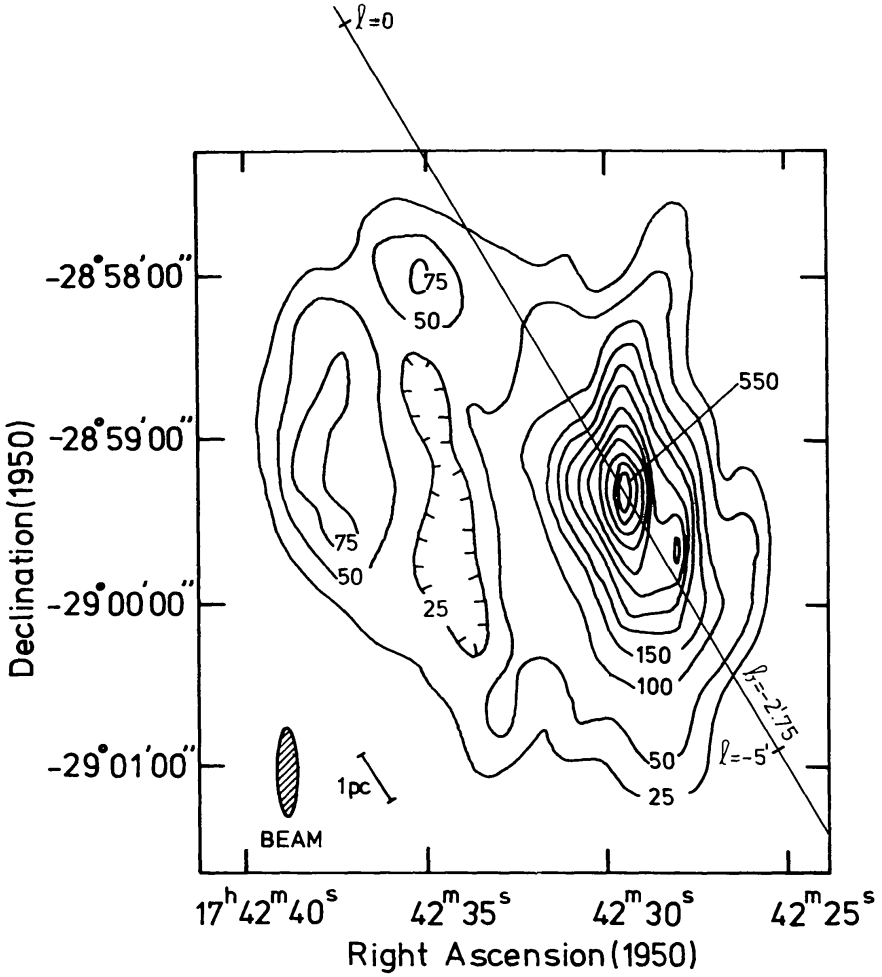

Figure 33 Full synthesis map of Sgr A at 5 GHz. This map, from combined Westerbork-Owens Valley Radio Synthesis Telescopes, is sometimes referred to as the "WORST" map. Half-power widths of synthesized beam 6.″3 × 34″ ($\alpha \times \delta$); contour unit 1.2 K in brightness temperature. The zero contour corresponds approximately to the 60-K contour in a 6-cm survey with the Parkes 64-m telescope by Whiteoak & Gardner (1973). The straight line is the latitude circle at $b = -2'.75$, which is probably the real galactic equator; the zero point of galactic longitude is marked; and the center of the concentrated source, which is presumably the actual center of the Galaxy, lies at $l = -3'.34$ (Ekers et al. 1975).

including high-resolution interferometer maps (Downes & Martin 1971, Whiteoak, Rogstadt & Lockhart 1974, Balick & Sanders 1974) or charts constructed from lunar occultation observations (Gopal-Krishna et al. 1972, Sandqvist 1974). The map in Figure 33 gives probably the best overall high-resolution picture.

It shows two major components, Sgr A West and Sgr A East, as well as structural details within these components. There is little doubt that both lie in the immediate vicinity of the galactic center. The eastern component has a nonthermal spectrum, as is shown by observations at longer wavelengths. It is probably a supernova remnant; in spectral index, diameter (about 7 pc), and luminosity it resembles common supernova remnants; there is even a hint of a shell structure. Its brightest part lies 1'.8 (5.2 pc) from the peak of Sgr A West.

Sgr A West has a flat spectrum between the wavelengths of 6 and 21 cm where Ekers et al. (1975) have determined its flux density. Its radiation at short wavelengths is probably mostly thermal, although at longer wavelengths it appears to emit also nonthermal radiation (cf Gopal-Krishna & Swarup 1976). Ekers et al. estimate the diameter to half power to be $1'x < 0'.6$, with the long axis in position angle 32°; the flux density at 6 cm is 26 Jy. The structure differs from that of other giant H II regions in the Galaxy by its much smoother structure, which as the authors remark could arise if the exciting stars are more evenly distributed, or if there is only a single exciting source, which may be associated with the compact nucleus described in Section 6.3.1. The central H II is also unique by its large internal motions (Section 6.3.2).

Pauls et al. (1976) describe a "halo" of 3′ radius surrounding Sgr A East and West, which at 3 cm has a flux density of 70 Jy. About 60% of this would be nonthermal.

Sgr A West lies in the midst of a unique agglomeration of infrared sources covering an area of about 20″ (1 pc) diameter (cf Section 7, Figure 35). The agglomeration contains among others the sharp maximum of 2.2 μ radiation, which is supposed to be the dynamical center of the Galaxy. Radio observations at 8085 MHz show some fine structure of the same 5″ to 10″ scale as the infrared (Balick & Sanders 1974, cf the inserts in their Figures 3 and 5); the shoulder at ~25″ SW of the maximum in Figure 33 may be an outlying condensation of the same category. It lies in the general direction where at 53 microns a conspicuous maximum has been observed (cf Figure 38). The central component of the fine structure has an ultracompact core (Section 6.3.1), which is probably the actual nucleus of our Galaxy. This coincides with the 2.2 μ maximum within the errors of a few seconds of the 2.2 μ position (Ekers et al. 1975, Borgman, Koornneef & de Vries 1974, Becklin & Neugebauer 1975).

6.3.1 THE COMPACT NUCLEUS Sgr A West has an extremely compact core. This was first observed in 1971 by Ekers & Lynden-Bell; later observations by Balick & Brown (1974) showed that it was smaller than 0″.1 and had flux densities of 0.6 and 0.8 Jy at 11 and 3.8 cm respectively, corresponding to a brightness temperature in excess of 10^7 K. The 1950 position of this small source is $\alpha = 17^h42^m29^s.291 \pm 0^s.005$, $\delta = -28°59'17''.6 \pm 0''.1$, or $l = -3'.34$, $b = -2'.75$. The source was subsequently ob-

served by Lo et al. (1975) with a medium-baseline interferometer at 3.7 cm. They found it to be smaller than about 0".02, with a flux density of 0.6 Jy. More recent observations at a wavelength of 3.8 cm, with a much longer baseline, indicate an overall size of 0".01 to 0".02, with about 25% of the flux, or 0.2 Jy, in a core of about 0".001 (private communication from Kellermann; cf Kellermann et al. 1977). The radio luminosity of the core is 10^{33} ergs sec^{-1}. The brightness temperature must be about 10^{10} K, and the radiation is probably nonthermal. The core diameter is smaller than 10 astronomical units, or 80 light-minutes. This is smaller than the limits measured in any other nucleus.

Davies, Walsh & Booth (1976) have suggested from their measurements at 0.408, 0.96, and 1.66 GHz that the observed diameter of the nuclear source would be mainly due to interstellar scattering. The new VLBI result by Kellermann et al. seems to show that the scattering is considerably less than proposed by Davies et al. However, judging from the scintillation observations of other distant galactic sources, the scattering towards the center is unlikely to be smaller than 0".001 at 3.8 cm. The true diameter may therefore be appreciably smaller still.

The existence of such an extremely compact radio-emitting body in the galactic center is intriguing and leads naturally to the question of whether it might contain the engine providing the energy and mass required for the expulsion phenomena discussed in the preceding sections.

It may be mentioned in this connection that the Schwarzschild radius of a mass of $5 \times 10^6\ M_\odot$, which may be the mass of the compact core (cf Section 6.3.2), is $\sim 1.5 \times 10^{12}$ cm, or 0.1 astronomical unit.

Several radio galaxies are known to contain cores of small dimensions, which are suspected to be the sources of the enormous energies poured into their radio lobes. The galactic nucleus is, however, 7 to 9 powers of ten weaker than the nuclei of strong radio galaxies and quasars, so that the confrontation may not be meaningful. It should be noted, however, that there is an enormous spread in the emission at radio frequencies, such as shown for instance by the large class of radio-quiet quasars, and by the very great differences in radio emission by the cores of common galaxies, as is indicated by a comparison of our Galaxy with the very similar nearby spirals M31 and M81. While no compact core is seen in M31, M81 has a nonthermal radio core that may be of similar dimension as that in the Galaxy, but has a 10^4 times higher radio power. Interferometer measures show that its diameter is less than 1300 au, or 7 light-days (Kellermann et al. 1976); intensity variations at cm waves indicate it to be smaller than one light-day.

6.3.2 HIGH-VELOCITY IONIZED GAS AROUND SGR A WEST AND THE MASS OF THE NUCLEUS Observations of the 109α hydrogen recombination line at 5010 MHz in Sgr A showed that this is exceptionally broad (Pauls, Mezger & Churchwell 1974). As observed with the Effelsberg telescope, with a beam width of $\sim$2'.5 or 7.5 pc, the line was found to have a half-width of $\sim$200 km sec^{-1} centered around zero velocity. The authors commented that such a width is almost certainly the result of systematic motions, and not of random turbulence.

New information on the nature of these motions has come from the observation

of the Ne II fine-structure line at 12.8 μ by Townes and co-workers (Wollman et al. 1976, Wollman 1976). The published observations were made at the Tololo Observatory. Subsequently, data with much better sensitivity as well as better resolution were obtained by Wollman with the Lick 3-m telescope. The reviewer is greatly indebted to Dr. Wollman for putting these results at his disposal prior to publication. Because of their eminent interest, a full reproduction of his principal results is given in Figure 34. The resolution of these observations, which is 28 times better than that of the hydrogen recombination lines, made it possible not only to investigate the distribution of the ionized gas around Sgr A West, but also to get some insight in the internal motions.

From the data in Figure 34, combined with less sensitive observations in surrounding fields, it was found that the ionized gas is concentrated in an area of about 15″ (or 3/4 pc) radius, the center of which coincides with the compact radio source discussed in the preceding subsection and indicated by an asterisk in Figure 34. As described in Section 7 a unique concentration of discrete infrared sources has been found in just the same area. I therefore propose to refer to this region as the "infrared core." Figure 34 shows the positions at which the high-resolution Ne II line measurements were made, projected onto a 10μ continuum map.

Some of the profiles, in particular in the southwestern part, are extremely wide; in the area b' the emission seems to cover an interval of about 1000 km sec^{-1} (half-width $\sim$ 500 km sec^{-1}). The central velocity is seen to change systematically from about +100 km sec^{-1} at $\Delta l = +8''$ to -200 km sec^{-1} at $\Delta l = -7''.5$, Δl being measured from the longitude of the compact radio source. The shift is perpendicular to the rotation axis of the Galaxy and in the direction of the galactic rotation. If interpreted as rotation it indicates a rotation velocity of roughly 150 km sec^{-1} at 7″.8, or 0.4 pc, from the center. The *circular* velocity at $R = 0.4$ pc is likely to be higher, for two reasons: firstly because the measures give the projection of the rotation on the line of sight, averaged over a column through the whole mass, and secondly because the large linewidths indicate that there must be large radial motions in addition to rotation. Therefore, the true "circular" velocity at $R = 0.4$ pc may well be between 200 and 250 km sec^{-1}, and possibly even higher. It should, however, be stressed that there remains a possibility that the observed systematic change of velocity is *not* due to rotation but to radial motions mimicking rotation around the galactic axis.

In a sense the ionized gas at 0.5 pc gives a repetition of what the H I nuclear disk gave at a thousand times larger distance.

In the case of a spherical mass distribution, or a point mass, the mass inside 0.4 pc would be between 4 and 6×10^6 $M_\odot$. The mass within the same radius as estimated from the distribution of the 2.2 μ radiation and the light distribution in M31 was 1.5×10^6 $M_\odot$ (interpolated from Table 1). It is therefore possible that practically the whole of the 4–6 $\times 10^6$ $M_\odot$ deduced from the Ne II observations would be concentrated in the ultracompact radio source; it might be the mass of a black hole in the center. The kinematics of the nuclear complex are evidently complicated. Radial streamings of comparable velocity must be present beside the rotation; otherwise the profiles of fields c and b', both at negative longitude relative

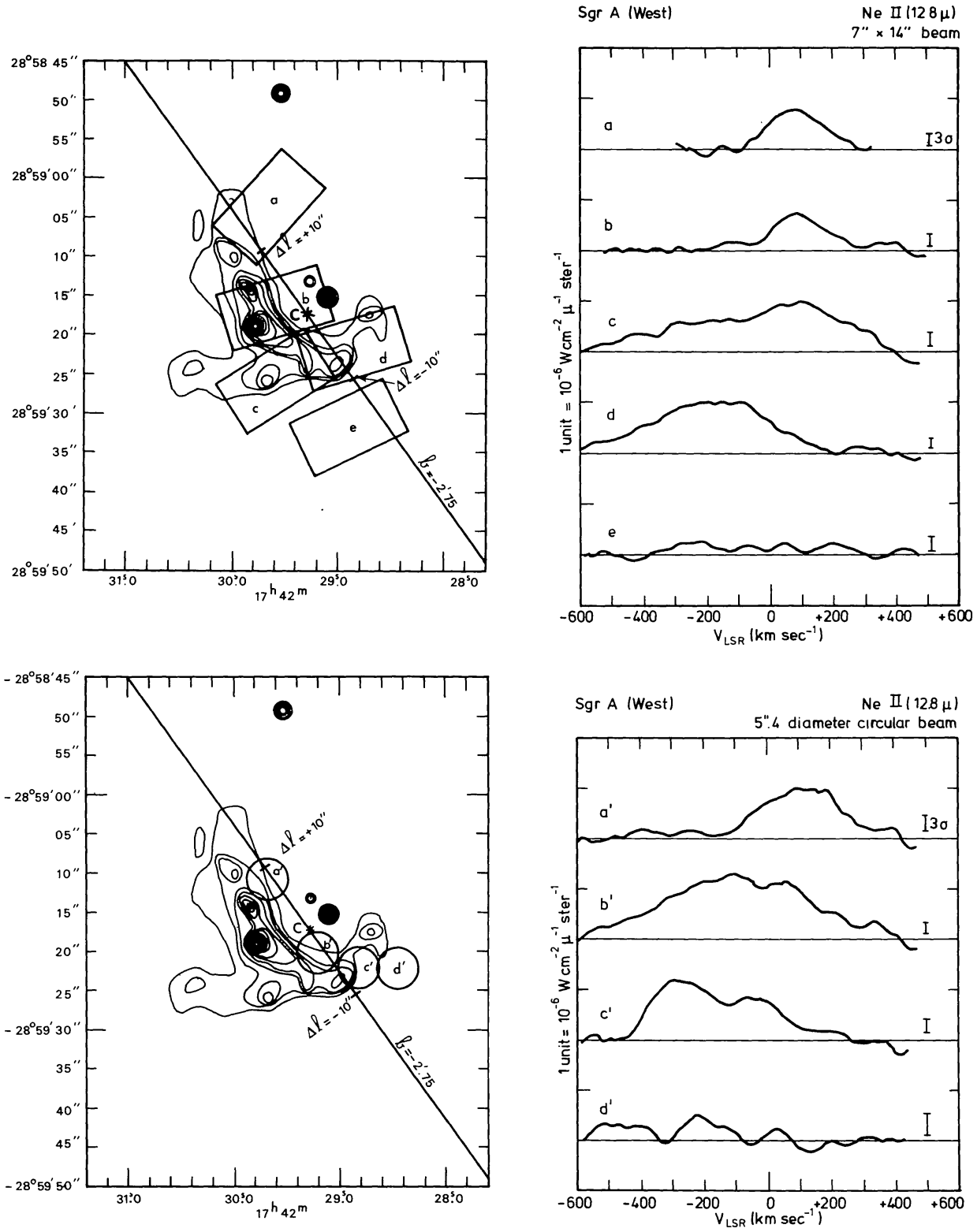

Figure 34 Profiles of the Neon II line at 12.8 μ. The regions measured are shown projected on a 10-μ continuum map. The straight line is the latitude circle at $b = -2'.75$, and the position of the galactic center is shown by an asterisk and a capital C (Wollman 1976, from observations with the Lick 3-m telescope).

to the center, could not have such long extensions to positive velocities. Nor could we otherwise have such large asymmetries.

The lifetime of these large-scale irregularities must be short, comparable with the time of revolution, which is roughly 15,000 years. To maintain the observed state of turmoil there should be major eruptions on time scales of at most 10,000 years, each imparting a kinetic energy of $10^{49}-10^{50}$ erg in the form of large-scale motions. This is of the order of what can be yielded by a type II supernova. But it is unlikely that supernovae would be sufficiently frequent.

It is more probable that the same unknown mechanism that is needed to expell the massive molecular features and the expanding H I arms is also responsible for the motions in this inner region.

Evidently, further observations of the Ne II line in the galactic nucleus are of extreme interest.

7 THE INFRARED CORE

Observations at infrared wavelengths have shown a remarkable concentration of objects in a region of 10 to 15″ radius around the center.

Radiation at 2.2 μ was first extensively observed by Becklin & Neugebauer (1968), who interpreted it as emission from stars at the center. They also observed at other wavelengths, and found relatively strong radiation at 10 and 20 μ concentrated in an area of about 1 pc diameter. Rieke & Low (1973), observing at various wavelengths between 3.5 and 20 μ, discovered that the area contained a number of discrete sources. Later observations with better resolving power (Borgman, Koornneef & de Vries 1974, Rieke, unpublished) yielded improved absolute positions of the Rieke & Low features, and brought out some more detail. The most detailed maps presently available are by Becklin & Neugebauer (1975). They are shown in Figures 35 (2.2 μ) and 36 (10 μ), the latter being from unpublished observations by Willner (Willner, Becklin & Neugebauer, private communication, Willner 1976). Individual sources in these maps are numbered, and will in the following be referred to as IRS 1, IRS 2, etc.

As suggested by Becklin & Neugebauer (1968), the near infrared (2–3 μ) emission comes probably mainly from the central concentration of the later-type stars of which the spheroidal bulges of galaxies are made; it contains an outstanding point-like object (IRS 7). As discussed in Section 2 these observations have given important information on the density distribution and total star density between about 0.2 and 50 pc from the center. An extension of the map to distances of about 0°.5 is shown in Figure 1. Source IRS 16 of Figure 35 coincides with the ultracompact central radio source; it provides an indication of the star density within 2″ of the actual center. The irregularity of the distribution in Figures 35 and 1 is mainly caused by the dominating role of a relatively small number of intrinsically very bright M-type stars, all situated in the region of the center.

The maps in Figures 35 and 36 are strikingly different. This is due to the fact that the emission at 2.2 μ is mainly direct stellar radiation, while that at 10 μ comes from solid particles, heated by stars, but radiating at a much lower temperature. The

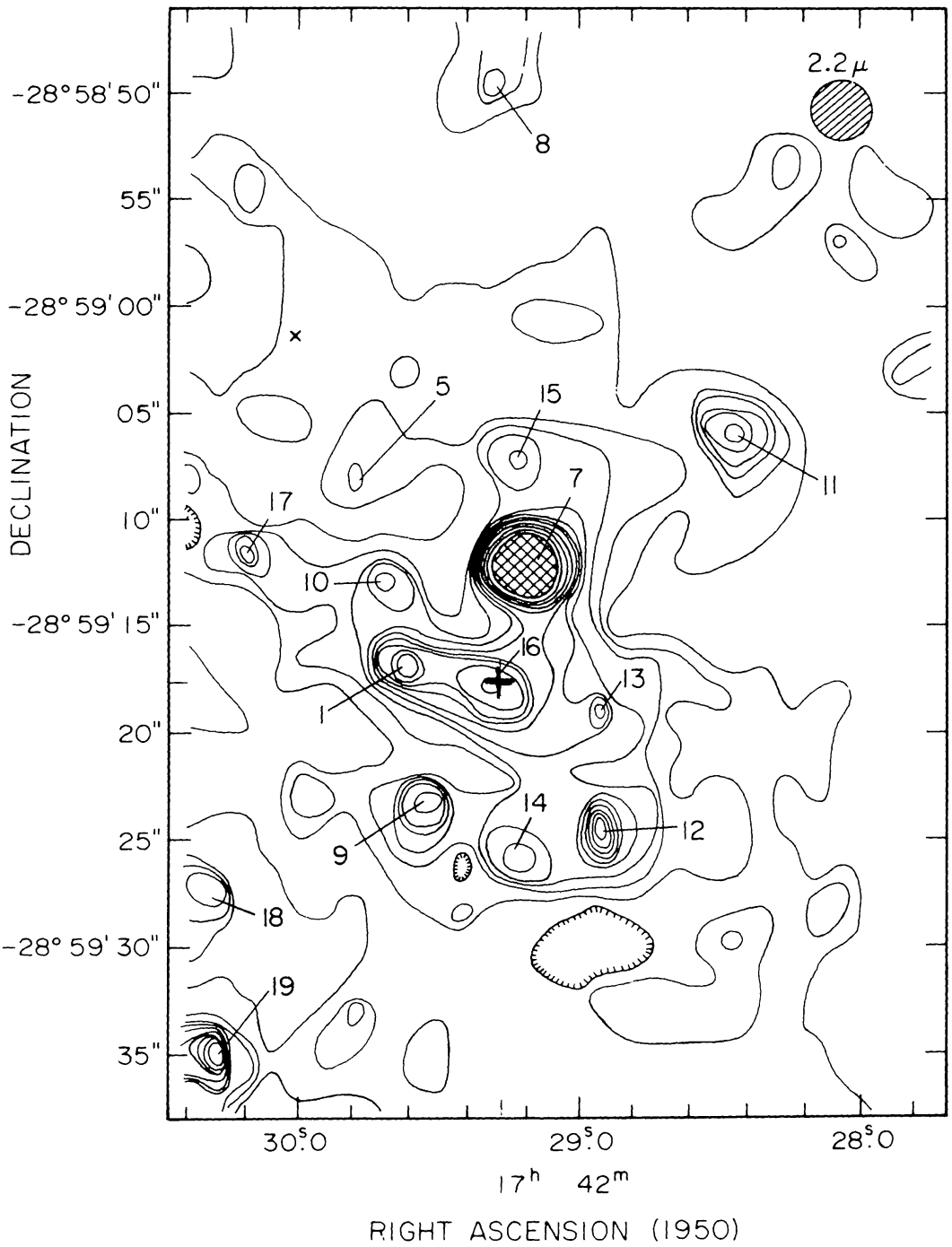

Figure 35 Map of the galactic center region at 2.2 μ, made with a 2".5 diaphragm on the 5-m Hale telescope. The contour levels each correspond to 2.5×10^{-18} W m^{-2} Hz^{-1} sr^{-1}. The crosshatching corresponds to 35 contour levels. The cross marks the galactic center. Discrete sources are indicated by numbers which will be referred to in the text as IRS 1, etc. (Becklin & Neugebauer 1975).

dust is apparently rather evenly distributed over a sort of ridge that is seen in the 10-μ picture to extend from IRS 2 to a little North of IRS 5. It is heated partly by the Population II stars (whose strong concentration towards the center causes the dust temperature to increase with decreasing distance from the center) and partly by high-luminosity O stars. The condensations in Figure 36 are presumably the locations of such newly formed stars. By an extensive analysis of the spectra between

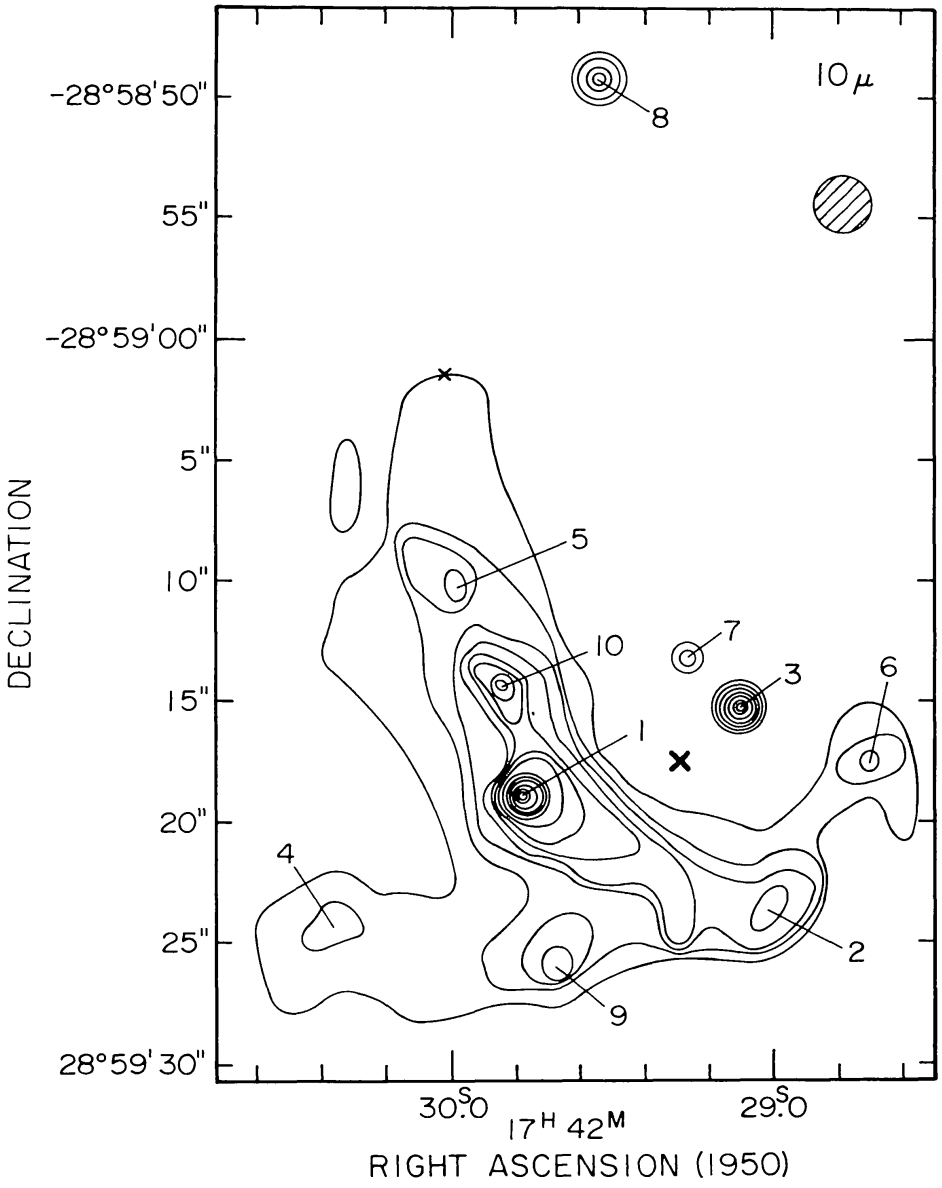

Figure 36 Map of the galactic center region at 10 μ, made with a 2.″3 circular aperture on the 5-m Hale telescope. The aperture size is shown by the circle in the upper right-hand corner. The contour interval is 4×10^{-16} W m^{-2} Hz^{-1} sr^{-1}. The cross marks the galactic center (Willner 1976, Becklin et al. 1977).

1.2 and 12.5 μ, Willner (1976) has found that IRS 7, 11, 12, 16, and 19 of Figure 35 are stars or star clusters (IRS 16 is the star concentration at the center) with luminosities of the order of 10^4 $L_\odot$. No. 7, with 10^5 $L_\odot$, is probably an MIa supergiant. All except IRS 7 are invisible at 10 μ; cf Becklin et al. 1977.

The "ridge" which contains the dust that produces the emission around 10 μ and longer is at the same time a density-bounded concentration of ionized gas, as is shown by the high resolution Ne II observations discussed in Section 6.3.2. Willner has further argued that the 10-μ sources do not come from increased dust density but rather from increased local heating of the dust; the heated regions have a typical size of 0.1 pc, comparable to that of compact H II regions.

The extinction towards most of the sources appears to be moderately uniform. From their photometric measurements in the infrared Becklin, Neugebauer and Willner (Willner 1976) conclude that the visual extinction is about 28 magnitudes, and that most of it occurs in the Galaxy at large. The dust density in the central region itself appears to be relatively small in comparison with the high gas density. The visual extinction across the central 10 pc is estimated to be only about 3^m (Gatley et al. 1977).

Radiation in the *far* infrared (25–300 μ) was first extensively studied by Hoffmann, Frederick & Emery (1971) (cf also Low & Aumann 1970, Harper 1974). The early observations were made with large apertures, and did not therefore reveal any of the fine structure. A radical improvement has recently become possible by the use of NASA's Gerard P. Kuiper Airborne Infrared Observatory. With this equipment Gatley et al. (1977) mapped a region of 10′ diameter around the center in three

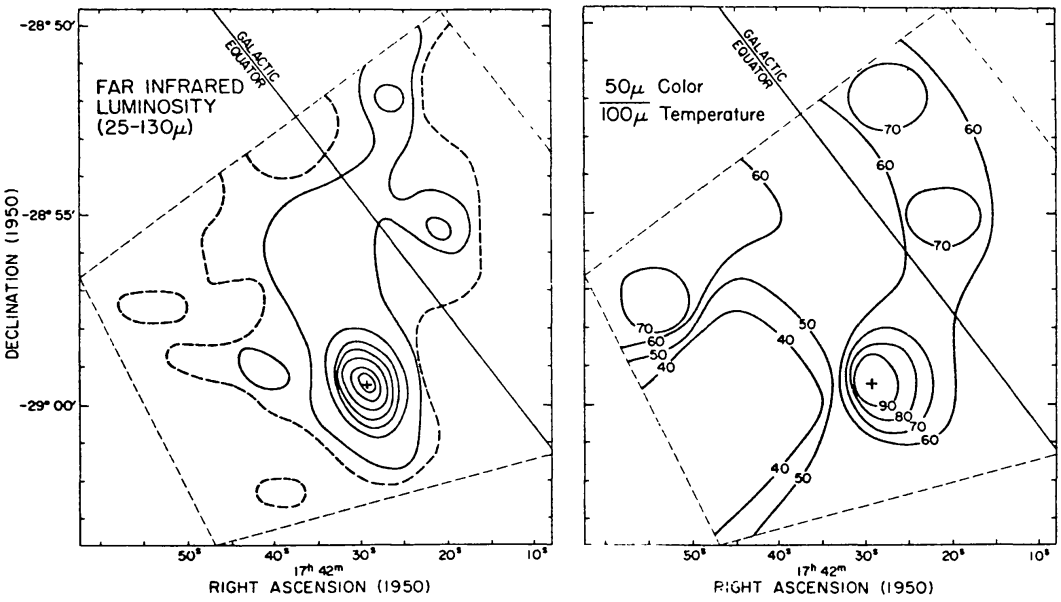

Figure 37 Map of the far-infrared luminosity of the galactic center region obtained by integration from 25- to 130-μ wavelength (left); the contour interval is equivalent to 1.0×10^{-10} W m^{-2} into a 1′ beam. The right-hand diagram gives the color temperatures (Gatley et al. 1977).

wavelength bands, at 30 μ, 50 μ, and 100 μ, with a resolution of $\sim 1'$. Figure 37a shows the distribution of the integrated luminosity between 25 and 130 μ; Figure 37b indicates the run of the color temperature obtained by fitting a Planck curve to their data. The far-infrared radiation is seen to be strongly concentrated to the same region as the near-infrared emission (the galactic center position is shown by a cross). The 25–130 μ luminosity of the central $1'$ is $2.3 \times 10^6\ L_\odot$, the color temperature is ~ 100 K, while the brightness temperature at 50 μ is ~ 40 K. From the comparison of these two temperatures the authors estimated that the optical depth $\tau_{50\mu} \sim 0.05$. The optical depth was found to be practically the same at almost all points, which indicates that the volume density of dust is fairly uniform over the whole region within about 15 pc from the center.

Observations with much higher resolving power with the same airborne observatory have been made and discussed by Harvey, Campbell & Hoffmann

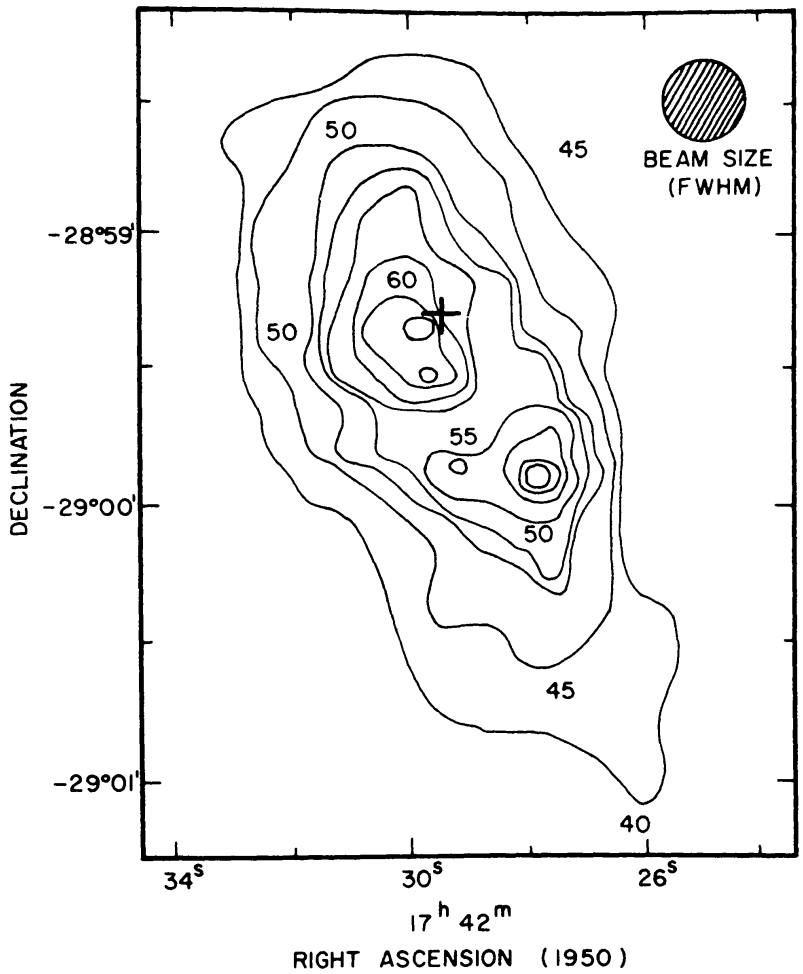

Figure 38 Map of the galactic center at 53 μ with a 17″ beam. The contour levels are at 5, 10, 15, 18, 21, 24, 27, and 30×10^{-16} W m^{-2} Hz^{-1} sr^{-1}. Dust temperatures are also indicated. The cross marks the position of the ultracompact radio source at the galactic center (Harvey, Campbell & Hoffmann 1976).

(1976). Their map at 53 μ, with 17″ resolution, is shown in Figure 38. It shows a strongly elongated structure, more or less (but not precisely) along the true galactic equator, in which there are two maxima, about 45″ (2 pc) apart; the NE maximum coincides with the galactic center (Sgr A West), the other with a *weak* 10 μ source. It may be noted that the "shoulder" shown in the 6-cm map (Figure 33) SW of the center lies in the same position angle, though at a somewhat smaller distance. The authors observed also at 100 and 175 μ, with a beam of $\sim$30″. Like Gatley et al. they find that the decrease in surface brightness with distance from the center (in this case between 0.7 and 2 pc) can be most readily explained by a temperature gradient, with little or no change in dust column density. The amount of dust required for the far-infrared emission is comparable to that required to explain the near-infrared and visual *extinction*. The optical depths they find from their model range from 0.1 at 53 μ to 0.01 at 175 μ. The paper contains an interesting graph of the energy distribution of Sgr A West between $\sim$10 and 400 μ.

ACKNOWLEDGMENT

I am grateful for the kindness with which colleagues have put unpublished material at my disposal. The article could not have been written in its present form but for the pre-publication data received from Drs. Bania, Burton, and Wollman. I am similarly indebted to Drs. Becklin, Cohen, Fukui, Kellermann, Lo, Sanders, Willner, and others for early information on new results. Valuable comments have been given by Drs. van Bueren, Dekker, Ekers, Mezger, Pauls, van den Bout, and van der Kruit. I want to thank Drs. Cohen, Davies, Downes, Mezger, and Townes for help of various kinds.

Literature Cited

Altenhoff, W. J., Downes, D., Goad, L., Maxwell, A., Rinehart, R. 1970. *Astron. Astrophys. Suppl.* 1:319
Balick, B., Sanders, R. H. 1974. *Ap. J.* 184: 415
Balick, B., Brown, R. L. 1974. *Ap. J.* 194: 265
Bania, T. M. 1977. *Ap. J.* Submitted for publication
Becklin, E. E., Matthews, K., Neugebauer, G., Willner, S. P. 1977. *Ap. J.* Submitted for publication
Becklin, E. E., Neugebauer, G. 1968. *Ap. J.* 151:145
Becklin, E. E., Neugebauer, G. 1969. *Ap. J. Lett.* 157:L31
Becklin, E. E., Neugebauer, G. 1975. *Ap. J. Lett.* 200:L71
Becklin, E. E., Neugebauer, G., Early, D. 1977. In preparation
Bieging, J. H. 1976. *Astron. Astrophys.* 51: 289
Bolton, J. G., Gardner, F. F., McGee, R. X., Robinson, B. J. 1964. *Nature* 204:30
Borgman, J., Koornneef, J., de Vries, M. 1974. *Proc. 8th Eslab Symp. H II Reg. Galactic Cent.*, p. 229
Burton, W. B. 1970. *Astron. Astrophys. Suppl.* 2:261
Burton, W. B. 1974. In *Galactic and Extra-Galactic Radio Astronomy,* ed. G. L. Verschuur, K. J. Kellermann, pp. 82–117. Berlin, Heidelberg, New York: Springer. 402 pp.
Burton, W. B., Gordon, M. A. 1977. *Astron. Astrophys.* Submitted for publication
Cohen, R. J. 1975. *MNRAS* 171:659
Cohen, R. J., Davies, R. D. 1976. *MNRAS* 175:1
Cohen, R. J., Few, R. W. 1976. *MNRAS* 176:495
Cohen, R. J. 1977. *MNRAS.* 178:547
Cugnon, P. 1968. *Bull. Astron. Inst. Neth.* 19:363
Davies, R. D., Walsh, D., Booth, R. S. 1976. *MNRAS* 177:319
de Bruyn, A. G. 1977. *Astron. Astrophys.* 58: 221
Downes, D., Maxwell, A. 1966. *Ap. J.* 146: 653

Downes, D., Martin, A. H. M. 1971. *Nature* 233:112
Downes, D. 1974. *Proc. 8th Eslab Symp. H II Reg. Galactic Cent.*, p. 247
Ekers, R. D., Lynden-Bell, D. 1971. *Astrophys. Lett.* 9:189
Ekers, R. D., Goss, W. M., Schwarz, U. J., Downes, D., Rogstad, D. H. 1975. *Astron. Astrophys.* 43:159
Fomalont, E. B., Weliachew, L. N. 1973. *Ap. J.* 181:781
Frank, J., Rees, M. J. 1976. *MNRAS* 176: 633
Fukui, Y., Iguchi, T., Karifu, N., Chicada, Y., Morimoto, M., Nagane, K., Miyazawa, K., Miyaji, T. 1977. *Publ. Astron. Soc. Jpn.* In press
Gardner, F. F., Whiteoak, J. B. 1970. *Astrophys. Lett.* 5:161
Gatley, I., Becklin, E. E., Werner, M. W., Wynn-Williams, C. G. 1977. Preprint
Gopal-Krishna, Swarup, G., Sarma, N. V. G., Hoshi, M. N. 1972. *Nature* 239:91
Gopal-Krishna, Swarup, G. 1976. *Astrophys. Lett.* 17:45
Gordon, M. A., Burton, W. B. 1976. *Ap. J.* 208:346
Harper, D. A. 1974. *Ap. J.* 192:557
Harvey, P. M., Campbell, M. F., Hoffmann, W. F. 1976. *Ap. J. Lett.* 205:L69
Hoffmann, W. F., Frederick, C. L., Emery, R. J. 1971. *Ap. J. Lett.* 164:L23
Johnson, H. M. 1961. *Ap. J.* 133:309
Kaifu, J., Kato, T., Iguchi, T. 1972. *Nature Phys. Sci.* 238:105 (*not Nature* 238:105, as has been erroneously cited by several authors)
Kellermann, K. I., Shaffer, D. B., Pauliny-Toth, I. I. K., Preuss, E., Witzel, A. 1976. *Ap. J. Lett.* 210:L121
Kellermann, K. I., Shaffer, D. B., Clark, B. G., Geldzahler, B. J. 1977. *Ap. J. Lett.* 214:L61
Kerr, F. J., Sinclair, M. W. 1966. *Nature* 212:166
Kerr, F. J. 1968. In *Radio Astronomy and the Galactic System, IAU Symp. No. 31*, p. 239, ed. H. van Woerden
Kinman, T. D. 1965. *Ap. J.* 142:1376
Leung, Chun Ming, Liszt, H. S. 1976. *Ap. J.* 208:732
Light, E. S., Danielson, R. E., Schwarzschild, M. 1974. *Ap. J.* 194:257
Lindblad, B. 1956. *Stockholm Obs. Ann.* 19: No. 2
Liszt, H. S., Sanders, R. H., Burton, W. B. 1975. *Ap. J.* 198:537
Liszt, H. S., Burton, W. B., Sanders, R. H., Scoville, N. Z. 1977. *Ap. J.* 213:38
Little, A. G. 1974. In *Galactic Radio Astronomy, IAU Symp. No. 60*, ed. F. J. Kerr, S. C. Simonson III, pp. 491–97
Lo, K. Y., Schilizzi, R. T., Cohen, M. H., Ross, H. N. 1975. *Ap. J. Lett.* 202:L63
Low, F. J., Aumann, H. H. 1970. *Ap. J. Lett.* 162:L79
Lynden-Bell, D., Rees, M. J. 1971. *MNRAS* 152:461
Martin, A. H. M., Downes, D. 1972. *Astrophys. Lett.* 11:219
McGee, R. X., Brooks, J. W., Sinclair, M. W., Batchelor, R. A. 1970. *Aust. J. Phys.* 23: 777
Mezger, P. G. 1974. *Proc. ESO/SRC/CERN Conf. Prog. New Large Telescopes*, p. 79
Mezger, P. G., Churchwell, E. B., Pauls, T. A. 1974. *Proc. Eur. Astron. Meet., 1st* 2:140
Mills, B. Y. 1956. *Observatory* 76:65
Milman, A. S. 1975. *Ap. J.* 202:673
Minkowski, R. 1965. *Stars and Stellar Systems*, eds. A. Blaauw, M. Schmidt, Vol. 5, p. 321. Univ. Chicago Press
Mirabel, I. F., Turner, K. C. 1972. *Bull. Am. Astr. Soc.* 4:413
Morton, D. C., Thuan, T. X. 1973. *Ap. J.* 180:705
Oort, J. H. 1968. In *Non-Stable Phenomena in Galaxies, Proc. IAU Symp. No. 29*, ed. Armenian Acad. Sci., pp. 41–44
Oort, J. H. 1974a. In *The Formation and Dynamics of Galaxies, IAU Symp. No. 58*, ed. J. R. Shakeshaft, pp. 378–82
Oort, J. H. 1974b. See Little 1974, pp. 539–47
Oort, J. H., Plaut, L. 1975. *Astron. Astrophys.* 41:71
Pauls, T., Mezger, P. G., Churchwell, E. 1974. *Astron. Astrophys.* 34:327
Pauls, T., Mezger, P. G. 1975. *Astron. Astrophys.* 44:259
Pauls, T., Downes, D., Mezger, P. G., Churchwell, E. 1976. *Astron. Astrophys.* 46:407
Peters, W. L. 1975. *Ap. J.* 195:617
Rieke, G. H., Low, F. J. 1973. *Ap. J.* 184:415
Robinson, B. J., McGee, R. X. 1970. *Aust. J. Phys.* 23:405
Robinson, B. J. 1974. See Little 1974, pp. 521–35
Rougoor, G. W., Oort, J. H. 1960. *Proc. Natl. Acad. Sci. USA* 46:1
Rougoor, G. W. 1964. *Bull. Astron. Inst. Neth.* 17:381
Ruiz, Maria Teresa. 1976. *Ap. J.* 207:382
Salpeter, E. E. 1964. *Ap. J.* 140:796
Sandage, A. R. 1961. *The Hubble Atlas of Galaxies, Carnegie Inst. Washington Publ. 618*, Plate 31
Sandage, A. R., Becklin, E. E., Neugebauer, G. 1969. *Ap. J.* 157:55
Sanders, R. H., Huntley, J. M. 1976. *Ap. J.* 209:53

Sanders, R. H., Lowinger, T. 1972. *Astron. J.* 77:292
Sanders, R. H., Prendergast, K. H. 1974. *Ap. J.* 188:489
Sanders, R. H., Wrixon, G. T. 1973. *Astron. Astrophys.* 26:365
Sanders, R. H., Wrixon, G. T. 1974. *Astron. Astrophys.* 33:9
Sanders, R. H., Wrixon, G. T., Mebold, U. 1977. To appear in *Astron. Astrophys.*
Sanders, R. H., Wrixon, G. T., Penzias, A. A. 1972. *Astron. Astrophys.* 16:322
Sandqvist, Aa. 1970. *Astron. J.* 75:135
Sandqvist, Aa. 1973. *Astron. Astrophys. Suppl.* 9:391
Sandqvist, Aa. 1974. *Astron. Astrophys.* 33:413
Saraber, M. J. M., Shane, W. W. 1974. *Astron. Astrophys.* 36:365
Schwarz, U. J., Shaver, P. A., Ekers, R. D. 1977. *Astron. Astrophys.* 54:863
Scoville, N. Z., Solomon, P. M., Thaddeus, P. 1972. *Ap. J.* 172:335
Scoville, N. Z. 1972. *Ap. J. Lett.* 175:L127
Scoville, N. Z., Solomon, P. M. 1973. *Ap. J.* 180:55
Scoville, N. Z., Solomon, P. M., Jefferts, K. B. 1974. *Ap. J. Lett.* 187:L63
Scoville, N. Z., Solomon, P. M., Penzias, A. A. 1975. *Ap. J.* 201:352
Segalovitz, A. 1975. *Astron. Astrophys.* 40:401
Shane, W. W. 1972. *Astron. Astrophys.* 16:118
Simonson, S. C. III, Mader, G. L. 1973. *Astron. Astrophys.* 27:337
Solomon, P. M., Scoville, N. Z., Jefferts, K. B., Penzias, A. A., Wilson, R. W. 1972. *Ap. J.* 178:125
van Albada, G. D., Shane, W. W. 1975. *Astron. Astrophys.* 42:433
van den Bergh, S. 1975. *Ann. Rev. Astron. Astrophys.* 13:217
van der Kruit, P. C. 1970. *Astron. Astrophys.* 4:462
van der Kruit, P. C. 1971. *Astron. Astrophys.* 13:405
van der Kruit, P. C. 1974. *Ap. J.* 192:1
van der Kruit, P. C., Oort, J. H., Mathewson, D. S. 1972. *Astron. Astrophys.* 21:169
Wannier, P. G., Penzias, A. A., Linke, R. A., Wilson, R. W. 1976. *Ap. J.* 204:26
Westbrook, W. E., Werner, M. W., Elias, J. H., Gezari, D. Y., Hausier, M. G., Lo, K. Y., Neugebauer, G. 1976. *Ap. J.* 209:94
Whiteoak, J. B., Gardner, F. F. 1973. *Astrophys. Lett.* 13:205
Whiteoak, J. B., Rogstad, D. H., Lockhart, I. A. 1974. *Astron. Astrophys.* 36:245
Willner, S. P. 1976. *Compact infrared sources: NGC 7538 and the galactic center.* PhD thesis. Calif. Inst. Technol. 56 pp.
Wollman, E. R., Geballe, T. R., Lacy, J. H., Townes, C. H., Rank, D. M. 1976. *Ap. J. Lett.* 205:L5
Wollman, E. R. 1976. *Ne II 12.8 μ emission from the galactic center and compact H II regions.* PhD thesis. Univ. Calif., Berkeley
Wrixon, G. T., Sanders, R. H. 1973. *Astron. Astrophys. Suppl.* 11:339